PB93-221752

REPORT NO.
UCB/EERC-93/05
MAY 1993

EARTHQUAKE ENGINEERING RESEARCH CENTER

MULTIPLE-SUPPORT RESPONSE SPECTRUM ANALYSIS OF THE GOLDEN GATE BRIDGE

by

YUTAKA NAKAMURA
ARMEN DER KIUREGHIAN
DAVID LIU

Report to the National Science Foundation

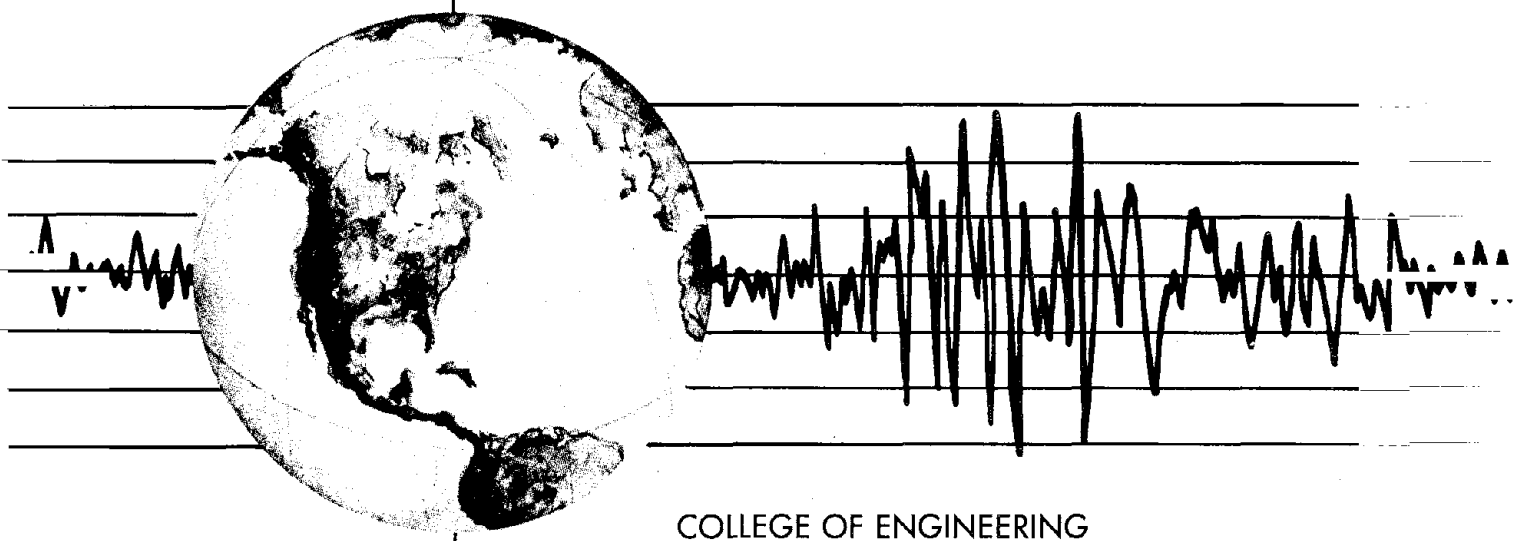

COLLEGE OF ENGINEERING

UNIVERSITY OF CALIFORNIA AT BERKELEY

For sale by the National Technical Information Service, U.S. Department of Commerce, Springfield, Virginia 22161

See back of report for up to date listing of EERC reports.

-101

REPORT DOCUMENTATION PAGE	1. REPORT NO. NSF/ENG-93001	2.	3. PB93-221752

4. Title and Subtitle
"Multiple-Support Response Spectrum Analysis of the Golden Gate Bridge"

5. Report Date
May 1993

6.

7. Author(s)
Yutaka Nakamura, Armen Der Kiureghian, and David Liu

8. Performing Organization Rept. No.
UCB/EERC-93/05

9. Performing Organization Name and Address
Earthquake Engineering Research Center
University of California, Berkeley
1301 So. 46th Street
Richmond, Calif. 94804

10. Project/Task/Work Unit No.

11. Contract(C) or Grant(G) No.
(C)
(G) BCS-9011112

12. Sponsoring Organization Name and Address
National Science Foundation
1800 G Street, N.W.
Washington, D.C. 20550

13. Type of Report & Period Covered

14.

15. Supplementary Notes

16. Abstract (Limit: 200 words)

The newly developed Multiple-Support Response Spectrum (MSRS) method is reviewed and applied to analysis of the Golden Gate Bridge. The MSRS method properly accounts for the effects of wave passage and incoherence of the support motions, the effect of local site conditions, and the effects of correlation between the support motions and between the dynamic modes of the structure. The peak response is given in terms of a combination rule involving the peak ground displacements and mean response spectra associated with the support ground motions: contributions of the pseudo-static and dynamic components of the response, as well as their covariance, are explicitly included. New results concerning the properties of influence coefficients and modal participation factors involved in the combination rule are derived. A 3-dimensional model of the Golden Gate Bridge with a total of 4,074 degrees of freedom and 6 pairs of support points, and site-specific response spectra are used for the response analysis.

The new response spectrum method is shown to offer a simple and viable alternative for seismic analysis of multiply supported structures subjected to spatially varying ground motions. The method is particularly effective when a comprehensive understanding of the spatial variability effect, through parametric studies, is required.

17. Document Analysis a. Descriptors

b. Identifiers/Open-Ended Terms

c. COSATI Field/Group

18. Availability Statement
Release Unlimited

19. Security Class (This Report)	21. No. of Pages
unclassified	85
20. Security Class (This Page)	22. Price
unclassified	

(ANSI-Z39.18) See Instructions on Reverse OPTIONAL FORM 272 (4-77)
(Formerly NTIS-35)

MULTIPLE-SUPPORT RESPONSE SPECTRUM ANALYSIS OF THE GOLDEN GATE BRIDGE

by

Yutaka Nakamura
Armen Der Kiureghian
University of California, Berkeley

and

David Liu
Imbsen & Associates, Inc., Sacramento

A report on research supported by
the National Science Foundation under
Grant No. BCS-9011112

Report No. UCB/EERC-93/05
Earthquake Engineering Research Center
College of Engineering
University of California at Berkeley

May 1993

ABSTRACT

The newly developed Multiple-Support Response Spectrum (MSRS) method (Der Kiureghian and Neuenhofer 1992) is reviewed and applied to the analysis of the Golden Gate Bridge. The MSRS method properly accounts for the effects of wave passage and incoherence of the support motions, the effect of local site conditions, and the effects of correlation between the support motions and between the dynamic modes of the structure.

In the MSRS method, the peak response is given in terms of a combination rule involving the peak ground displacements and mean response spectra associated with the support ground motions, and a set of cross-support and cross-mode correlation coefficients that are determined in terms of the individual spectra and the coherency function describing the nature of the spatial variability of the ground motion. Contributions of the pseudo-static and dynamic components of the response, as well as their covariance, are explicitly included in the combination rule. New results concerning the properties of influence coefficients and modal participation factors involved in the combination rule are derived in this report.

The Golden Gate Bridge is a three-span suspension bridge connecting San Francisco and Marin Counties in California. The main span is 1280m long and the two side spans (from main tower to pylon support) are each 343m long. A 3-dimensional model with a total of 4,074 degrees of freedom and 6 pairs of support points is used for the response analysis. Site-specific response spectra consistent with a set of artificially generated accelerograms are used for the three components of ground motion at each support point.

The mean peak values of selected displacement and bending moment responses of the two tower structures of the bridge are computed by the MSRS method, including the first 100 modes and using an appropriate wave velocity and a coherency function for the region. Parametric studies demonstrate the effect of wave passage and incoherence on the dynamic and pseudo-static components of the response. The computed results by the MSRS method are compared with values computed by time history analysis using the artificial time histories. The results by the MSRS method show a consistent trend with the results by the time history analysis; however, a close agreement between the two sets of results cannot be claimed. Reasons for the apparent discrepancy are discussed.

It is found that the new response spectrum method offers a simple and viable alternative for seismic analysis of multiply supported structures subjected to spatially varying ground motions. The method is particularly effective when a comprehensive understanding of the spatial variability effect, through parametric studies, is required. Due to inherent uncertainties in models describing wave passage, incoherence and site response effects, such parametric studies are imperative in design of critical structures having long spans, such as bridges and viaducts.

ACKNOWLEDGMENT

This study was supported by the National Science Foundation Grant No. BCS-9011112 with Dr. S-C. Liu as Program Director. The first author was supported by Shimizu Corporation during his studies at the University of California at Berkeley. The third author contributed to this study by providing the necessary structural model and input data. The authors gratefully acknowledge the permission of the Golden Gate Bridge Authority to receive and analyze the data reported herein.

TABLE OF CONTENTS

LIST OF TABLES

LIST OF FIGURES

CHAPTER 1
INTRODUCTION

Observations during recent earthquakes, notably the Loma Prieta earthquake of October 17, 1989 have clearly demonstrated that seismic ground motions can vary significantly over distances of the same order of magnitude as the dimensions of some extended structures, such as bridges. This phenomenon can give rise to differential support motions for multiply supported structures. The effect on most structures is beneficial, i.e., the response is reduced compared to the case where the supports move uniformly. However, there are situations where such differential support motions may actually increase the response. The failure of several bridges during the Loma Prieta earthquake has highlighted the need for a better understanding of this phenomenon, and for the development of simple and accurate analysis tools for use in engineering practice.

Three phenomena are responsible for variations of ground motions in space: (1) the difference in the arrival times of seismic waves at different stations, known as the "wave passage" effect; (2) loss of coherence of the motion due to reflections and refraction of the waves in the heterogeneous medium of the ground, as well as due to the differences in the manner of superposition of waves arriving from an extended source, collectively known as the "incoherence" effect; and (3) the difference in the local soil conditions at each station and the manner in which they influence the amplitude and frequency content of the bedrock motion, known as the "site response" effect.

Presently, dynamic analysis with spatially varying input motions is performed either by the time history approach, or by the method of random vibrations. For the former approach, one is required to define the input accelerations at the various support points in terms of their complete time histories. The primary disadvantage of the time history approach is that the results produced from the analysis are specific to the set of selected time histories. Often the results vary significantly when an alternative set of records with equal validity is considered. A further disadvantage is that the analysis requires extensive amounts of computation, thus precluding the possibility of analysis with alternative sets of records.

The random vibration approach is based on a statistical characterization of the set of motions at the support points, usually in terms of auto- and cross-power spectral densities. The primary advantage of the random vibration approach is that it provides a statistical measure of the response, which is not controlled by an arbitrary choice of the

input motions. This approach is particularly appealing from the viewpoint of design, where consideration should be given to entire families of potential ground motions at the stations of interest.

Der Kiureghian and Neuenhofer (1991) have recently developed a new multiple-support response spectrum (MSRS) method based on the principles of random vibration theory. The MSRS method can be seen as an extension of the well known complete quadratic combination (CQC) rule, developed by Der Kiureghian (1981), which is now a recommended rule of practice by several codes. The MSRS method properly accounts for the effects of wave passage and incoherence of the support motions, the effect of spatially varying site response, and the effects of correlation between the support motions and between the dynamic modes of the structure.

In the MSRS method, the peak response is given in terms of a combination rule involving the peak ground displacements and mean response spectra associated with the support ground motions, and a set of cross-support and cross-mode correlation coefficients. The latter are determined in terms of the individual response spectra and a coherency function, which describes the nature of the spatial variability of the ground motion in the region. Contributions of the pseudo-static and dynamic components of the response, as well as their covariance, are explicitly included in the combination rule.

The object of this study is to demonstrate the validity and practicality of the MSRS method by its application to the Golden Gate Bridge, which is a three-span suspension bridge connecting San Francisco and Marin. Liu and Imbsen (1990) developed a three-dimensional model of the bridge and carried out time history response analysis for support ground motions artificially generated to be compatible with a set of target response spectra. The MSRS results generated in this study are compared with the results of the time history analysis by Liu and Imbsen.

Following this introductory chapter, Chapter 2 deals with the review of the equations of motion for a multiply-supported structure, and definition of terms that enter into the MSRS modal combination rule. New results concerning the properties of influence coefficients and modal participation factors that are involved in the combination rule are derived. Chapter 3 describes the model of the Golden Gate Bridge and the support excitations. Chapter 4 presents a parametric study of the cross-correlation coefficients of the Golden Gate Bridge for the specified input. Chapter 5 presents the results of multiple-support response spectrum analysis of the Golden Gate Bridge and the comparison with the time history analysis results. Finally, Chapter 6 presents a summary of the report and major results of the study.

CHAPTER 2
THE MULTIPLE-SUPPORT RESPONSE SPECTRUM METHOD

2.1 Introduction

This chapter reviews the equations of motion of multiply-supported structures and the multiple-support response spectrum (MSRS) method developed by Der Kiureghian and Neuenhofer (1991). In addition to these reviews, new results concerning the properties of an influence matrix, effective influence coefficients and effective modal participation factors are derived in this chapter.

2.2 Equations of Motion of Multiply-Supported Structure

The equations of motion for a discretized, n-degrees-of-freedom linear system subjected to m support motions can be written in the matrix form (Clough and Penzien, 1975)

$$\begin{bmatrix} \mathbf{M} & \mathbf{M}_c \\ \mathbf{M}_c^{\mathrm{T}} & \mathbf{M}_g \end{bmatrix} \begin{Bmatrix} \ddot{\mathbf{x}} \\ \ddot{\mathbf{u}} \end{Bmatrix} + \begin{bmatrix} \mathbf{C} & \mathbf{C}_c \\ \mathbf{C}_c^{\mathrm{T}} & \mathbf{C}_g \end{bmatrix} \begin{Bmatrix} \dot{\mathbf{x}} \\ \dot{\mathbf{u}} \end{Bmatrix} + \begin{bmatrix} \mathbf{K} & \mathbf{K}_c \\ \mathbf{K}_c^{\mathrm{T}} & \mathbf{K}_g \end{bmatrix} \begin{Bmatrix} \mathbf{x} \\ \mathbf{u} \end{Bmatrix} = \begin{Bmatrix} \mathbf{0} \\ \mathbf{F} \end{Bmatrix} \tag{2.1}$$

where $\mathbf{x} = \{x_1, \ldots, x_n\}^{\mathrm{T}}$ is the n-vector of (total) displacements at the unconstrained degrees of freedom; $\mathbf{u} = \{u_1, \ldots, u_m\}^{\mathrm{T}}$ is the m-vector of prescribed support displacements; $\mathbf{M}$, $\mathbf{C}$ and $\mathbf{K}$ are $n \times n$ mass, damping and stiffness matrices associated with the unconstrained degrees of freedom, respectively; $\mathbf{M}_g$, $\mathbf{C}_g$ and $\mathbf{K}_g$ are the $m \times m$ matrices associated with the support degrees of freedom; $\mathbf{M}_c$, $\mathbf{C}_c$ and $\mathbf{K}_c$ are the $n \times m$ coupling matrices associated with both sets of degrees of freedom; and $\mathbf{F}$ is the m-vector of reacting forces at the support degrees of freedom. Both $\mathbf{x}$ and $\mathbf{u}$ may contain translational as well as rotational components.

In the analysis of such systems, it is common to decompose the response into pseudo-static and dynamic components. Following the conventional procedure (Clough and Penzien, 1975), we define

$$\mathbf{x} = \mathbf{x}^s + \mathbf{x}^d \tag{2.2}$$

where the pseudo-static component, $\mathbf{x}^s$, is the solution to Eq. 2.1 when the inertia and damping terms are discarded, and is given by

$$\mathbf{x}^s = -\mathbf{K}^{-1}\mathbf{K}_c\mathbf{u} = \mathbf{R}\mathbf{u} \tag{2.3}$$

in which $\mathbf{R} = -\mathbf{K}^{-1}\mathbf{K}_c$ is denoted as the influence matrix. Substituting Eqs. 2.2 and 2.3 in Eq. 2.1, the dynamic component of the response is obtained in the differential form

$$\begin{aligned}\mathbf{M}\ddot{\mathbf{x}}^d + \mathbf{C}\dot{\mathbf{x}}^d + \mathbf{K}\mathbf{x}^d &= -(\mathbf{MR} + \mathbf{M}_c)\ddot{\mathbf{u}} - (\mathbf{CR} + \mathbf{C}_c)\dot{\mathbf{u}} \\ &\approx -(\mathbf{MR} + \mathbf{M}_c)\ddot{\mathbf{u}} \end{aligned} \tag{2.4}$$

where the right-hand side is approximated by neglecting the damping forces, which are usually much smaller than the corresponding inertia forces on the same side. This approximation is exact when the damping matrix is proportional to the stiffness matrix. It is noted that $\mathbf{M}_c = \mathbf{0}$ if a lumped mass model is used.

To formulate a response spectrum method, it is necessary to employ the normal mode approach. Let $\Phi = [\phi_1 \ldots \phi_n]$, ω_i and ζ_i, $i = 1, \cdots, n$, denote the modal matrix, natural frequencies and modal damping ratios of the structure with its supports fixed. Using the transformation $\mathbf{x}^d = \Phi\mathbf{y}$, $\mathbf{y} = [y_1, \cdots, y_n]^{\mathrm{T}}$ in Eq. 2.4 and employing orthogonality of the mode shapes (assuming proportional damping), the decoupled equations of motions are

$$\ddot{y}_i + 2\zeta_i\omega_i\dot{y}_i + \omega_i^2 y_i = \sum_{k=1}^{m} \beta_{ki}\ddot{u}_k(t) \qquad i = 1, \cdots, n \tag{2.5}$$

where the index k refers to the degrees of freedom associated with the prescribed support motions, the subscript i denotes the mode number, and β_{ki} is the modal participation factor given by

$$\beta_{ki} = -\frac{\phi_i^{\mathrm{T}}(\mathbf{M}\mathbf{r}_k + \mathbf{M}_c\mathbf{i}_k)}{\phi_i^{\mathrm{T}}\mathbf{M}\phi_i} \tag{2.6}$$

where $\mathbf{r}_k$ is the k-th column of $\mathbf{R}$ and $\mathbf{i}_k$ is the k-th column of an $m \times m$ identity matrix. It is convenient to define a normalized modal response $s_{ki}(t)$, representing the response of a single-degree-of-freedom oscillator of unit mass, frequency ω_i and damping ζ_i, which is subjected to the base motion $u_k(t)$. From Eq. 2.5, $s_{ki}(t)$ satisfies the equation

$$\ddot{s}_{ki} + 2\zeta_i\omega_i\dot{s}_{ki} + \omega_i^2 s_{ki} = \ddot{u}_k(t) \tag{2.7}$$

Obviously, $y_i(t) = \sum_{k=1}^{m} \beta_{ki} s_{ki}(t)$.

A generic response quantity of interest, $z(t)$ (e.g., a nodal displacement, an internal force, stress or strain component), in general can be expressed as a linear function of the nodal displacements **x**, i.e.,

$$z(t) = \mathbf{q}^{\mathrm{T}}\mathbf{x}(t) = \mathbf{q}^{\mathrm{T}}\left[\mathbf{x}^{s}(t) + \mathbf{x}^{d}(t)\right] \tag{2.8}$$

where **q** is a response transfer vector which usually depends on the geometry and stiffness properties of the structure. Substituting for the pseudo-static component of **x** from Eq. 2.3 and for the dynamic component in terms of the normalized modal responses, the generic response $z(t)$ is written as

$$z(t) = \sum_{k=1}^{m} a_k u_k(t) + \sum_{k=1}^{m}\sum_{i=1}^{n} b_{ki} s_{ki}(t) \tag{2.9}$$

in which

$$a_k = \mathbf{q}^{\mathrm{T}}\mathbf{r}_k \qquad k = 1,\cdots,m \tag{2.10}$$

$$b_{ki} = \mathbf{q}^{\mathrm{T}}\phi_i\beta_{ki} \qquad k = 1,\cdots,m\ ; \quad i = 1,\cdots,n \tag{2.11}$$

are denoted effective influence coefficients and effective modal participation factors, respectively. It is important to note that a_k and b_{ki} are functions only of the structural properties, and that $s_{ki}(t)$ is dependent only on the i-th modal frequency and damping ratio and the k-th input motion. The first sum on the right hand side of Eq. 2.9 represents the pseudo-static component of the response and the double-sum term represents the dynamic component.

2.3 Properties of the Influence Matrix, Effective Influence Coefficients and Effective Modal Participation Factors

(i) Influence Matrix

In the previous section, the influence matrix **R** was defined as

$$\mathbf{R} = \left[\mathbf{r}_1\ \mathbf{r}_2 \cdots \mathbf{r}_{\mathrm{m}}\right] = -\mathbf{K}^{-1}\mathbf{K}_c \tag{2.12}$$

As defined by Eq. (2.3), the vector of the pseudo-static components, $\mathbf{x}^s$, is given by

$$\mathbf{x}^s = \begin{Bmatrix} x_1^s \\ x_2^s \\ \vdots \\ x_n^s \end{Bmatrix} = \mathbf{R}\mathbf{u} = \begin{bmatrix} \mathbf{r}_1 & \mathbf{r}_2 & \cdots & \mathbf{r}_m \end{bmatrix} \begin{Bmatrix} u_1 \\ u_2 \\ \vdots \\ u_m \end{Bmatrix} \tag{2.13}$$

where $\mathbf{u}$ denotes the vector of support displacements. Now consider the case where all the support displacements are unity, i.e., $\mathbf{u} = \{1\ 1\ \cdots\ 1\}^{\mathrm{T}}$. If all support motions are translational, this condition corresponds to a rigid body motion of the entire structure by a unit amount in each translational coordinate direction. Let $\mathbf{x}^{s,1}$ denote the corresponding vector of nodal displacements at the unconstrained degrees of freedom. If $\mathbf{x}$ includes only translational degrees of freedom and the coordinate systems for $\mathbf{x}$ and $\mathbf{u}$ coincide, then $\mathbf{x}^{s,1} = \{1\ 1\ \cdots\ 1\}^{\mathrm{T}}$. Otherwise, the elements of $\mathbf{x}^{s,1}$ will not all be unity, but they can be determined by observing the geometry of the structure. From Eq. 2.13, one has

$$\begin{bmatrix} \mathbf{r}_1 & \mathbf{r}_2 & \cdots & \mathbf{r}_m \end{bmatrix} \begin{Bmatrix} 1 \\ 1 \\ \vdots \\ 1 \end{Bmatrix} = \sum_{k=1}^{m} \mathbf{r}_k = \mathbf{x}^{s,1} \tag{2.14}$$

The above relation gives an expression for the sum of columns of $\mathbf{R}$ that is useful in checking the accuracy of calculations.

Next consider the case where the k-th component of $\mathbf{u}$ is unity and the other components are all zero, i.e., $\mathbf{u}^k = \left\{0 \cdots 0\ \overset{k}{1}\ 0 \cdots 0\right\}^{\mathrm{T}}$. Let $\mathbf{x}^{s,k}$ be the corresponding solution of the nodal displacements. From Eq. 2.13, one has

$$\mathbf{x}^{s,k} = \mathbf{R}\mathbf{u}^k = \mathbf{r}_k \tag{2.15}$$

Thus, the influence matrix can be expressed as follows

$$\mathbf{R} = \begin{bmatrix} \mathbf{r}_1 & \mathbf{r}_2 & \cdots & \mathbf{r}_m \end{bmatrix} = \begin{bmatrix} \mathbf{x}^{s,1} & \mathbf{x}^{s,2} & \cdots & \mathbf{x}^{s,m} \end{bmatrix} \tag{2.16}$$

It follows that one can obtain the influence matrix by solving for $\mathbf{x}^{s,k}$ for each $\mathbf{u}^k$, $k = 1, \cdots, m$, instead of using Eq. 2.12. This approach is preferable when $\mathbf{K}^{-1}$ and $\mathbf{K}_c$ are not directly available. From Eq. 2.14, it is also clear that $\mathbf{x}^{s,1} = \sum_{k=1}^{m} \mathbf{x}^{s,k}$.

(ii) Effective Influence Coefficients

Using Eqs. 2.10 and 2.14, one obtains the following property of the effective influence coefficients

$$\sum_{k=1}^{m} a_k = \mathbf{q}^{\mathrm{T}} \sum_{k=1}^{m} \mathbf{r}_k = \mathbf{q}^{\mathrm{T}} \mathbf{x}^{s,1} \tag{2.17}$$

In particular, if the response quantity of interest is the nodal displacement at degree of freedom l, then the response transfer vector $\mathbf{q}$ is

$$\mathbf{q} = \left\{ 0 \cdots 0 \overset{l}{1} 0 \cdots 0 \right\}^{\mathrm{T}} \tag{2.18}$$

From Eq. 2.17, the sum of the effective influence coefficients a_k $(k = 1, \cdots, m)$ for the nodal displacement is found to be

$$\sum_{k=1}^{m} a_k = x_l^{s,1} \tag{2.19}$$

where $x_l^{s,1}$ is the l-th element of $\mathbf{x}^{s,1}$, which would be equal to unity under the conditions specified earlier. The above identity can be used to check the accuracy of computed effective influence coefficients a_k.

(iii) Effective Modal Participation Factors

For a lumped mass model, the modal participation factor β_{ki} for mode i and input component u_k (Eq. 2.6) reduces to

$$\beta_{ki} = -\frac{\boldsymbol{\phi}_i^{\mathrm{T}} \mathbf{M} \mathbf{r}_k}{\boldsymbol{\phi}_i^{\mathrm{T}} \mathbf{M} \boldsymbol{\phi}_i} \tag{2.20}$$

β_{ki} can be interpreted as the participation ratio of the i-th mode in the shape vector $-\mathbf{r}_k$, i.e.,

$$-\mathbf{r}_k = \boldsymbol{\phi}_1 \beta_{k1} + \boldsymbol{\phi}_2 \beta_{k2} + \cdots + \boldsymbol{\phi}_n \beta_{kn} \tag{2.21}$$

The above relation is verified by premultiplying Eq. 2.21 by $\boldsymbol{\phi}_i^{\mathrm{T}} \mathbf{M}$ and using the orthogonality property of the mode shapes.

Premultiplying Eq. 2.21 by $\mathbf{q}^{\mathrm{T}}$ and using the definitions of a_k and b_{ki} from Eqs. 2.10 and 2.11, one has

$$-a_k = b_{k1} + b_{k2} + \cdots + b_{kn} = \sum_{i=1}^{n} b_{ki} \tag{2.22}$$

Hence, the sum of b_{ki} values for all modes is identical to $-a_k$. The above equation can be used to check the accuracy of the computed effective modal participation factors, b_{ki}. However, in practice, for structures with many degrees of freedom usually only a subset of the modes are considered. In that case, unfortunately the above equation is not useful, since the b_{ki} values for truncated modes will remain unknown. One can show that the magnitudes of b_{ki} do not necessarily decrease with increasing mode number and, therefore, the sum in Eq. 2.22 may not converge when terms for any subset of the modes are neglected.

2.4 The Multiple-Support Response Spectrum Method

In this section, the multiple-support response spectrum (MSRS) method is briefly reviewed without any derivation. The detailed development is given by Der Kiureghian and Neuenhofer (1991, 1992).

The MSRS method properly accounts for the effects of variability in the support motions that arises from the wave passage effect, the incoherence effect, as well as the spatially varying site response effect. The method is based on the principles of random vibration theory and accurately accounts for the cross-correlations that occur between the support motions and modes of vibration of the structure.

The combination rule for the mean of the absolute peak response is given in the form

$$\begin{aligned} \mathrm{E}[\max|z(t)|] = \Bigg[& \sum_{k=1}^{m}\sum_{l=1}^{m} a_k a_l \rho_{u_k u_l} u_{k,\max} u_{l,\max} \\ & + 2\sum_{k=1}^{m}\sum_{l=1}^{m}\sum_{j=1}^{n} a_k b_{lj} \rho_{u_k s_{lj}} u_{k,\max} D_l(\omega_j, \zeta_j) \\ & + \sum_{k=1}^{m}\sum_{l=1}^{m}\sum_{i=1}^{n}\sum_{j=1}^{n} b_{ki} b_{lj} \rho_{s_{ki} s_{lj}} D_k(\omega_i, \zeta_i) D_l(\omega_j, \zeta_j) \Bigg]^{1/2} \end{aligned} \tag{2.23}$$

in which a_k and b_{ki} are effective influence coefficients and effective modal participation factors defined by Eqs. 2.10 and 2.11, respectively, $u_{k,\max}$ denotes the peak ground displacement at support degree of freedom k, $D_k(\omega_i, \zeta_i)$ denotes the displacement response spectrum ordinate at support degree of freedom k for the frequency and damping of mode i, and $\rho_{u_k u_l}$, $\rho_{u_k s_{lj}}$ and $\rho_{s_{ki} s_{lj}}$ are cross-correlation coefficients between

the support motions and the modes of the structure. The first term inside the brackets with summations over the support degrees of freedom represents the pseudo-static component of the response, the third term with double-summations over the support degrees of freedom and the modes of the structure represents the dynamic component of the response, and the second term represents the contribution arising from the covariance between the pseudo-static and dynamic components.

The cross-correlation coefficients $\rho_{u_k u_l}$, $\rho_{u_k s_{lj}}$ and $\rho_{s_{ki} s_{lj}}$ in Eq. 2.23 are defined by

$$\rho_{u_k u_l} = \frac{1}{\sigma_{u_k} \sigma_{u_l}} \int_{-\infty}^{\infty} G_{u_k u_l}(\mathrm{i}\omega)\, d\omega \tag{2.24}$$

$$\rho_{u_k s_{lj}} = \frac{1}{\sigma_{u_k} \sigma_{s_{lj}}} \int_{-\infty}^{\infty} H_j(-\mathrm{i}\omega)\, G_{u_k \ddot{u}_l}(\mathrm{i}\omega)\, d\omega \tag{2.25}$$

$$\rho_{s_{ki} s_{lj}} = \frac{1}{\sigma_{s_{ki}} \sigma_{s_{lj}}} \int_{-\infty}^{\infty} H_i(\mathrm{i}\omega)\, H_j(-\mathrm{i}\omega)\, G_{\ddot{u}_k \ddot{u}_l}(\mathrm{i}\omega)\, d\omega \tag{2.26}$$

in which $H_i(\mathrm{i}\omega) = \left[\omega_i^2 - \omega^2 + 2\mathrm{i}\zeta_i \omega_i \omega\right]^{-1}$ represents the frequency response function of mode i, and σ_{u_k} and $\sigma_{s_{ki}}$ are the root-mean-squares of the ground displacement $u_k(t)$ and the normalized modal response $s_{ki}(t)$, respectively, where $\mathrm{i} = \sqrt{-1}$ denotes the imaginary unit. These are given by the integrals

$$\sigma_{u_k}^2 = \int_{-\infty}^{\infty} G_{u_k u_k}(\omega)\, d\omega \tag{2.27}$$

$$\sigma_{s_{ki}}^2 = \int_{-\infty}^{\infty} \left|H_i(\mathrm{i}\omega)\right|^2 G_{\ddot{u}_k \ddot{u}_k}(\omega)\, d\omega \tag{2.28}$$

in which $G_{u_k u_k}(\omega)$ and $G_{\ddot{u}_k \ddot{u}_k}(\omega)$ are the power spectral densities of the ground displacement and acceleration processes, respectively. In Eqs. 2.24, 2.25, and 2.26, $G_{\ddot{u}_k \ddot{u}_l}(\mathrm{i}\omega)$, $G_{u_k \ddot{u}_l}(\mathrm{i}\omega)$, $G_{u_k u_l}(\mathrm{i}\omega)$ are cross-power spectral densities defined by

$$G_{\ddot{u}_k \ddot{u}_l}(\mathrm{i}\omega) = \gamma_{kl}(\mathrm{i}\omega) \left[G_{\ddot{u}_k \ddot{u}_k}(\omega)\, G_{\ddot{u}_l \ddot{u}_l}(\omega)\right]^{1/2} \tag{2.29}$$

$$G_{u_k \ddot{u}_l}(\mathrm{i}\omega) = -\omega^{-2}\, \gamma_{kl}(\mathrm{i}\omega) \left[G_{\ddot{u}_k \ddot{u}_k}(\omega)\, G_{\ddot{u}_l \ddot{u}_l}(\omega)\right]^{1/2} \tag{2.30}$$

$$G_{u_k u_l}(\mathrm{i}\omega) = -\omega^{-4}\,\gamma_{kl}(\mathrm{i}\omega)\left[G_{\ddot{u}_k\ddot{u}_k}(\omega)\,G_{\ddot{u}_l\ddot{u}_l}(\omega)\right]^{1/2} \tag{2.31}$$

in which $\gamma_{kl}(\mathrm{i}\omega)$ is the coherency function that characterized the spatial variability of the ground motion.

For the purpose of the application in this study, the following model of the coherency function is employed

$$\gamma_{kl}(\mathrm{i}\omega) = \exp\left[-\left(\frac{\alpha\,\omega\,d_{kl}}{v_s}\right)^2\right]\exp\left(\mathrm{i}\frac{\omega\,d_{kl}^{\mathrm{L}}}{v_{app}}\right) \tag{2.32}$$

In this model, α is an incoherence parameter, d_{kl} denotes the horizontal distance between stations k and l, d_{kl}^{L} denotes the projected horizontal distance in the longitudinal direction of wave propagation, v_s is the shear wave velocity of the medium, and v_{app} is the surface apparent wave velocity. It can be shown that the first term on the right hand side accounts for the effect of incoherency, whereas the second term accounts for the effect of wave passage.

The cross-correlation coefficients in Eqs. 2.24 - 2.26 can be interpreted in terms of a pair of oscillators, representing modes i and j of the structure, which are respectively subjected to the support motions $u_k(t)$ and $u_l(t)$, as shown in Fig. 2.1. Specifically, $\rho_{u_k u_l}$ denotes the cross-correlation coefficient between the two support displacements, $\rho_{u_k s_{lj}}$ denotes the cross-correlation coefficient between the displacement at support k and the response of the oscillator at support l, and $\rho_{s_{ki} s_{lj}}$ denotes the cross-correlation coefficient between the responses of the two oscillators, all taken at the same time instant. These coefficients incorporate the effects of cross-modal and cross-support correlations that arise in the response of the structure to the spatially varying ground motion.

Most seismic design codes specify the earthquake motion in terms of the response spectrum and not the power spectral density. Therefore, it is desirable to develop a method that is based on the response spectrum specification of the input motion. To compute the power spectral density consistent with a given mean response spectrum $D(\omega,\zeta)$, the following approximation is used in this study

$$G_{\ddot{u}\ddot{u}}(\omega) = \frac{\omega^{p+2}}{\omega^p + \omega_f^p}\left(\frac{2\zeta\,\omega}{\pi} + \frac{4}{\pi\tau}\right)\left[\frac{D(\omega,\zeta)}{p_s(\omega)}\right]^2 \qquad \omega \geq 0 \tag{2.33}$$

In this expression, the term $\omega^{p+2} / \left(\omega^p + \omega_f^p\right)$ is a correction factor for low frequencies in which ω_f and p are parameters, τ is the strong-motion duration of the excitation, and $p_s(\omega)$ is the peak factor for the oscillator response (Der Kiureghian, 1980). In this study, the following values are used: $p = 3$, $\omega_f = 0.705$ rad / sec, $\tau = 20$ seconds, and $\zeta = 0.05$.

The data flow diagram for MSRS analysis is shown in Fig. 2.2. This method employs information that is commonly available in seismic design applications. It is important to note that the same set of cross-correlation coefficients are applicable to all response quantities of interest.

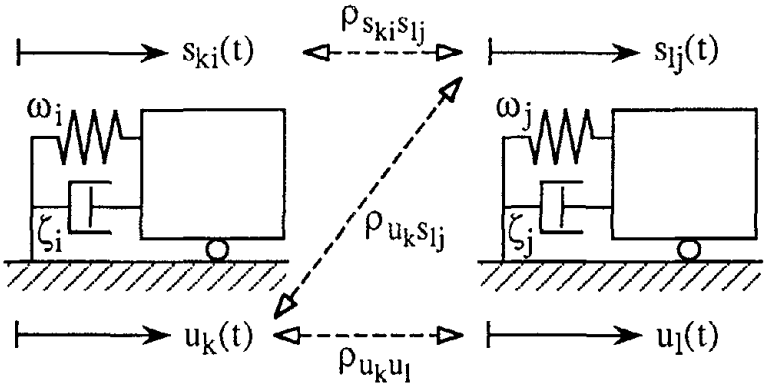

Fig. 2.1 Pair of Oscillators and Cross-Correlation Coefficients

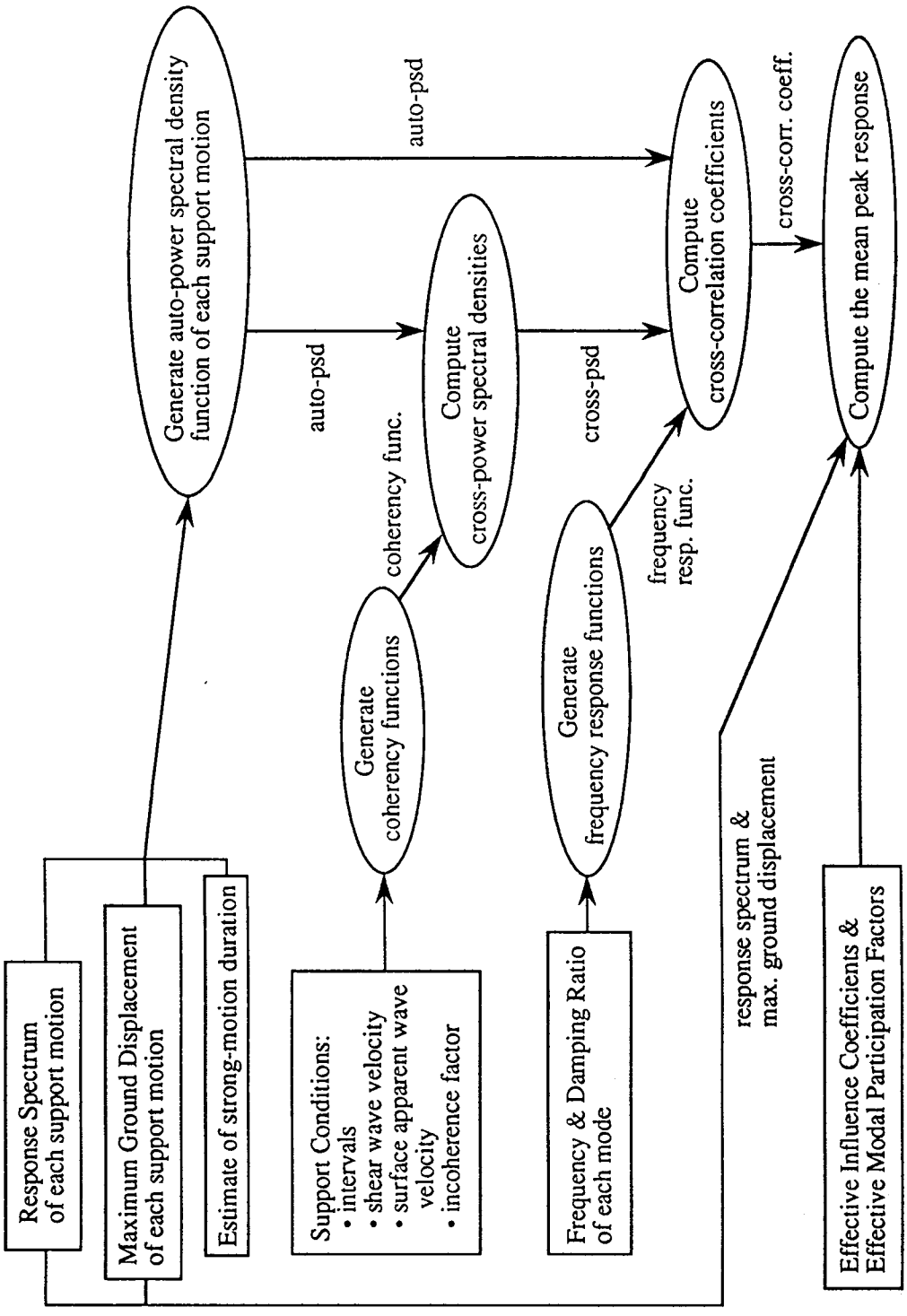

Fig. 2.2 Data Flow Diagram for Multiple-Support Response Spectrum Analysis

CHAPTER 3
DESCRIPTION OF THE GOLDEN GATE BRIDGE

3.1 Introduction

The object of this study is to demonstrate the validity and practicality of the multiple-support response spectrum (MSRS) method for application to bridge structures. The Golden Gate Bridge is selected for this study since a dynamic model and extensive time-history analysis are available for this bridge from another study (Liu and Imbsen, 1990). This chapter presents a brief description of the Bridge, the structural model and the support excitations.

3.2 Description of the Bridge

The dimensions of the Golden Gate Bridge are shown in Fig. 3.1. The main span is 1281m (4200ft) long and the two side spans (from the main towers to the pylon supports) are each 343m (1125ft) long. The roadway and the floor system are a closed box consisting of two stiffening trusses and the top and bottom lateral bracing systems. The top and bottom lateral bracings are, respectively, in the planes of the top and bottom chords of the stiffening trusses. The deck superstructure is suspended from two main cables, 92.4cm (36.4in) in diameter, which are spaced 27.5m (90ft) apart.

(i) Main Cables and Anchorage

Main cables, each consisting of 61 strands, are supported on the top of the tower shafts and anchored by gravity-type mass concrete anchorages at the ends. At the shore ends of the side spans, the cables are tied down to the concrete pylons so that they are maintained at the proper elevations. At the anchorages, each strand is held by a cast steel strand shoe pinned between a pair of heat treated eye-bars.

(ii) Main Towers and Piers

The steel towers are each made up of two shafts that are connected by four horizontal portal struts at upper levels and X-diagonal bracings below the roadway. The towers are 210.5m (690ft) high from the piers to the bases of cable castings, and rise 227m (746ft) above the mean water level to the intersection of the main and the side span cable tangents. The tower shafts are built up of plates and angles arranged in cellular form. The main towers are built on massive concrete piers which are founded on the rock formation below. The tower shafts are anchored to the concrete pier through pairs of steel angles.

(iii) Pylons

The Pylons, located at the shore-ends of the side spans, are of concrete frame and panel construction. Pylons contain anchorage steelwork that restrains the main cable vertically at equal distances from the main towers. Pylons also provide vertical support and transverse restraint to the stiffening trusses.

(iv) The Suspended Structure

The suspended structure consists of two parallel trusses, 7.6m (25ft) deep, spaced 27.5m (90ft) apart. The two trusses and the top and bottom lateral bracing systems form a closed box configuration. The new orthotropic steel deck is carried on the floor beams which occur at every truss panel point, 7.6m (25ft) apart, and is framed into the vertical members of the stiffening trusses. The entire stiffening system is suspended every 15.3m (50ft) by double suspenders of wire rope.

The main span truss is connected to the tower at each end through a hinge and sliding joint located on the bridge centerline. This allows free longitudinal movement at the centerline of up to 1m (39in) [43cm toward shore and 57cm toward channel]. Also, rotation about the vertical and horizontal axes are unrestrained. At the curbs the total longitudinal movement allowed is 1.44m (56.6in). Only transverse shear force is transferred to the tower.

The side span trusses are pinned to the tower allowing only rotational movements. All longitudinal forces applied to the side span are delivered directly to the tower.

At the pylons the ends of the side spans are free to slide longitudinally, restrained transversely, and free to rotate in both vertical and horizontal planes.

3.3 Description of the Structure Model

An original 3-dimensional model of the main bridge was developed by T.Y. Lin, International (TYLI). This model was used as a basis with substantial modifications made by Imbsen & Associates, Inc. for use in the earthquake response analysis. The original TYLI model included a total of 9,933 frame elements connecting 4,775 nodes. This was substantially reduced by using a superelement formulation for the stiffening trusses while maintaining the same level of refinement in the behavior modeling. The final model has 2017 elements connecting 806 active nodes with a total 4,074 active degrees of freedom making it more tractable for earthquake response analysis. The detailed development of the structure model is given by Liu and Imbsen (1990).

Computed periods and damping ratios of the first 100 modes of the Bridge model are shown in Table 3.1, and in Figs. 3.2 and 3.3. Ambient vibration measurements were conducted by Abdel-Ghaffar and Scalan (1985). The computed periods show good

agreement with the measured values. The first mode is the transverse vibration of the main span deck with a natural period of 20.56 sec. The modes with significant contributions to the response of the towers are the 62nd (1.86sec), 63rd (1.84sec), 81st (1.41sec), 83rd (1.37sec), 91st (1.30sec), and 95th (1.29sec) modes (Liu and Imbsen, 1990).

3.4 Description of Support Excitations

The Bridge is located in the close vicinity of two significant fault systems. The San Andreas fault is about 7 miles west of the Bridge and the Hayward fault is about 10 miles east of the Bridge. Both are capable of generating large magnitude earthquakes.

The Golden Gate Bridge has 6 support locations; north anchor, north pylon, Marin tower, S.F. tower, south pylon, and south anchor. The bridge model has two support points (east side and west side) at each support location. During an earthquake the Bridge is subjected to a three-component ground motion at each support location (identical for east and west sides), i.e., longitudinal, transverse, and vertical ground motions. In all there are 18 ground motion components, which are given numbers shown in Fig. 3.1.

To carry out time history analysis of the bridge response, Liu and Imbsen (1990) used a set of artificial time histories which were generated to be compatible with the target response spectrum while properly accounting for the wave passage and incoherence effects. The target response spectrum corresponds to the "maximum credible" earthquake occurring on the San Andreas fault for the site. Peak ground acceleration is 0.65g and peak ground displacement is 100cm (40in) at the maximum credible earthquake level. Maximum ground accelerations and displacements of the generated time histories are listed in Table 3.2.

Displacement response spectra for each support motion computed from the generated time histories are shown in Figs. 3.4 - 3.7, and they are used in the application of the MSRS method to the Golden Gate Bridge. Seismic waves are assumed to propagate in the direction of south to north. To estimate the value of the surface apparent wave velocity v_{app}, longitudinal displacement time histories for six support locations (Fig. 3.8) are used. Although the coherency function is defined for the ground accelerations, they include too many high frequency peaks to estimate v_{app}. Computed time lags between the deepest troughs in the displacement time histories indicate a value of v_{app} in the range of 2000 to 3000 m/s. This, however, is a very crude estimate. Therefore, a parametric study will be performed to examine the influence of this parameter.

In this study, we assume that the longitudinal, transverse and vertical components of the ground motion at each support point are mutually statistically independent.

Table 3.1 Computed Periods and Damping Ratios of the Golden Gate Bridge

Mode	T (sec)	f (Hz)	ζ	Mode	T (sec)	f (Hz)	ζ
1	20.563	0.0486	0.0200	51	2.183	0.4580	0.0367
2	12.639	0.0791	0.0161	52	2.166	0.4617	0.0370
3	12.619	0.0792	0.0160	53	2.164	0.4621	0.0370
4	11.763	0.0850	0.0158	54	2.064	0.4845	0.0386
5	8.942	0.1118	0.0156	55	2.027	0.4933	0.0393
6	8.338	0.1199	0.0158	56	2.010	0.4974	0.0396
7	7.843	0.1275	0.0160	57	2.005	0.4987	0.0397
8	7.800	0.1282	0.0160	58	1.997	0.5007	0.0398
9	6.477	0.1544	0.0169	59	1.973	0.5068	0.0403
10	6.350	0.1575	0.0171	60	1.889	0.5294	0.0419
11	6.147	0.1627	0.0173	61	1.884	0.5307	0.0420
12	5.927	0.1687	0.0176	62	1.858	0.5382	0.0426
13	5.178	0.1931	0.0189	63	1.838	0.5441	0.0430
14	5.150	0.1942	0.0189	64	1.789	0.5589	0.0441
15	5.116	0.1955	0.0190	65	1.767	0.5661	0.0446
16	5.073	0.1971	0.0191	66	1.704	0.5867	0.0462
17	4.939	0.2025	0.0194	67	1.693	0.5907	0.0465
18	4.846	0.2064	0.0196	68	1.662	0.6015	0.0473
19	4.832	0.2070	0.0196	69	1.654	0.6048	0.0475
20	4.691	0.2132	0.0200	70	1.644	0.6083	0.0478
21	4.571	0.2188	0.0203	71	1.644	0.6084	0.0478
22	4.470	0.2237	0.0206	72	1.606	0.6227	0.0488
23	4.329	0.2310	0.0211	73	1.586	0.6305	0.0494
24	4.020	0.2488	0.0222	74	1.569	0.6375	0.0499
25	3.880	0.2577	0.0228	75	1.540	0.6494	0.0508
26	3.755	0.2663	0.0233	76	1.516	0.6595	0.0516
27	3.729	0.2682	0.0234	77	1.487	0.6725	0.0526
28	3.714	0.2692	0.0235	78	1.477	0.6769	0.0529
29	3.641	0.2746	0.0239	79	1.462	0.6841	0.0534
30	3.514	0.2845	0.0245	80	1.413	0.7075	0.0552
31	3.262	0.3065	0.0260	81	1.413	0.7077	0.0552
32	3.233	0.3093	0.0262	82	1.371	0.7293	0.0568
33	3.233	0.3093	0.0262	83	1.365	0.7326	0.0571
34	3.151	0.3174	0.0267	84	1.361	0.7349	0.0572
35	3.131	0.3194	0.0269	85	1.357	0.7372	0.0574
36	2.936	0.3406	0.0283	86	1.347	0.7424	0.0578
37	2.935	0.3407	0.0284	87	1.343	0.7445	0.0579
38	2.902	0.3446	0.0286	88	1.328	0.7532	0.0586
39	2.816	0.3551	0.0294	89	1.327	0.7536	0.0586
40	2.747	0.3640	0.0300	90	1.327	0.7537	0.0586
41	2.617	0.3821	0.0313	91	1.300	0.7692	0.0598
42	2.593	0.3856	0.0315	92	1.296	0.7714	0.0600
43	2.507	0.3989	0.0325	93	1.293	0.7733	0.0601
44	2.389	0.4186	0.0339	94	1.290	0.7755	0.0603
45	2.386	0.4190	0.0339	95	1.286	0.7774	0.0604
46	2.360	0.4238	0.0342	96	1.272	0.7862	0.0611
47	2.303	0.4343	0.0350	97	1.271	0.7868	0.0611
48	2.301	0.4346	0.0350	98	1.234	0.8104	0.0629
49	2.250	0.4444	0.0357	99	1.230	0.8128	0.0631
50	2.192	0.4563	0.0366	100	1.225	0.8166	0.0634

Table 3.2 Ground Motion Parameters

	Maximum Ground Acceleration (g)			Maximum Ground Displacement (cm)		
Support	Long.	Trans.	Vert.	Long.	Trans.	Vert.
North Anchor	0.54	0.69	0.56	32.77	43.69	27.43
North Pylon	0.60	0.50	0.56	32.77	44.96	29.21
Marin Tower	0.73	0.65	0.60	34.29	47.75	23.37
S.F. Tower	0.70	0.60	0.74	37.34	45.97	20.57
South Pylon	0.58	0.60	0.83	38.35	44.45	28.96
South Anchor	0.68	0.58	0.76	37.85	44.20	25.65

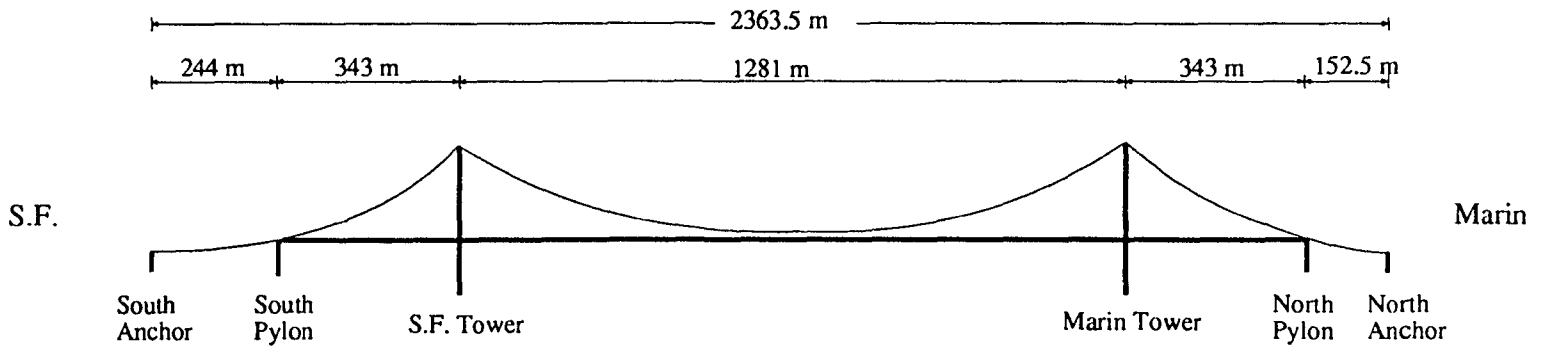

	South Anchor	South Pylon	S.F. Tower	Marin Tower	North Pylon	North Anchor
Longitudinal	6	5	4	3	2	1
Transverse	12	11	10	9	8	7
Vertical	18	17	16	15	14	13

Fig. 3.1 Dimensions of the Golden Gate Bridge and Numbering of 18 Support Motions

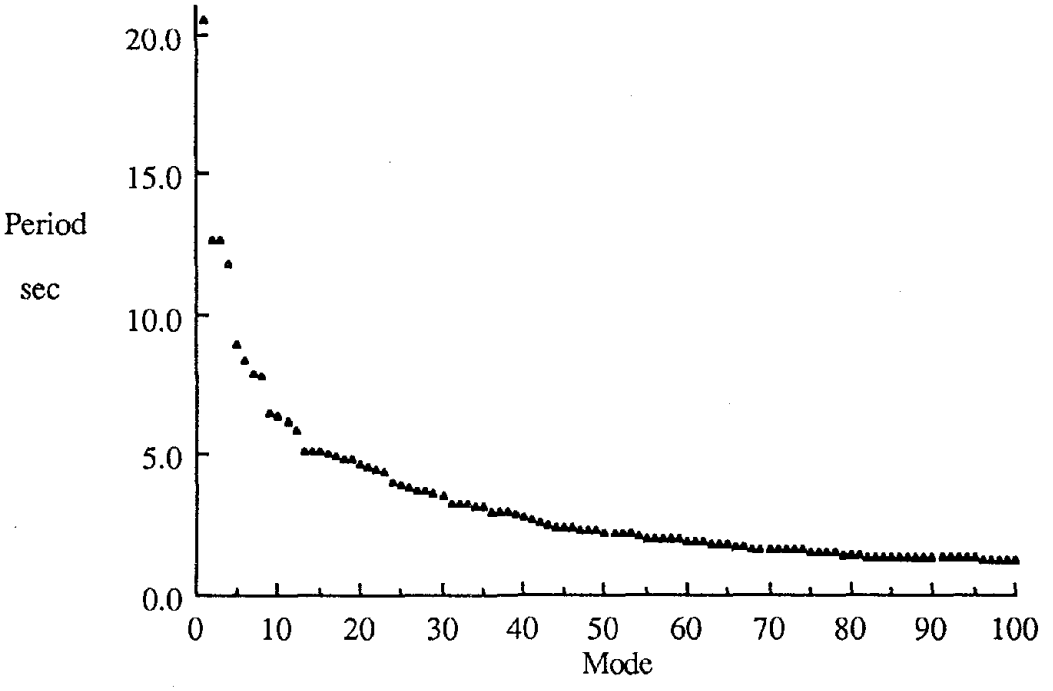

Fig. 3.2 Computed Periods of the Golden Gate Bridge

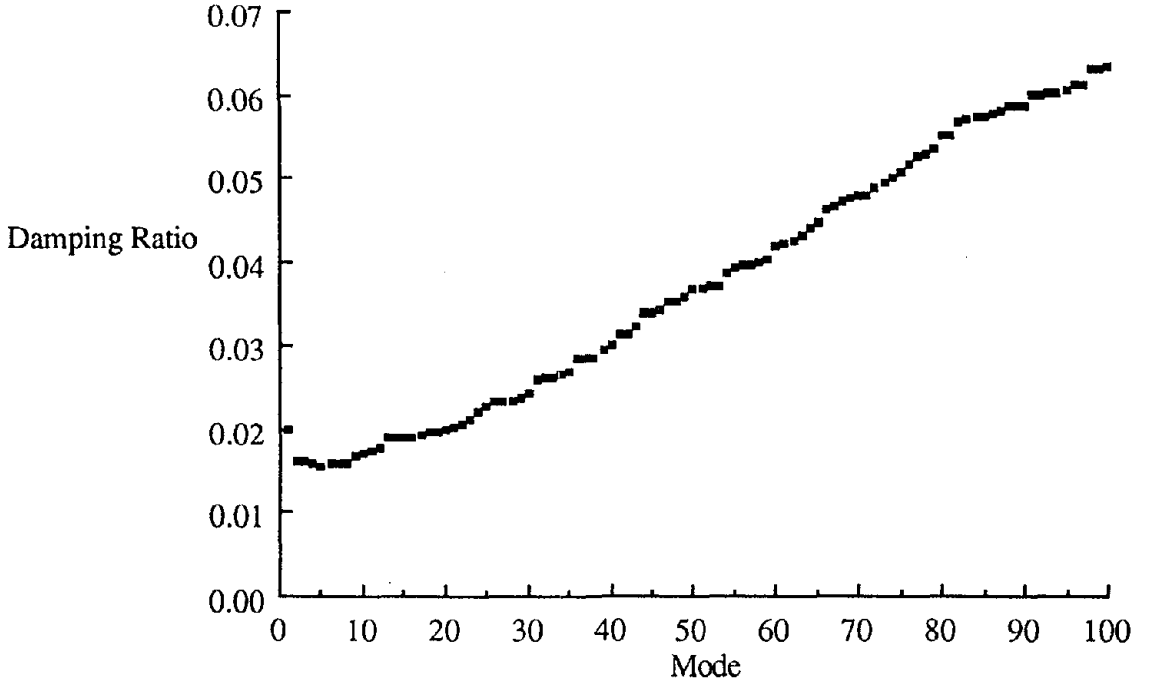

Fig. 3.3 Assumed Modal Damping Ratios of the Golden Gate Bridge

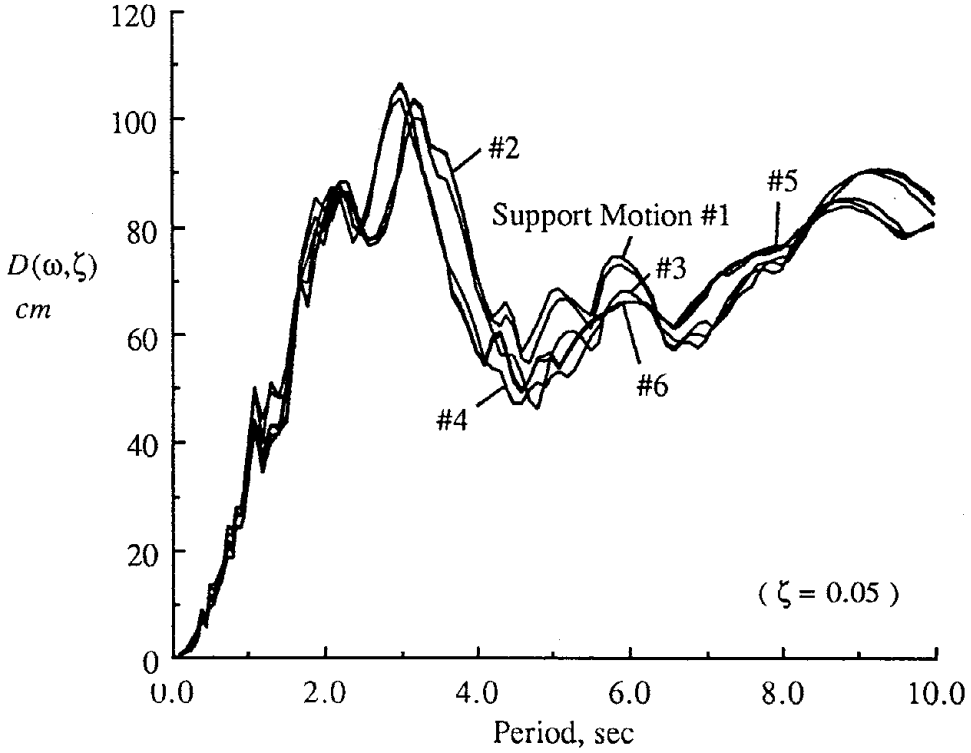

Fig. 3.4 Displacement Response Spectra for Longitudinal Components of Six Support Ground Motions

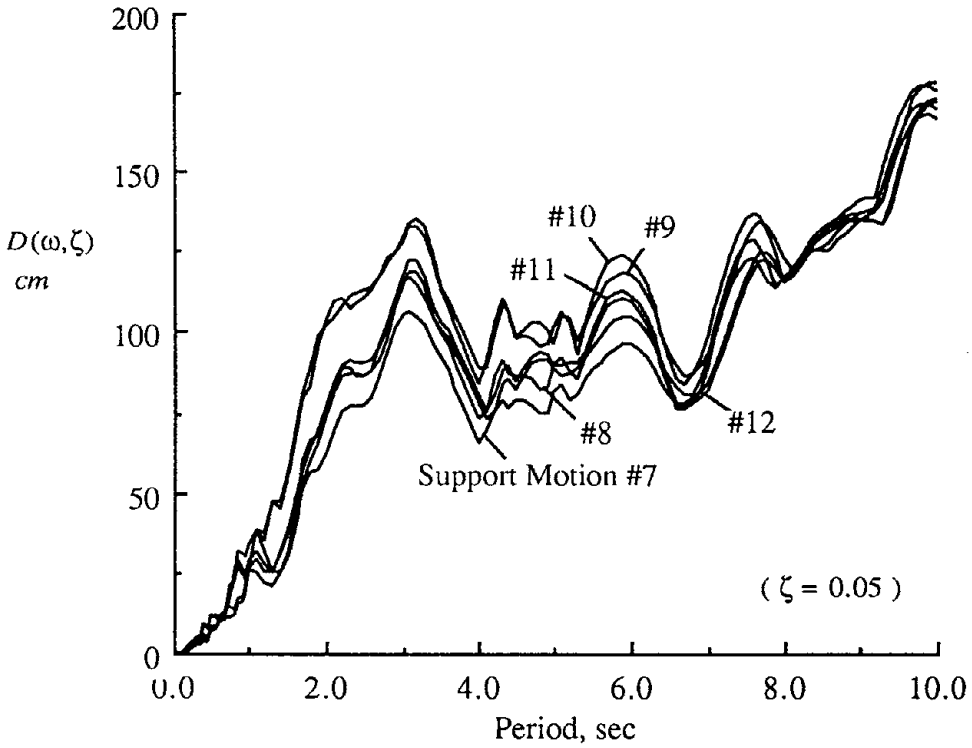

Fig. 3.5 Displacement Response Spectra for Transverse Components of Six Support Ground Motions

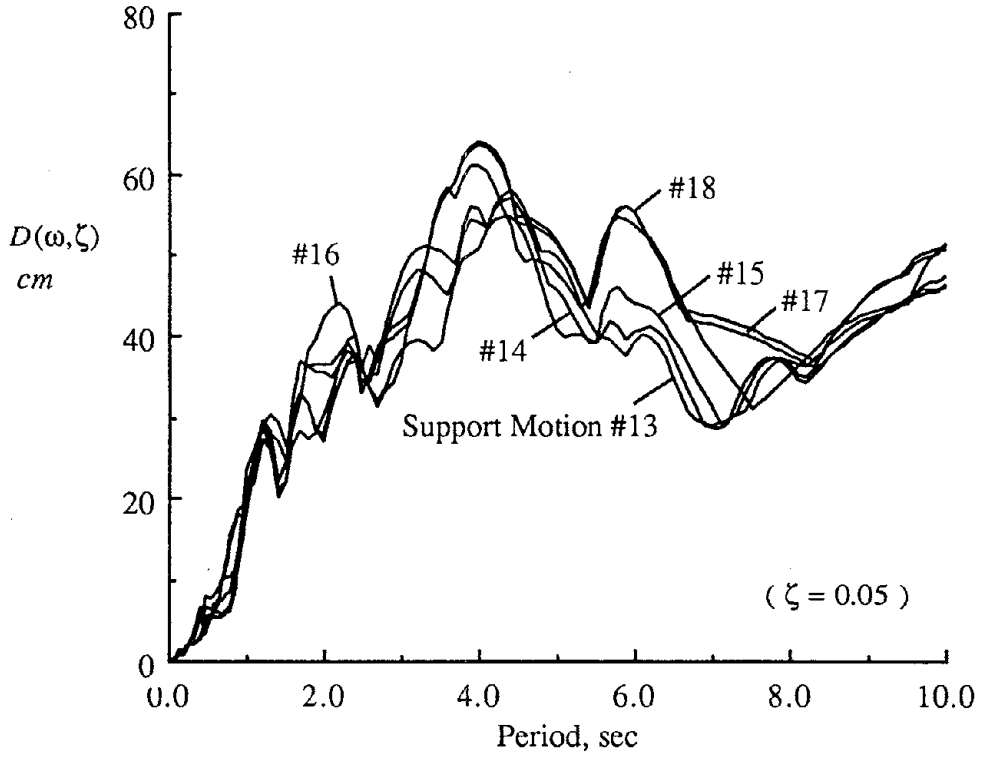

Fig. 3.6 Displacement Response Spectra for Vertical Components of Six Support Ground Motions

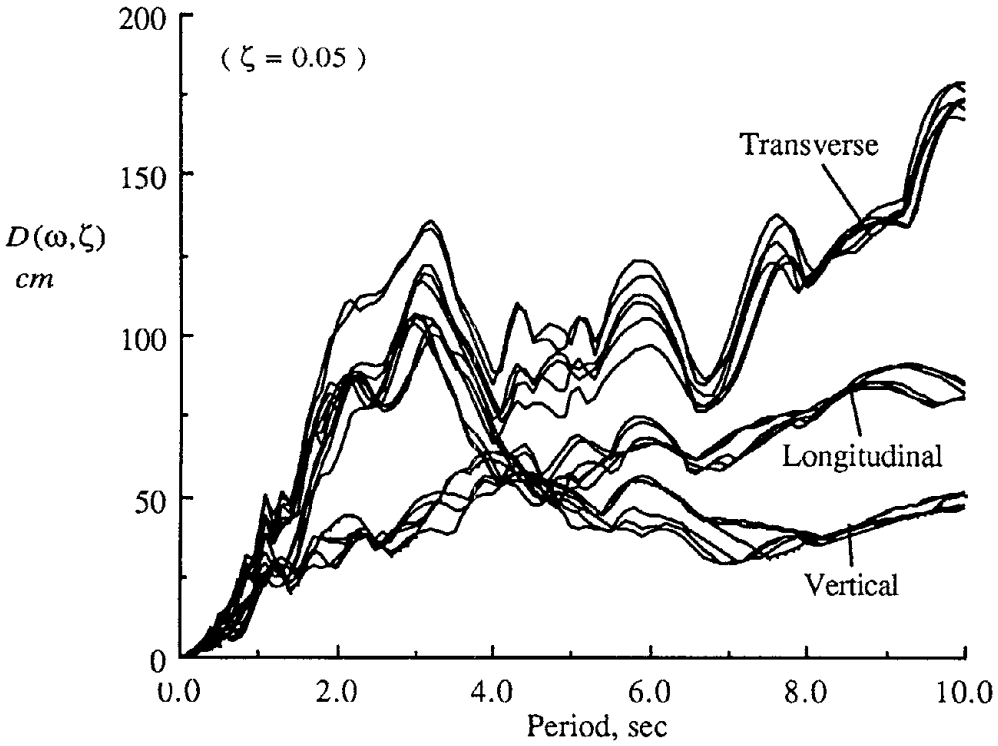

Fig. 3.7 Displacement Response Spectra for All Components of Six Support Ground Motions

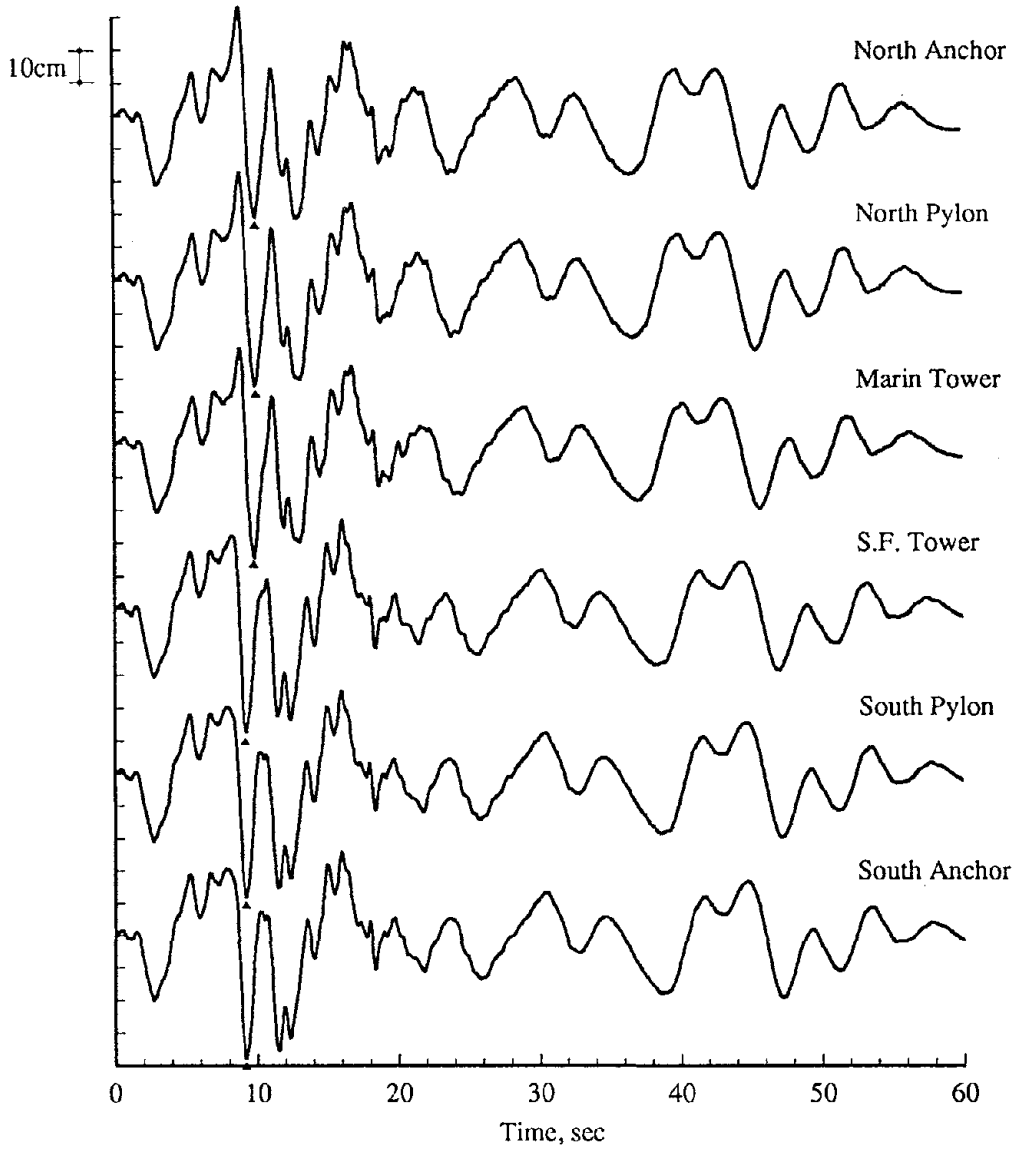

Fig. 3.8 Generated Longitudinal Displacement Time Histories for Six Support Locations

CHAPTER 4
CROSS-CORRELATION COEFFICIENTS OF THE GOLDEN GATE BRIDGE

4.1 Introduction

In this chapter we investigate the significance of the cross-correlation coefficients $\rho_{u_k u_l}$, $\rho_{u_k u_l}$ and $\rho_{s_{ki} s_{lj}}$ for the Golden Gate Bridge defined by Eqs. 2.24 - 2.26. To compute the cross-correlation coefficients, Eq. 2.33 is used to generate the power spectral densities consistent with the displacement response spectra at each support point, as shown in Figs. 3.4 - 3.7. For the coherency function, the model in Eq. 2.32 is assumed with α, v_s and v_{app} representing average values for the entire region. We consider ranges of values of the quantities α / v_s and v_{app} for a parametric study. The parameter α / v_s is varied between 0 and 1/1500 (sec/m), and v_{app} is varied between 1000 and 3000 (m/sec). These ranges are believed to be representative for the Golden Gate Bridge area and for the simulated time histories. As a matter of curiosity, the effect of reversing the wave direction, i.e., waves propagating from Marin to San Francisco instead of the San Francisco to Marin direction, on the three cross-correlation coefficients is investigated. This direction might be representative of waves emanating from an earthquake on the north segment of the San Andreas fault.

In the following sections, we investigate each of the three cross-correlation coefficients required in the combination rule of Eq. 2.23.

4.2 Cross-Correlation Coefficient Between Ground Displacements at Station *k* and *l*

Fig. 4.1 shows plots of the cross-correlation coefficient $\rho_{u_k u_l}$ between the longitudinal ground displacement at south anchor, $u_6(t)$, and the longitudinal displacement at other locations along the bridge. Fig. 4.2 shows similar plots for the longitudinal ground displacement at the S.F. tower, $u_4(t)$, and other locations along the bridge. In these figures, the horizontal axes represent the distance from the south anchor to each location along the bridge. Figs. 4.1(a) and 4.2(a) include only the wave passage effect and neglect the incoherence effect, i.e. $\alpha / v_s = 0$, whereas Figs. 4.1(b) and 4.2(b) include the incoherence effect. Results for other stations or ground motion components show similar trends and are not shown here.

These results indicate that both the wave passage effect and the incoherence effect reduce the value of the correlation coefficient $\rho_{u_k u_l}$. As will be shown in subsequent

sections, this is not necessarily the case for the effect of wave passage on cross-correlation coefficients $\rho_{u_k s_{lj}}$ and $\rho_{s_{ki} s_{lj}}$.

The results in Figs. 4.1 and 4.2 are for the wave direction S.F. to Marin. Reversing this direction (i.e., replacing d_{kl}^{L} by $-d_{kl}^{L}$) only changes the sign of the imaginary part of the coherency function (Eq. 2.32) or the cross-power spectral density function $G_{u_k u_l}(i\omega)$ in Eq. 2.24. Since the imaginary part of this function is anti-symmetric, this change does not affect the integral in Eq. 2.24 and $\rho_{u_k u_l}$ remains unchanged with the reversal in the direction of wave passage. This lack of dependence on the direction of wave passage does not apply to $\rho_{u_k s_{lj}}$ and $\rho_{s_{ki} s_{lj}}$, due to the presence of the complex response function $H_i(i\omega)$ in Eqs. 2.25 and 2.26.

In application to the Golden Gate Bridge, the cross-correlation coefficients $\rho_{u_k u_l}$ are large, and one cannot neglect the contributions of the cross terms in the first sum of the combination rule (Eq. 2.23), which represents the pseudo-static component of the response.

4.3 Cross-Correlation Coefficient Between Ground Displacement at Station *k* and Oscillator Response at Station *l*

Figs. 4.3 and 4.4 show plots of the cross-correlation coefficient $\rho_{u_k s_{lj}}$ between the longitudinal ground displacement at south anchor and the oscillator response to the longitudinal motion at the S.F. tower. Fig. 4.5 shows similar results for the longitudinal ground displacement at south pylon and the oscillator response at the S.F. tower. Figs. 4.6 - 4.8 show similar results for the longitudinal ground displacement at the S.F. tower and the oscillator response at the Marin tower. In these figures, the horizontal axes represent the oscillator frequency, and the points in each curve correspond to the first 100 modes of the bridge (Table 3.1). In each figure, part (a) includes only the wave passage effect, and part (b) includes both the wave passage and the incoherence effects. Figs. 4.3, 4.5, 4.6 show the results for the wave direction S.F. to Marin, and Figs. 4.4 and 4.7 show the results for the wave direction Marin to S.F. Fig. 4.8 compares the results for both wave directions. Although the wave direction from Marin to S.F. is not realistic for the simulated time histories, the results here are generated for the purpose of curiosity and for better understanding the influence of wave passage on the bridge response. For the purpose of comparison, the coefficient $\rho_{u_3 s_{4j}}$ for the wave direction S.F. to Marin is also plotted in Fig. 4.8. Compared to $\rho_{u_4 s_{3j}}$, the coefficient $\rho_{u_3 s_{4j}}$ represents the case where the location of the oscillator has been changed from station 3 (the Marin tower) to station 4 (the S.F. tower). It is seen that $\rho_{u_3 s_{4j}}$ for the wave direction S.F. to Marin is almost identical to $\rho_{u_4 s_{3j}}$ for the wave direction Marin to S.F. Hence, plots with the wave

direction Marin to S.F. may also be considered as values of the coefficients $\rho_{u_k s_{lj}}$ with the oscillator position switched (i.e., $\rho_{u_l s_{kj}}$) but with the wave direction S.F. to Marin.

For the first mode of the bridge, which has a long period T = 20.563sec, $\rho_{u_k s_{lj}}$ has a relatively large negative value. For other modes with shorter periods, $\rho_{u_k s_{lj}}$ is relatively small, particularly when the oscillator is placed at the station where waves arrive at a later time. When waves arrive first at the station where the oscillator is placed and then arrive at the station without the oscillator, $\rho_{u_k s_{lj}}$ has relatively large positive values (e.g., compare $\rho_{u_3 s_{4j}}$ and $\rho_{u_4 s_{3j}}$ in Fig. 4.8 for the wave direction S.F. to Marin). The reason for the higher positive correlation is that the time required for the oscillator to respond coincides with the time for the waves to travel to the second station and, hence, the oscillator response is directly related to the motion at the second station at the same time instant.

The incoherence effect always reduces $\rho_{u_k s_{lj}}$, but the wave passage effect does not necessarily reduce $\rho_{u_k s_{lj}}$. Furthermore, for the value of the parameters considered, the wave passage has a more pronounced effect than the incoherence (see Fig. 4.7(a)). Fig. 4.8 clearly indicates that the direction of wave passage has a significant influence on $\rho_{u_k s_{lj}}$.

4.4 Cross-Correlation Coefficient Between Responses of Oscillators at Station *k* and *l*

Figs. 4.9 - 4.18 show typical results for the cross-correlation coefficient $\rho_{s_{ki} s_{lj}}$. Each plot shows the results for a single mode i (either mode 62 with frequency $f_{62} = 0.538$ Hz, or mode 81 with frequency $f_{81} = 0.708$ Hz) verses a variable oscillator frequency ω_j. The selected modes are the ones which have dominant contributions to the responses of the two towers. In each figure, part (a) includes only the wave passage effect, whereas part (b) includes both the wave passage and the incoherence effects. The selected support points (subscripts k and l) are indicated in the caption for each figure. Figs. 4.9 - 4.14 are the results for the wave direction S.F. to Marin, and Figs. 4.15 and 4.16 are the results for the wave direction Marin to S.F. Figs. 4.17 and 4.18 compare the results for both wave directions. It can be shown that switching the wave direction is nearly equal to switching the locations of the two oscillators.

From Figs. 4.9 - 4.18, it is seen that $\rho_{s_{ki} s_{lj}}$ has a positive or negative peak when the frequencies of the two oscillators at stations k and l are close, and decays with increasing distance between the two frequencies. However, the decay of $\rho_{s_{ki} s_{lj}}$ is not necessarily monotonous, and the curves can be oscillatory and take on positive as well as negative values. It is seen that the incoherence effect always reduces the magnitude of $\rho_{s_{ki} s_{lj}}$, but

the wave passage effect does not necessarily reduce the magnitude. One noteworthy point is that $\rho_{s_{ki}s_{lj}}$ can be significantly different from zero even for well spaced modes.

Figs. 4.17 and 4.18 clearly indicate that the direction of wave passage has a significant influence on $\rho_{s_{ki}s_{lj}}$. It is notable that the plots for the two directions intersect when the oscillators at two stations are identical, i.e., when $\omega_i = \omega_j$, and $\zeta_i = \zeta_j$. $\rho_{s_{ki}s_{lj}}$ is independent of the direction of wave passage for identical oscillators at two stations, because the term $H_i(i\omega)\, H_j(i\omega)$ in Eq. 2.26 is then real valued and the imaginary part of $G_{\ddot{u}_k\ddot{u}_l}(i\omega)$ does not contribute to the integral. As indicated earlier, the plots for the Marin to S.F. direction are nearly identical to the plots for the S.F. to Marin direction when the locations of the two oscillators are switched.

4.5 Concluding Remarks

From the results in this chapter, the following main conclusions can be derived for the cross-correlation coefficients of the Golden Gate Bridge.

(1) The cross-correlation coefficient $\rho_{u_k u_l}$ between the ground displacements at stations k and l is large, and its contribution to the pseudo-static component of the response cannot be neglected.

(2) The cross-correlation coefficient $\rho_{u_k s_{lj}}$ between the ground displacement at station k and oscillator response at station l has a relatively small value, except for the first mode.

(3) The cross-correlation coefficient $\rho_{s_{ki}s_{lj}}$ between the responses of two oscillators at stations k and l depends on the separation between the two frequencies. $\rho_{s_{ki}s_{lj}}$ can be significant even for well spaced modes if there is not a strong incoherence effect.

(4) The incoherence effect reduces the magnitudes of all three cross-correlation coefficients $\rho_{u_k u_l}$, $\rho_{u_k s_{lj}}$, and $\rho_{s_{ki}s_{lj}}$. The wave passage effect reduces only $\rho_{u_k u_l}$, and has a significant influence on $\rho_{s_{ki}s_{lj}}$.

(5) The wave direction does not affect $\rho_{u_k u_l}$, but has a significance influence on $\rho_{u_k s_{lj}}$ and $\rho_{s_{ki}s_{lj}}$. However, because of symmetric terms involved in the modal combination rule in Eq. 2.23, the cumulative effect of the wave direction on the response of the bridge may not be significant.

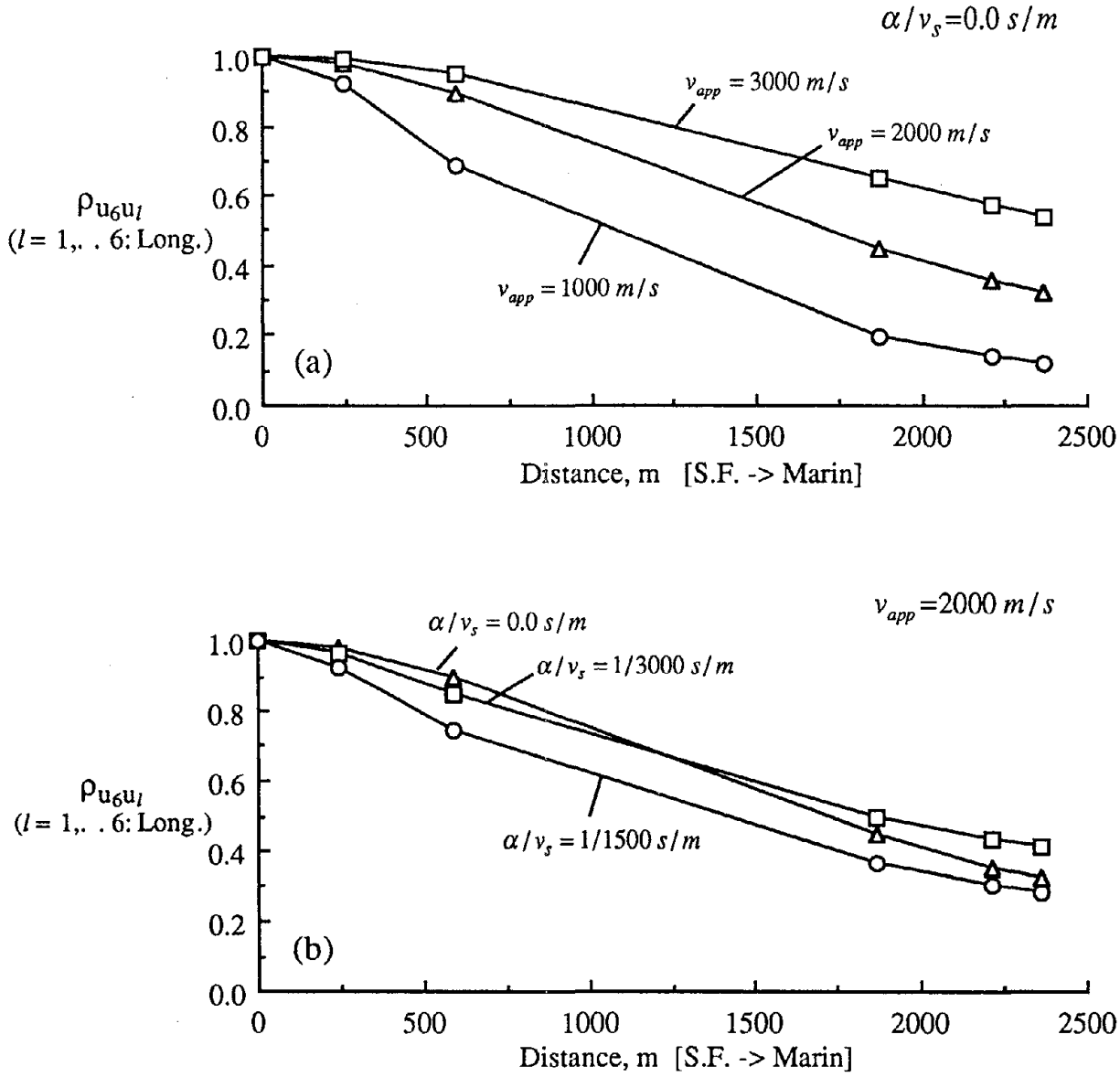

Fig. 4.1 Cross-Correlation Coefficients Between Longitudinal Ground Displacements at the South Anchor and the Other Support Points

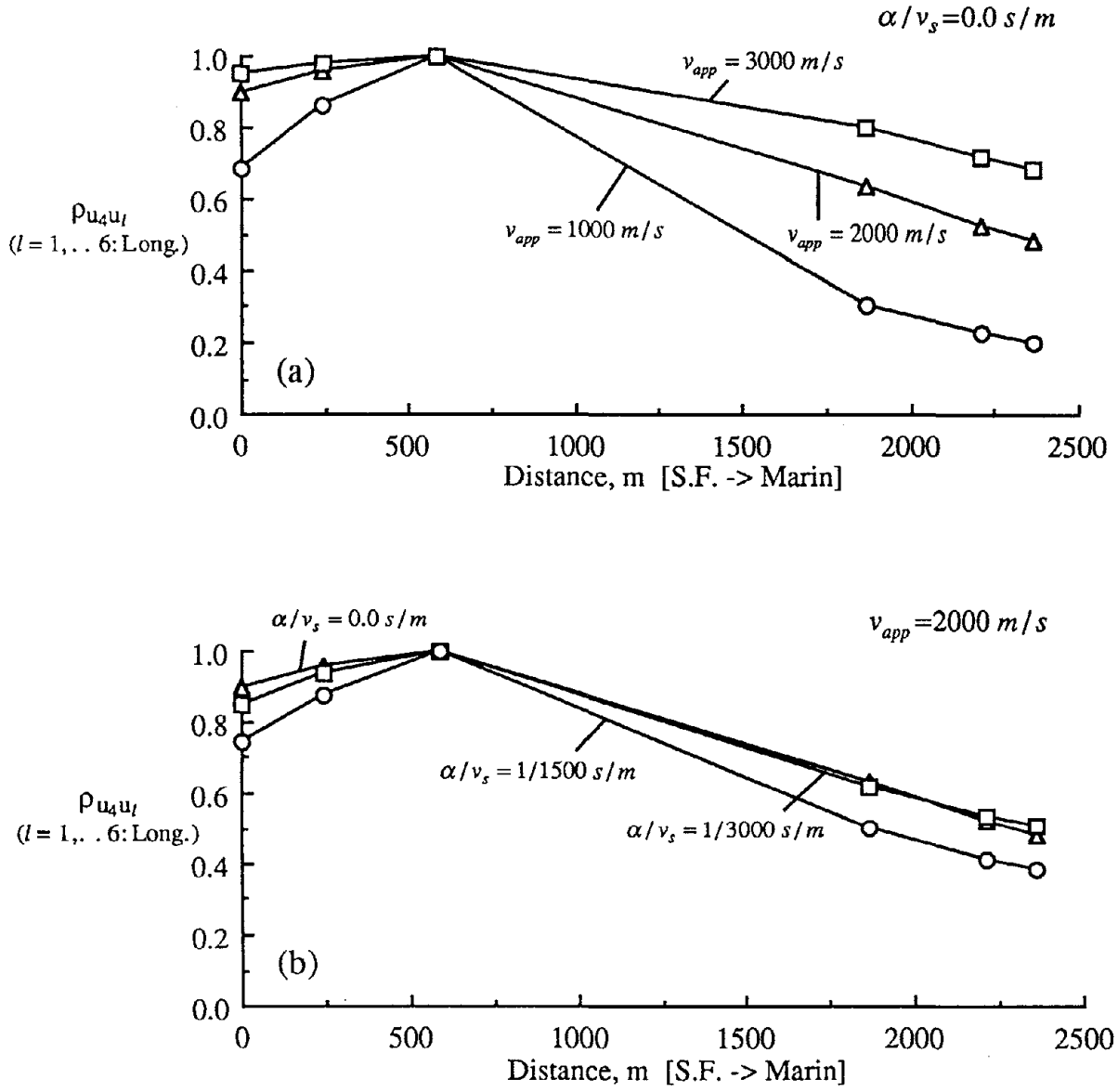

Fig. 4.2 Cross-Correlation Coefficients Between Longitudinal Ground Displacements at the S.F. Tower and the Other Support Points

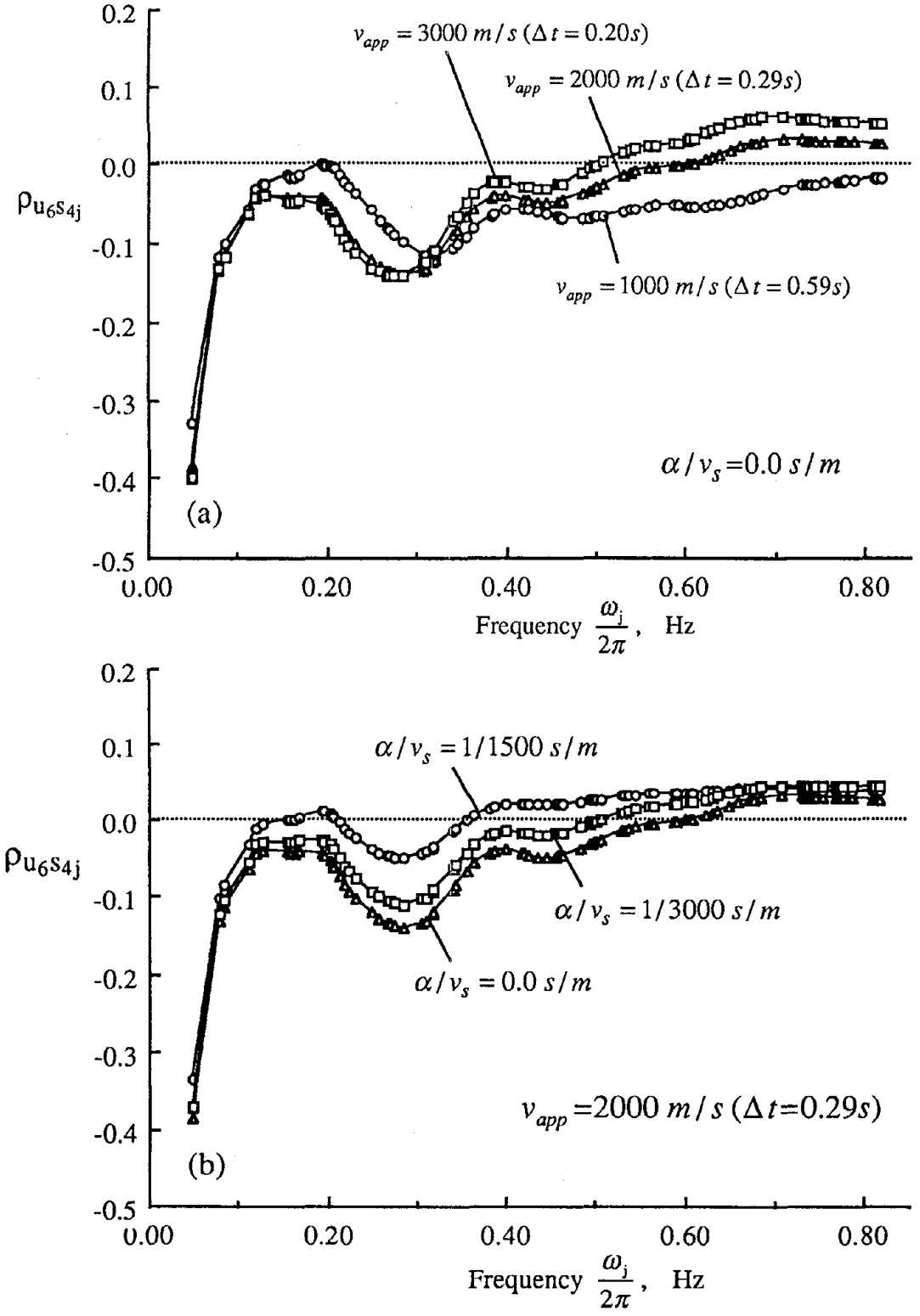

Fig. 4.3 Cross-Correlation Coefficients Between Long. Ground Displ. at the South Anchor and Response of Oscillator at the S.F. Tower for Wave Direction S.F. to Marin

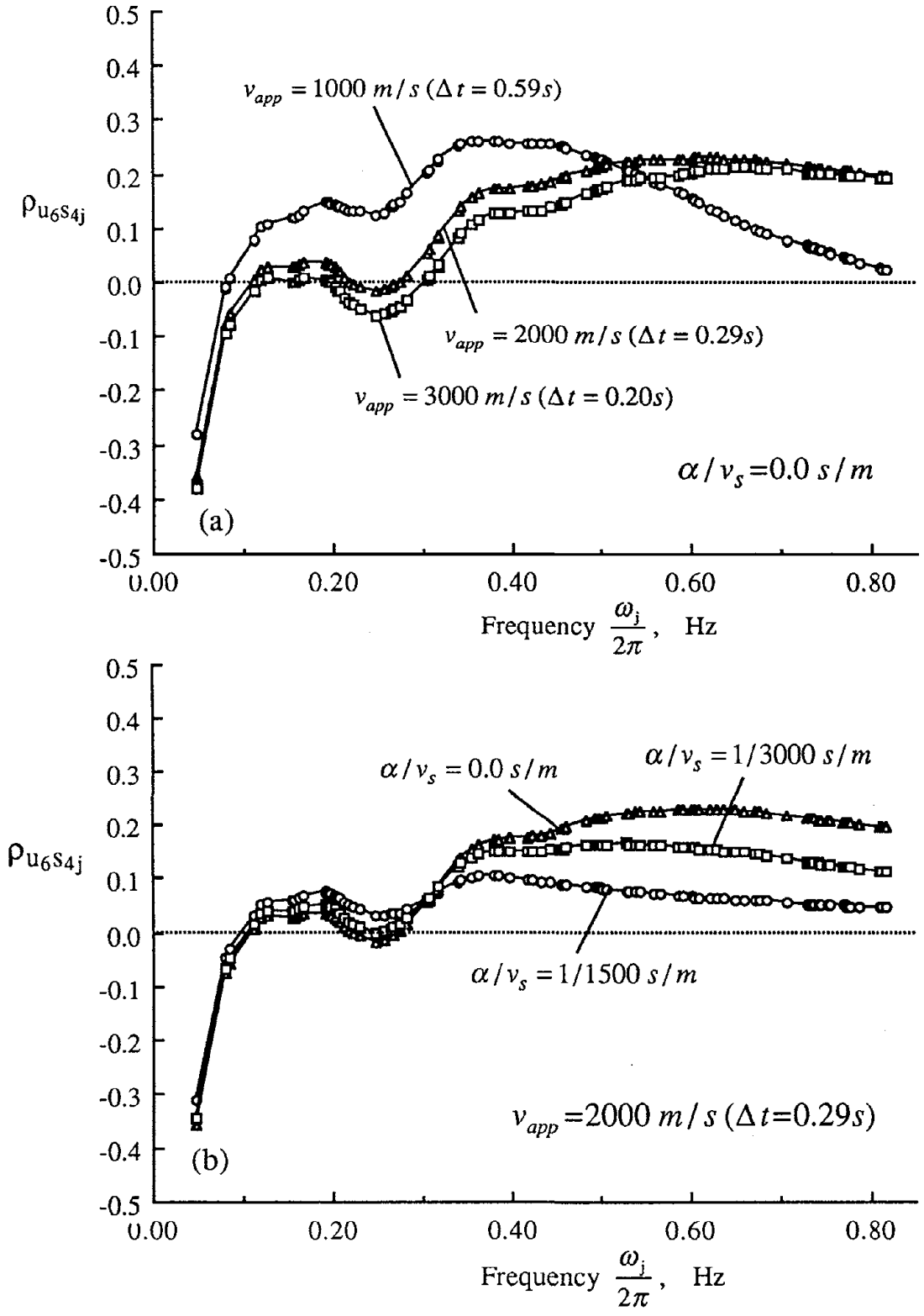

Fig. 4.4 Cross-Correlation Coefficients Between Long. Ground Displ. at the South Anchor and Response of Oscillator at the S.F. Tower for Wave Direction Marin to S.F.

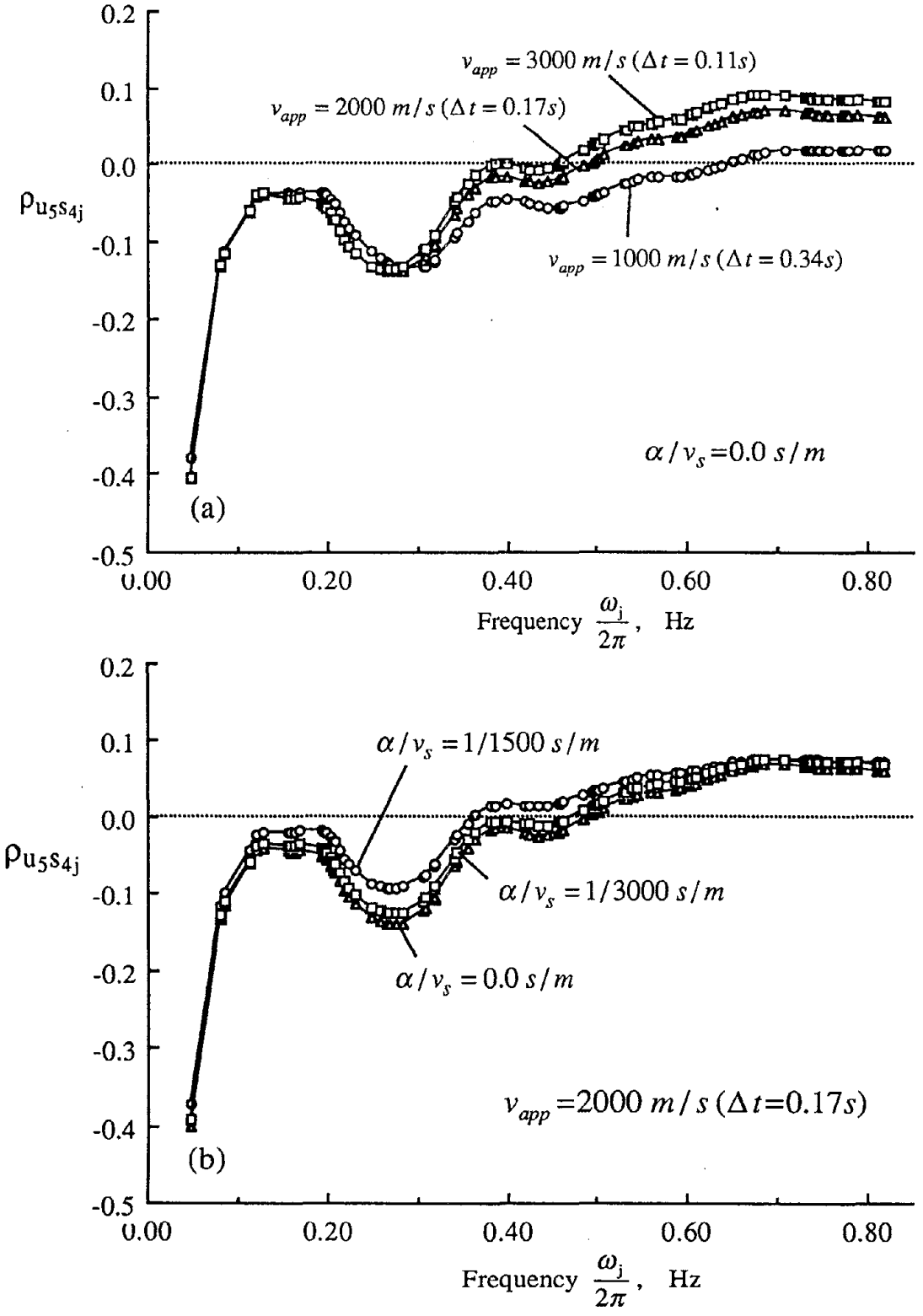

Fig. 4.5 Cross-Correlation Coefficients Between Long. Ground Displ. at the South Pylon and Response of Oscillator at the S.F. Tower for Wave Direction S.F. to Marin

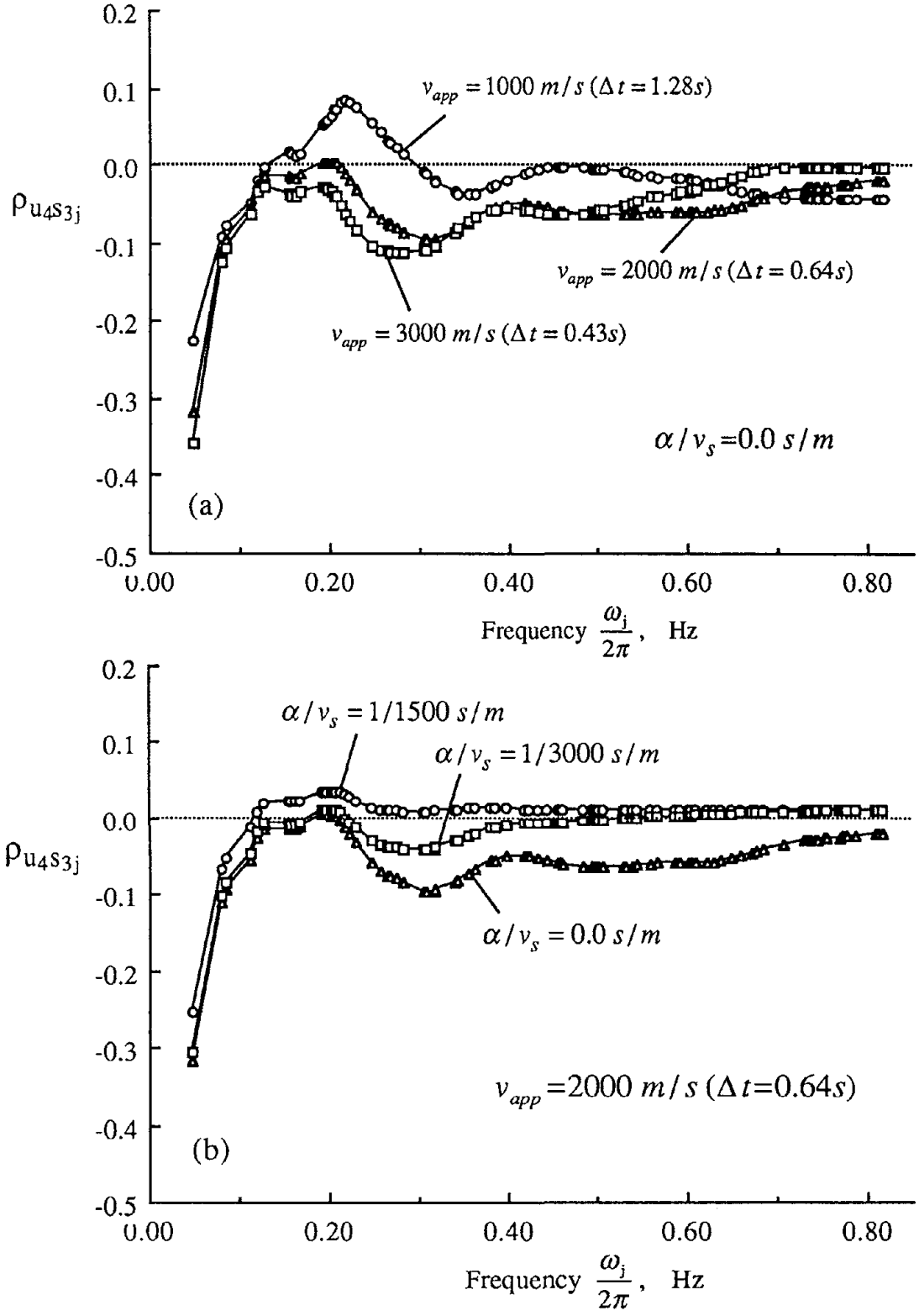

Fig. 4.6 Cross-Correlation Coefficients Between Long. Ground Displ. at the S.F. Tower and Response of Oscillator at the Marin Tower for Wave Direction S.F. to Marin

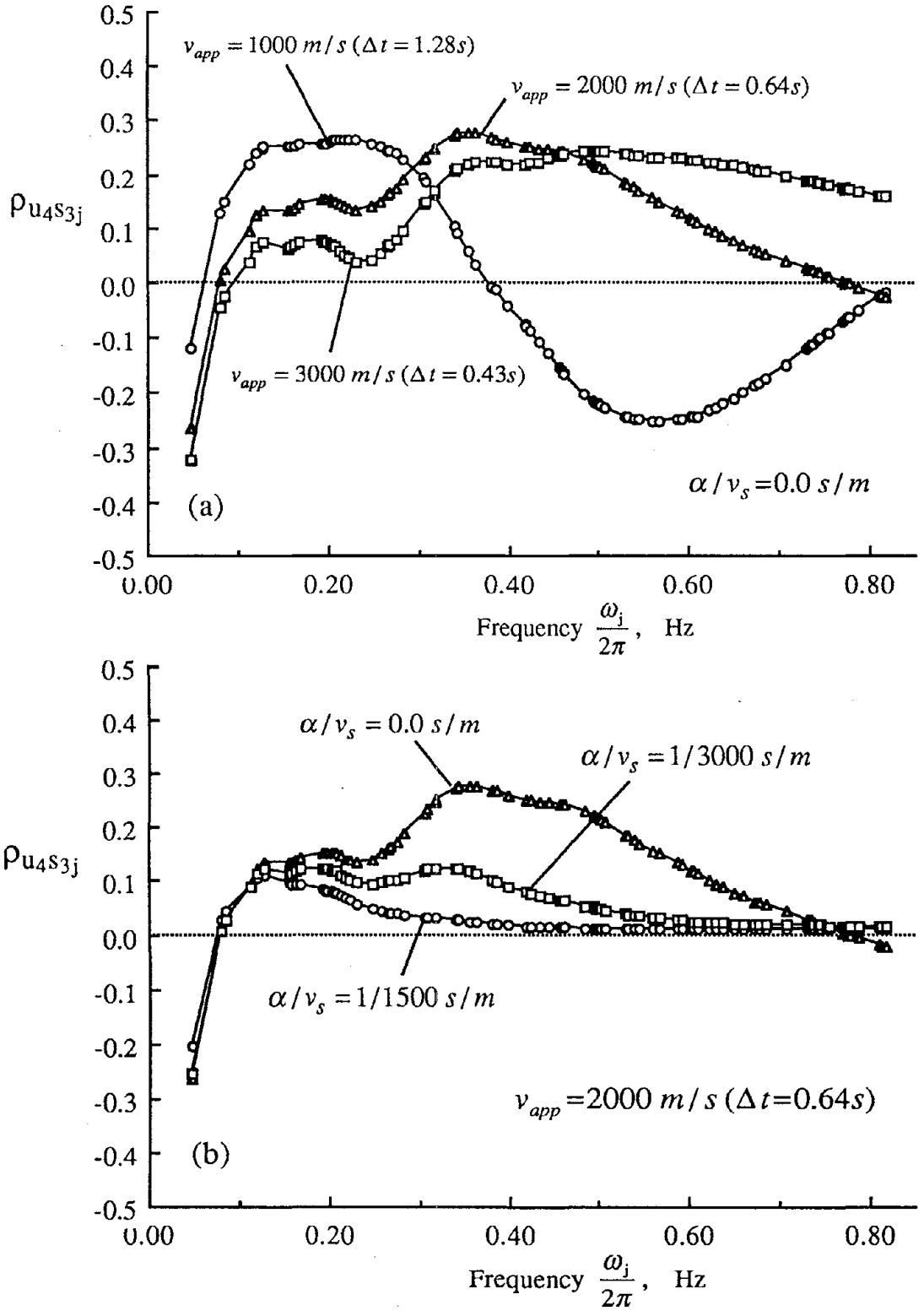

Fig. 4.7 Cross-Correlation Coefficients Between Long. Ground Displ. at the S.F. Tower and Response of Oscillator at the Marin Tower for Wave Direction Marin to S.F.

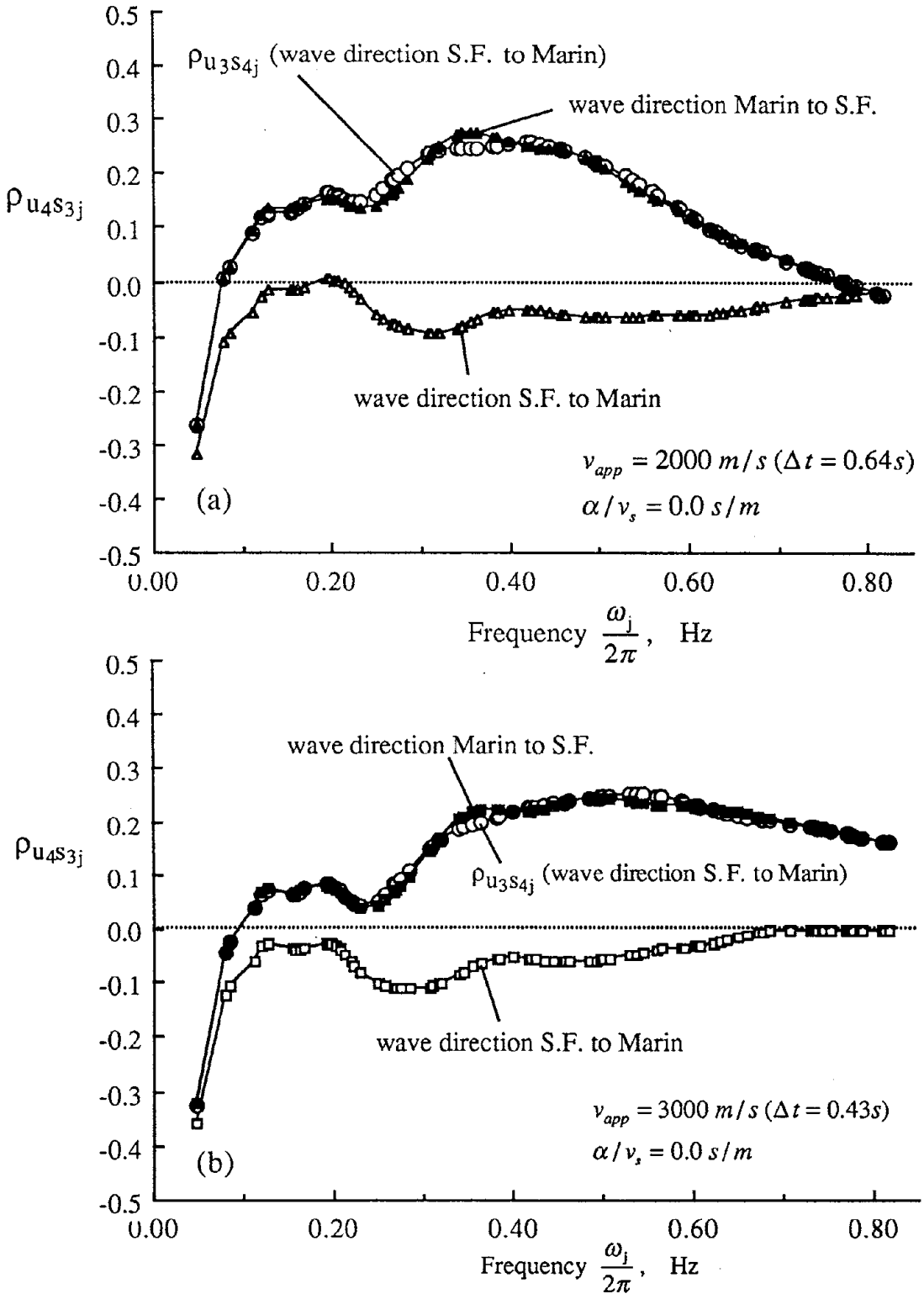

Fig. 4.8 Cross-Correlation Coefficients Between Long. Ground Displ. at the S.F. Tower and Response of Oscillator at the Marin Tower for Two Wave Directions

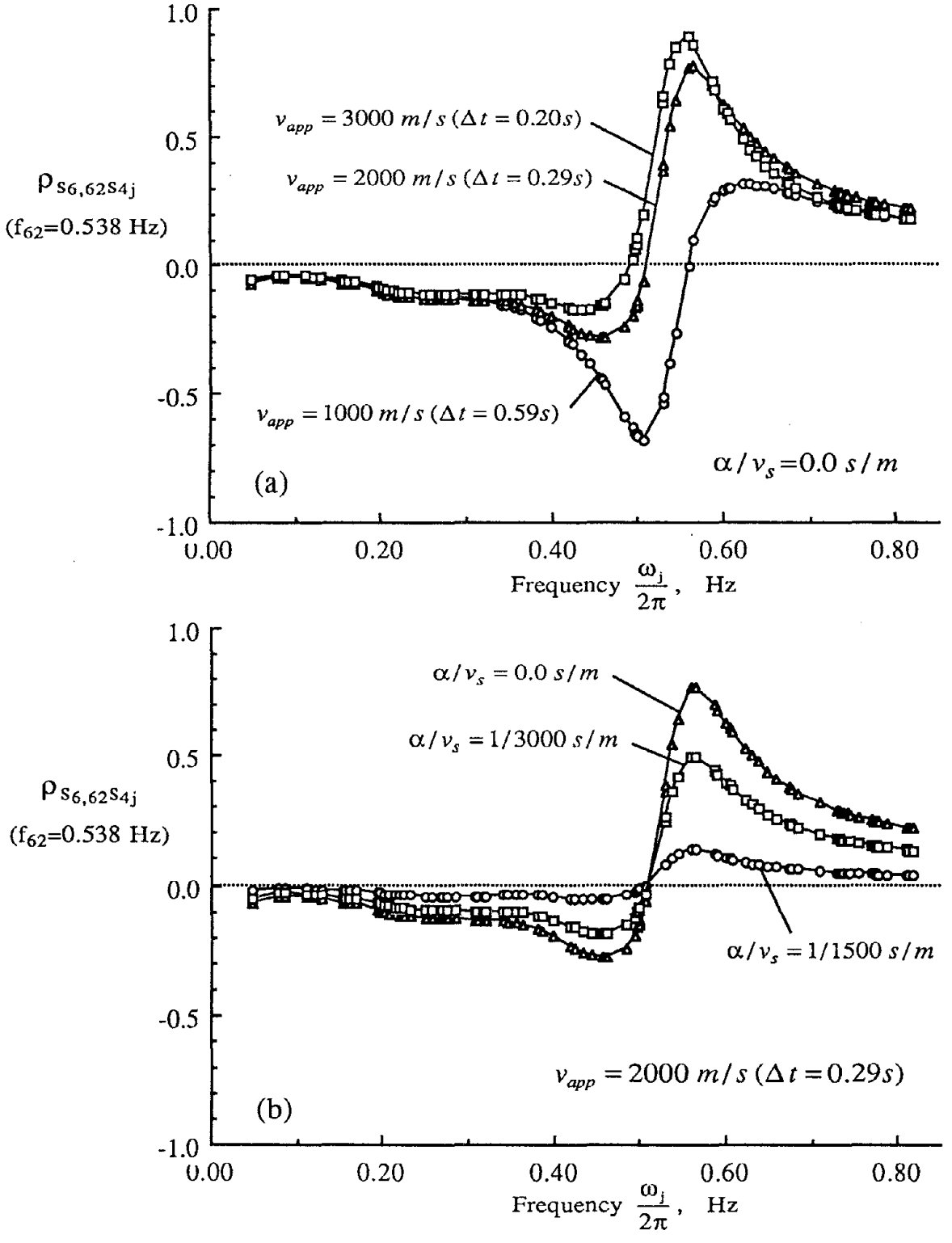

Fig. 4.9 Selected Cross-Correlation Coefficients Between Responses of Oscillators at the South Anchor and the S.F. Tower for Wave Direction S.F. to Marin

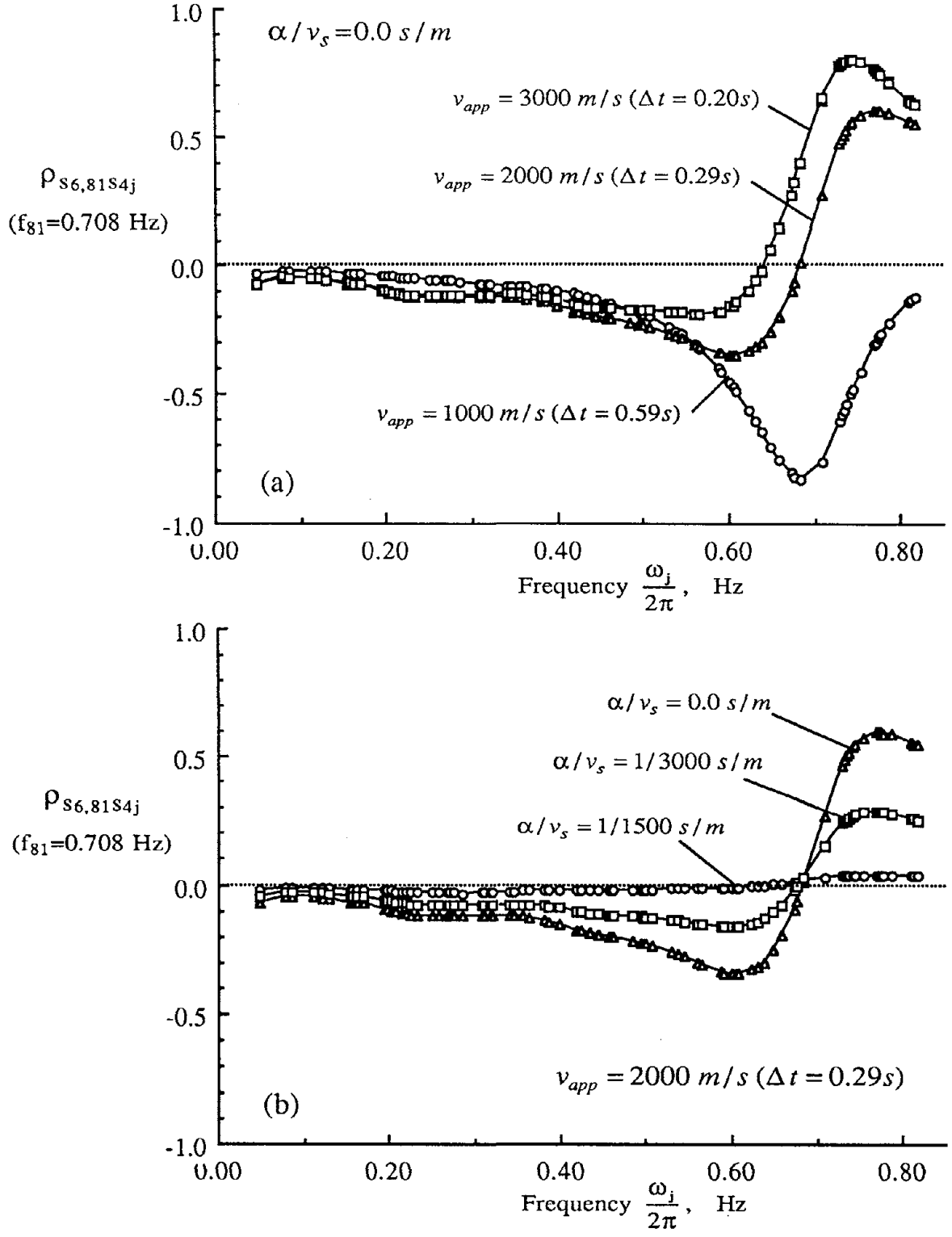

Fig. 4.10 Selected Cross-Correlation Coefficients Between Responses of Oscillators at the South Anchor and the S.F. Tower for Wave Direction S.F. to Marin

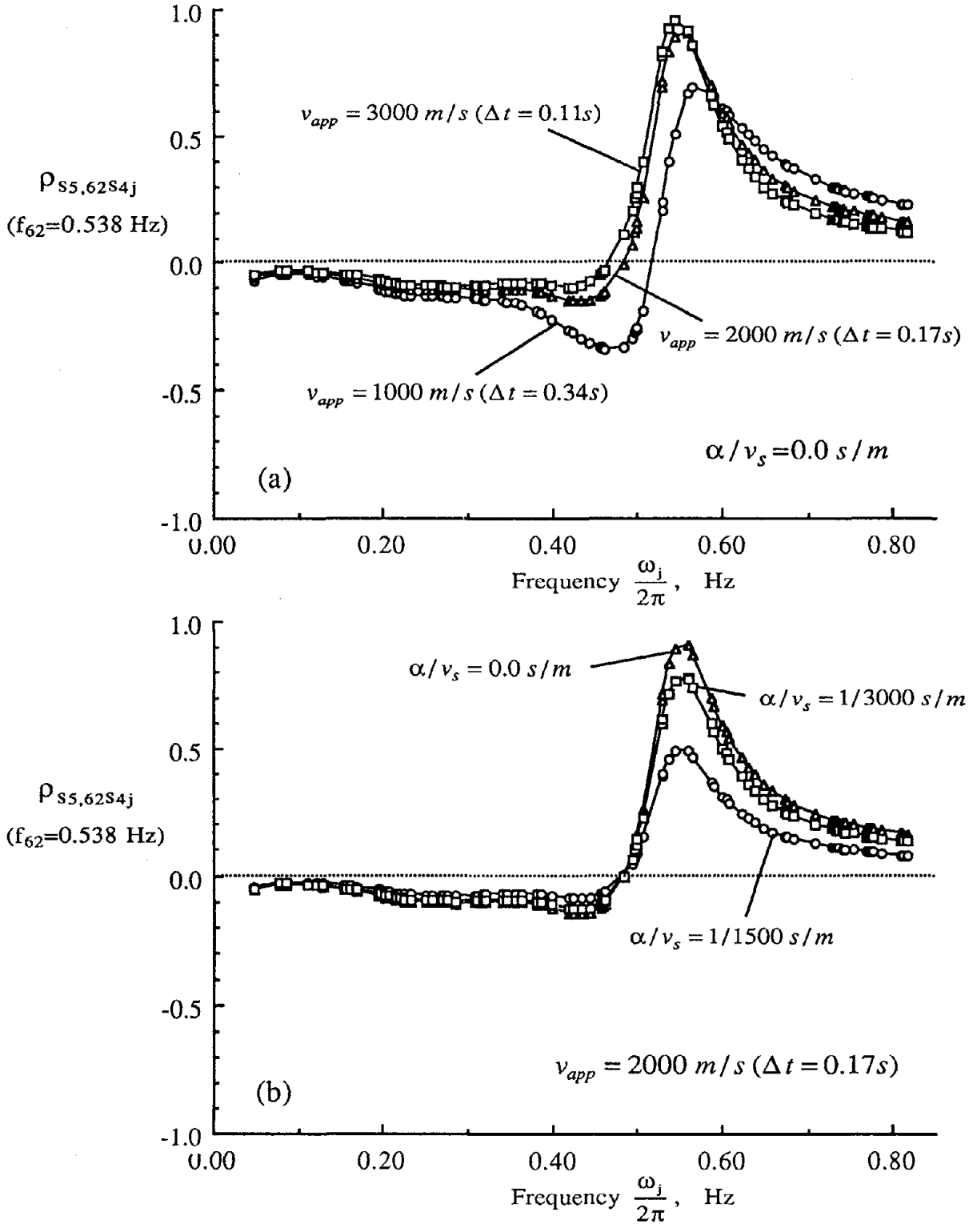

Fig. 4.11 Selected Cross-Correlation Coefficients Between Responses of Oscillators at the South Pylon and the S.F. Tower for Wave Direction S.F. to Marin

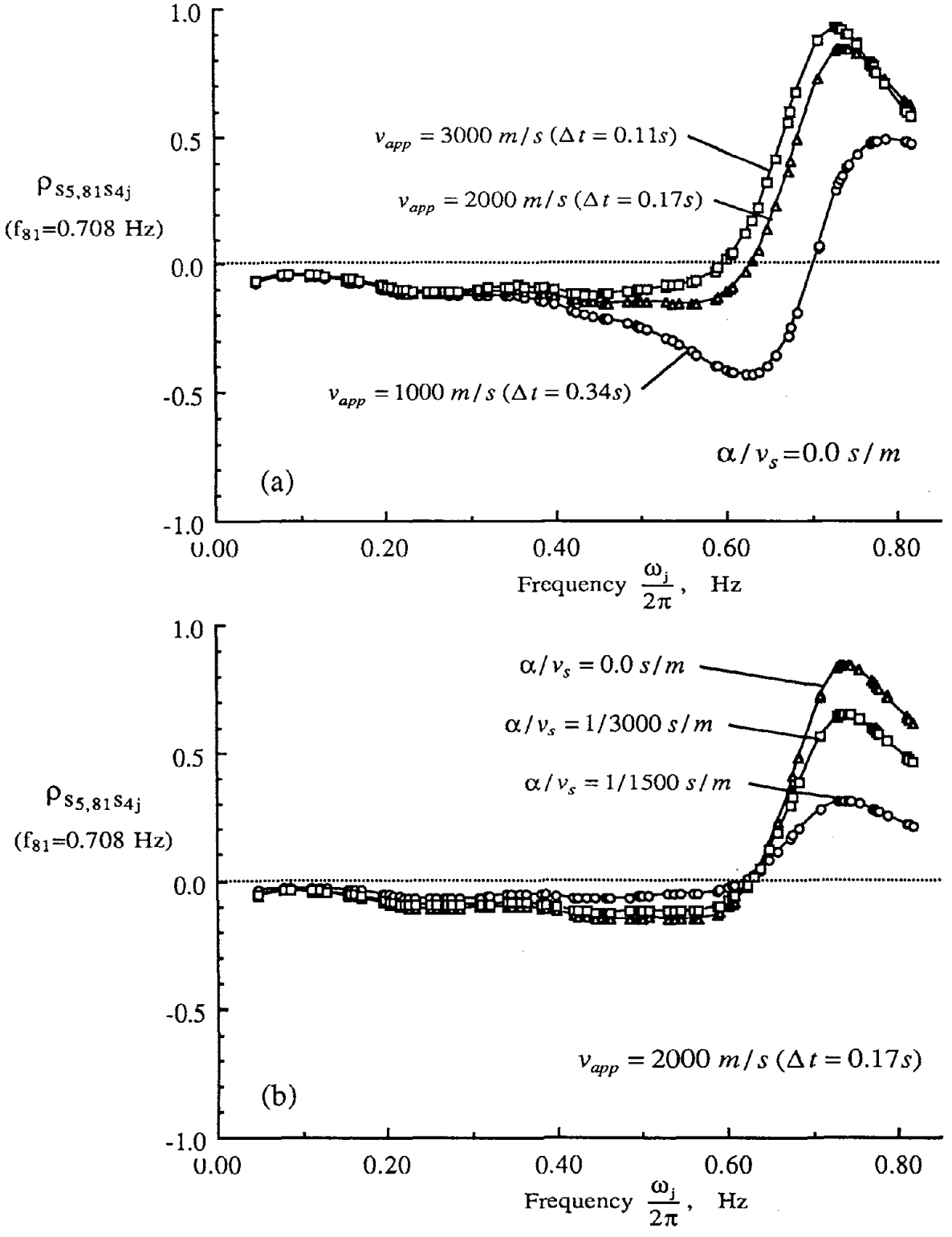

Fig. 4.12 Selected Cross-Correlation Coefficients Between Responses of Oscillators at the South Pylon and the S.F. Tower for Wave Direction S.F. to Marin

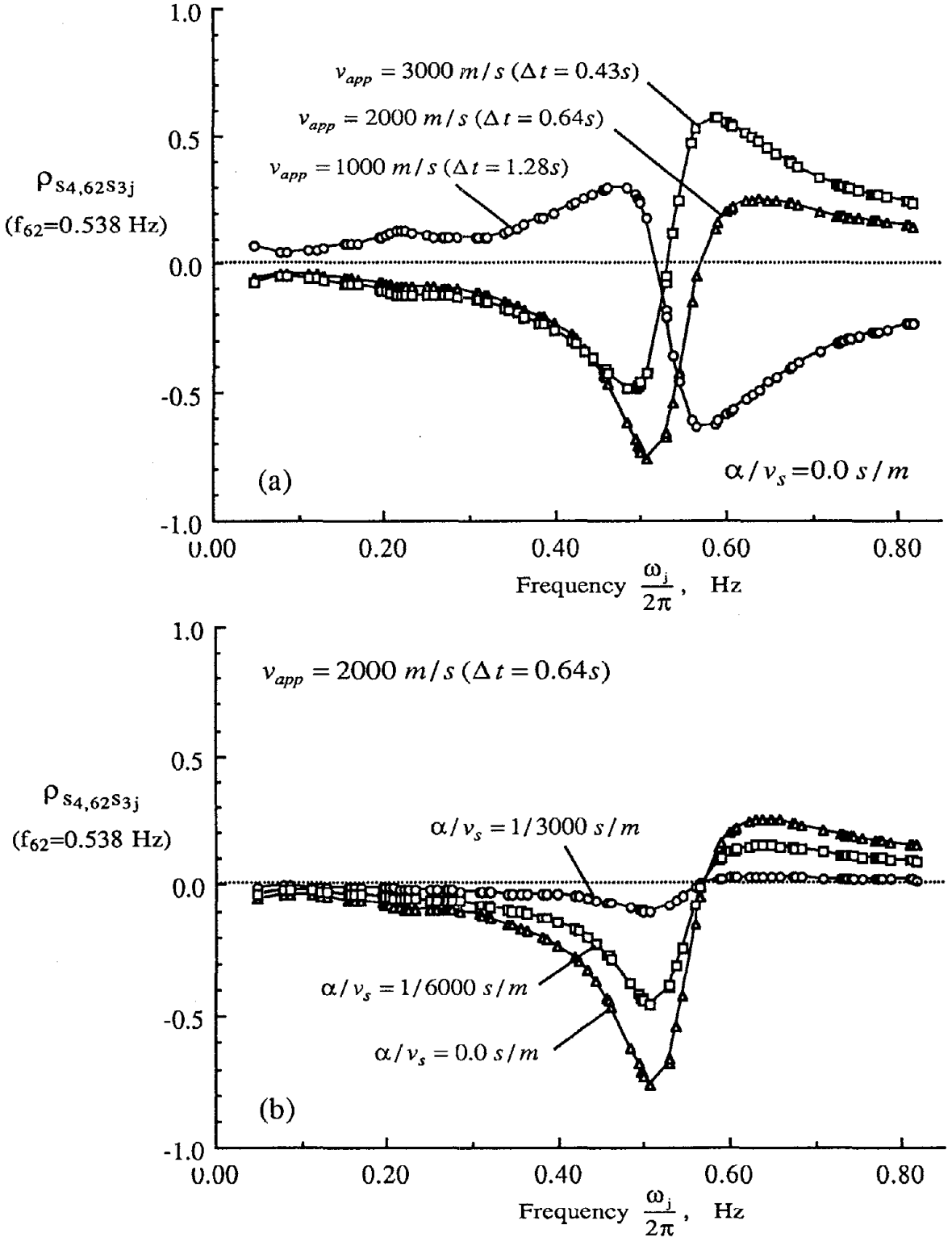

Fig. 4.13 Selected Cross-Correlation Coefficients Between Responses of Oscillators at the S.F. Tower and the Marin Tower for Wave Direction S.F. to Marin

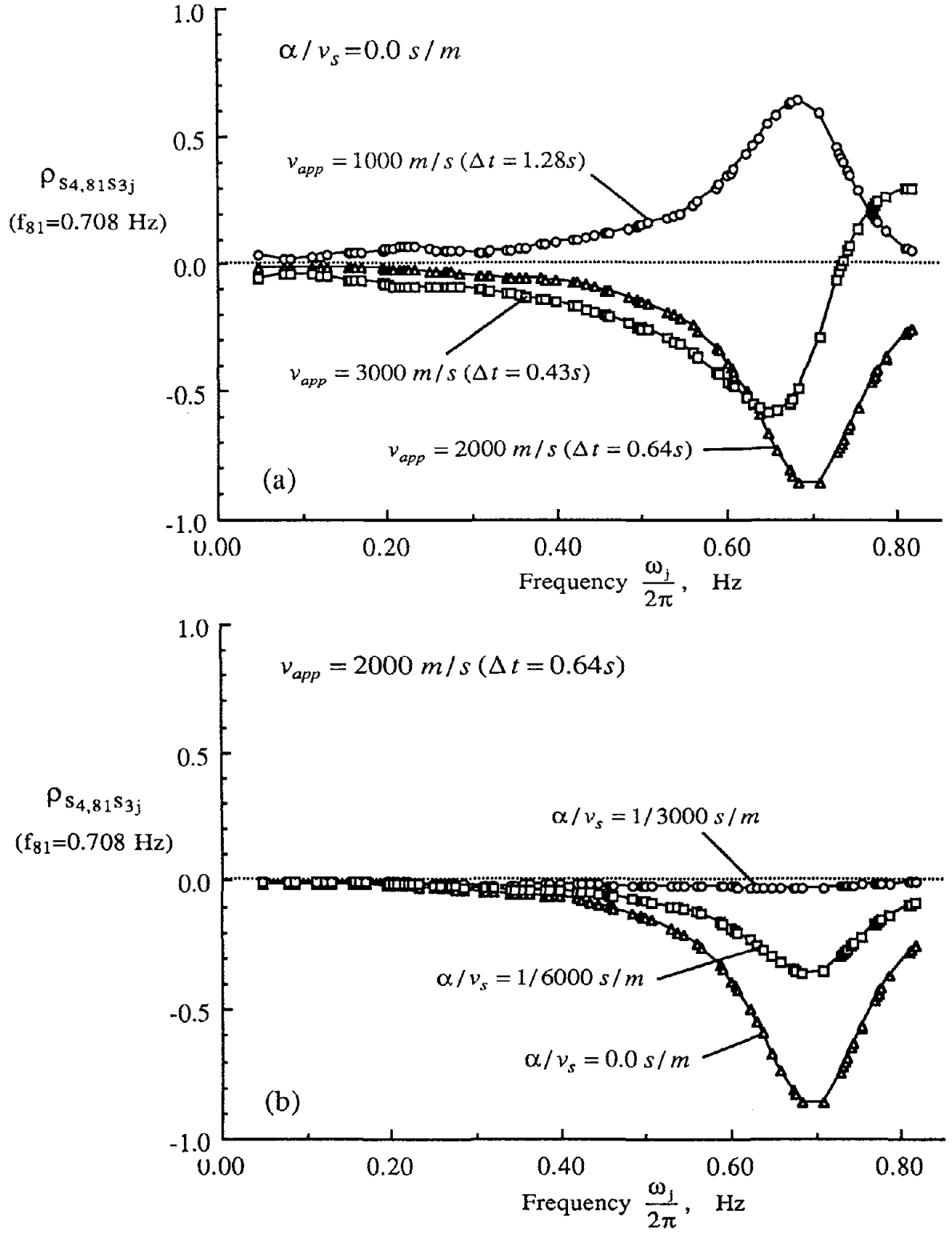

Fig. 4.14 Selected Cross-Correlation Coefficients Between Responses of Oscillators at the S.F. Tower and the Marin Tower for Wave Direction S.F. to Marin

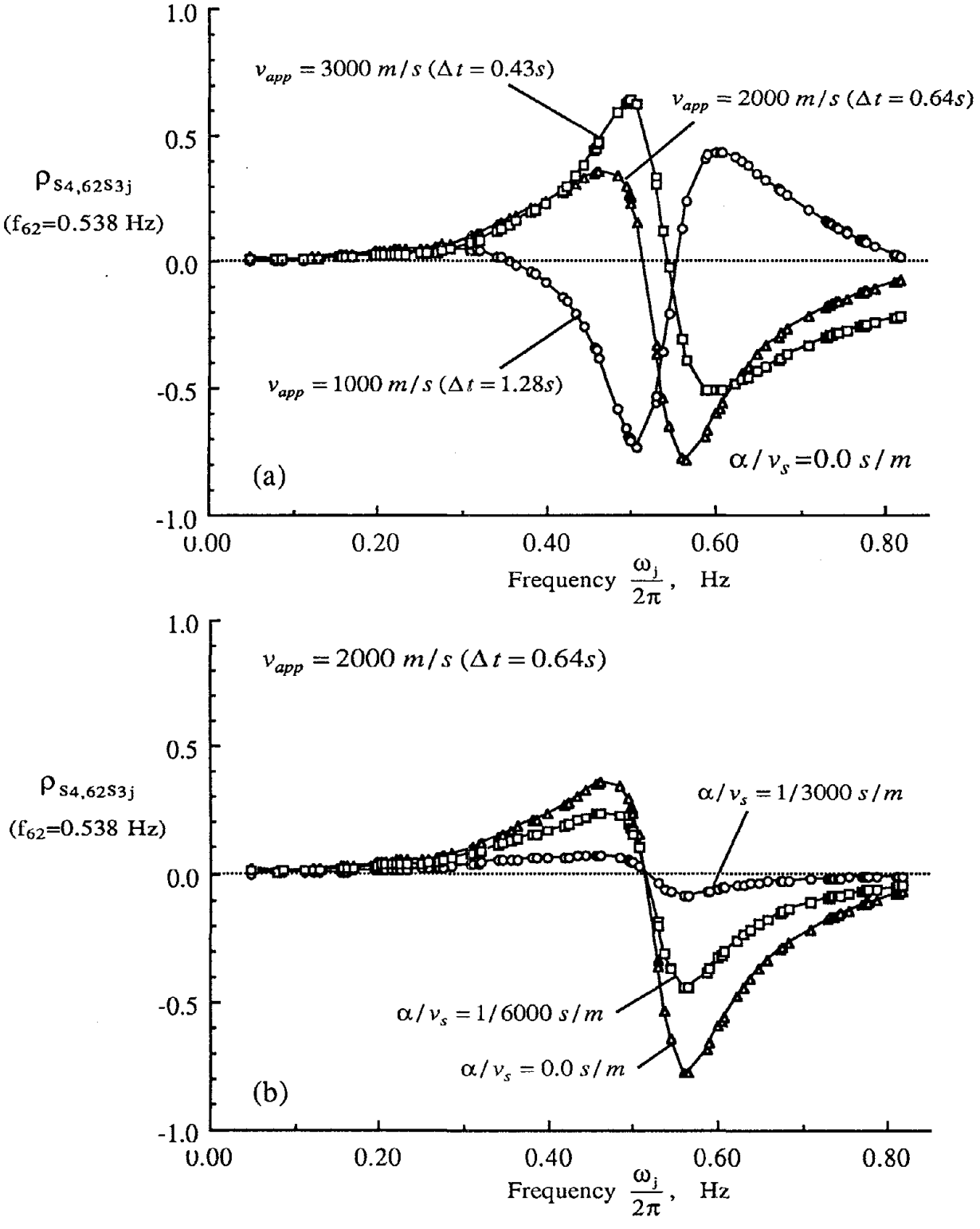

Fig. 4.15 Selected Cross-Correlation Coefficients Between Responses of Oscillators at the S.F. Tower and the Marin Tower for Wave Direction Marin to S.F.

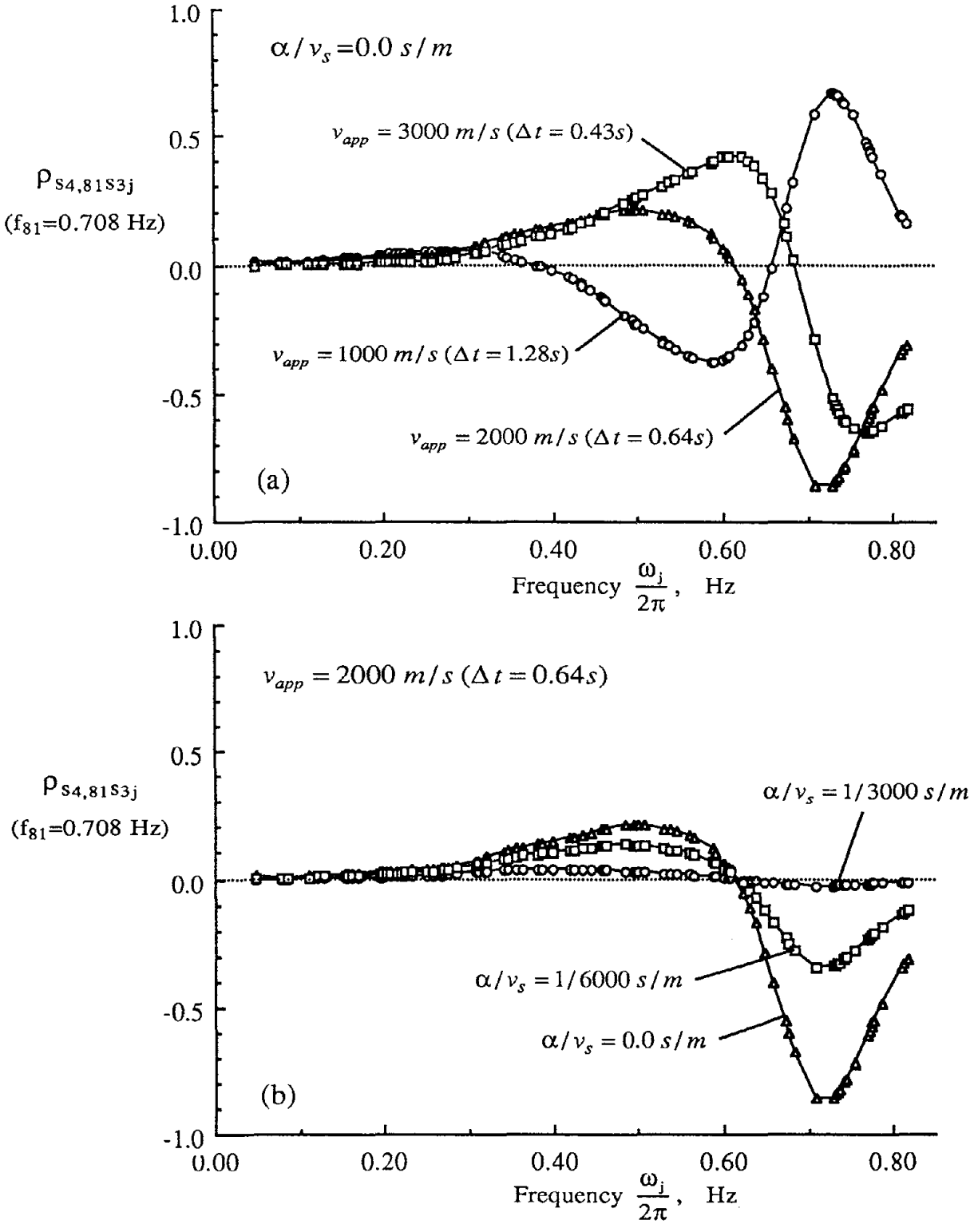

Fig. 4.16 Selected Cross-Correlation Coefficients Between Responses of Oscillators at the S.F. Tower and the Marin Tower for Wave Direction Marin to S.F.

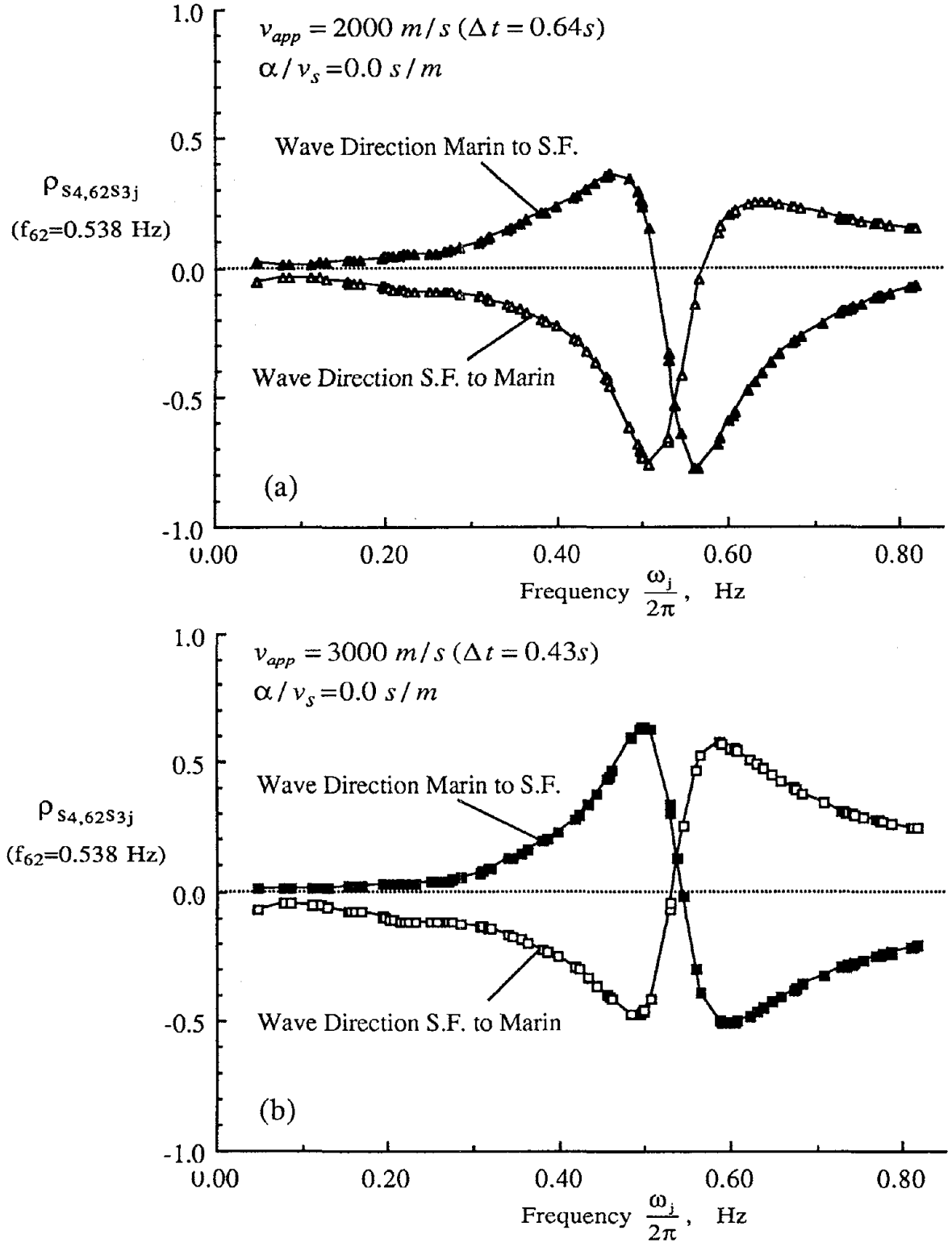

Fig. 4.17 Selected Cross-Correlation Coefficients Between Responses of Oscillators at the S.F. Tower and the Marin Tower for Two Wave Directions

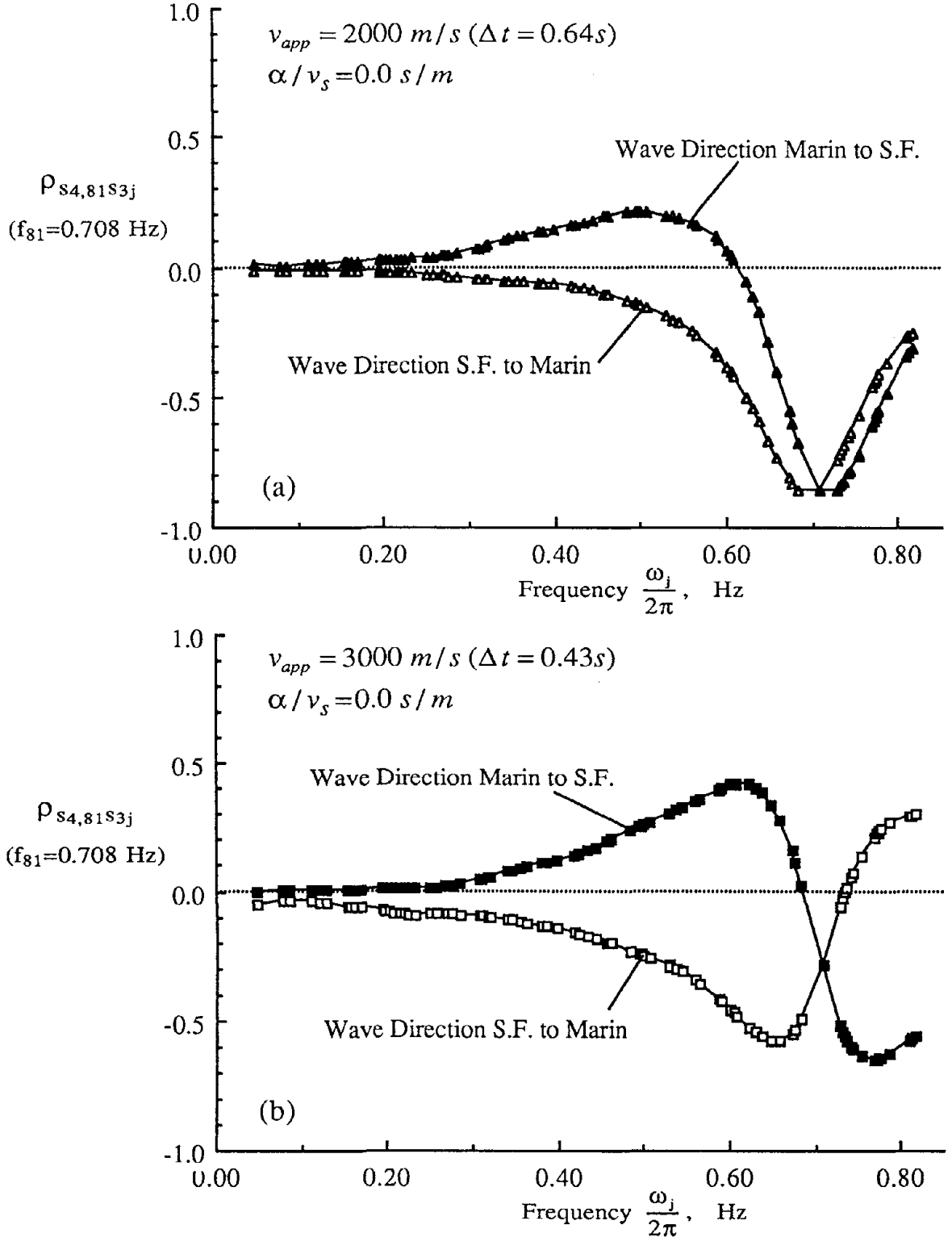

Fig. 4.18 Selected Cross-Correlation Coefficients Between Responses of Oscillators at the S.F. Tower and the Marin Tower for Two Wave Directions

CHAPTER 5
RESULTS OF ANALYSIS OF THE GOLDEN GATE BRIDGE

5.1 Introduction

This chapter presents the results of multiple-support response spectrum (MSRS) analysis of the Golden Gate Bridge, and investigates the effects of differential support motions on selected responses of the Bridge. The mean peak longitudinal displacements of the mid-height points (on the east and west side shafts) of the S.F. and Marin towers and their mean peak base moments are computed by the MSRS method (Eq. 2.23), including the first 100 modes. To investigate the effects of incoherence and wave passage, parameter α / v_s is varied between 0 and 1/1500 (sec/m), and v_{app} is varied between 1000 and 3000 (m/s). In all cases, the direction of propagation of seismic waves is assumed to be from S.F. to Marin (i.e., south to north). Finally, the results of the MSRS analysis are compared with the results of the time-history analysis by Imbsen and Associates (1990).

To compute the mean peak response by Eq. 2.23, the ordinates of the mean displacement response spectra for the first 100 modes (Table 3.1) are necessary. These modes have variable damping ratio, as shown in Table 3.1. The displacement response spectra used in this analysis were given only for the damping ratio ζ=0.05 (Figs. 3.4 - 3.7). To simplify the analysis, an approximation of the displacement response spectrum for mode i, $D(\omega_i,\zeta_i)$, is obtained from a formula of the form

$$D(\omega_i,\zeta_i) = H(\zeta_i)\, D(\omega_i,0.05) \tag{5.1}$$

where $H(\zeta)$ is a decreasing function of ζ normalized such that $H=1$ when ζ=0.05. Rosenblueth and Elorduy (1969) suggest obtaining the damped response of an oscillator by modifying the undamped response by the function

$$\left(\frac{1}{1+2\omega\zeta\tau}\right)^{1/2} \tag{5.2}$$

where τ is the duration of the ground motion. Normalizing this with respect to ζ=0.05 gives a formula for $H(\zeta)$ in the form

$$H(\zeta) = \left(\frac{1+a}{1+20a\zeta}\right)^{1/2} \tag{5.3}$$

where a is a constant. SEAONC (1990) suggests that a good fit to the amplification factors by Newmark and Hall can be obtained by using $a = 4$. Kawashima and Aizawa (1986) suggested the following $H(\zeta)$ based on regression analysis of spectra for 103 sets of strong accelerograms (206 records)

$$H(\zeta) = \frac{1.5}{40\zeta + 1} + 0.5 \tag{5.4}$$

These forms of $H(\zeta)$ are reasonably consistent with one another for damping values up to ζ=0.50. In the present study, the Kawashima-Aizawa relation, which is incorporated into the Japanese seismic code for bridges, is adopted.

5.2 Results

Figs. 5.1 - 5.6 show the squared displacements of the mid-height point (east side) of the S.F. and Marin towers in the longitudinal direction. In these figures, 'pseudo-static', 'cross' and 'dynamic' terms represent the double-sum term, the triple-sum term and the quadruple-sum term inside the brackets in Eq. 2.23, respectively. In Figs. 5.1 and 5.2, we include only the wave passage effect as a parameter and neglect the incoherence effect. In Figs. 5.3 and 5.4, we include both effects and use the incoherence effect as a varying parameter. Figs. 5.5 and 5.6 compare the MSRS results with the results for two extreme cases: (a) the "uniform excitation" case, which assumes no wave passage or incoherence effects ($v_{app} = \infty$ and $\alpha = 0$), i.e., $\gamma_{kl}(i\omega) = 1$, (b) the "independent excitation" case, which assumes statistically independent motions at all supports, i.e., $\gamma_{kl}(i\omega) = 0$ for $k \neq l$.

In all cases for the displacement response, the cross term (between the pseudo-static and dynamic parts arising from their covariance) has a relatively small negative value, but it is not small enough to be neglected. This indicates that all terms in the combination rule must be retained for the displacement responses of the Golden Gate Bridge. Among the three terms, the dynamic term is relatively large, particularly for the Marin tower. The pseudo-static term for the S.F. tower is larger than that for the Marin tower, and the dynamic term for the S.F. tower is smaller than that for the Marin tower.

Figs. 5.1 - 5.4 indicate that both the wave passage and incoherence effects slightly decrease the pseudo-static and cross terms, and have a large influence on the dynamic term of the response. The wave passage effect (which is inversely related to v_{app}) decreases the dynamic term for the Marin tower, but does not necessarily decrease the dynamic term for the S.F. Tower. It is noteworthy that a small incoherence effect

increases the dynamic term, but a larger incoherence effect decreases that term.

For the moment responses at the bases of the two towers, the pseudo-static term and the cross term are negligible and the response is primarily due to the dynamic term. This is due to the flexible nature of the bridge structure. For this reason, plots similar to Figs. 5.1 - 5.6 are not presented for these responses.

Figs. 5.7 - 5.9 show the total values for the mean peak longitudinal displacements of the mid-height points of the S.F. and Marin towers. In Fig. 5.7, only the wave passage effect is included, and in Fig. 5.8, both the wave passage and incoherence effects are included. In Fig. 5.9, the computed responses by the MSRS method for $v_{app} = 3000\ m/s$ and $\alpha / v_s = 0.0$ are compared with the two extreme cases described before. These values of the parameters for the coherency function are chosen, since they are believed to be most consistent with the generated time histories. Figs. 5.7 - 5.9 indicate that the displacement responses of the mid-height points of the Marin tower are larger than those of the S.F. tower in all cases. As mentioned earlier, the wave passage effect decreases the displacement responses of the Marin tower, but not those of the S.F. tower. It is again noted that a small incoherence effect increases the displacement responses of both towers, but a larger incoherence effect decreases these responses. The increase is due to the elimination by the incoherence effect of certain negative cross-correlation terms arising from the wave passage effect. Fig. 5.9 shows that the assumption of uniform excitation results in increased estimates of the displacement responses by 31% and 12% for the S.F. and Marin towers, respectively, whereas the assumption of independent excitations results in decreases of 4% and 16% in the estimated responses of the two towers, respectively.

Figs. 5.10 - 5.12 show the mean peak base moments of the S.F. and Marin towers. In Fig. 5.10, only the wave passage effect is included, and in Fig. 5.11, both the wave passage and incoherence effects are included. In Fig. 5.9, the assumption of uniform excitation is seen to result in increased estimates of the base moment responses by 35% and 10% for the S.F. and Marin towers, respectively, whereas the assumption of independent excitations results in a decrease of 16% in the Marin tower moment and practically no change in the S.F. tower moment.

5.3 Comparison with Time-History Results

The results generated by the response spectrum method should be viewed as statistical in nature. Specifically, they represent approximations to the mean peak response over an ensemble of input motions, provided the spectra employed in the analysis themselves

represent the mean spectra over the same ensemble. On the other hand, a time-history analysis produces the deterministic response to a single realization of the input motions. A comparison between the response spectrum and time-history results, hence, is not a proper comparison for the purpose of validating the response spectrum method. The proper comparison should involve the averages of peak responses over an ensemble of time-history results, as was done by Der Kiureghian (1981) in the validation of the original CQC method. In the present case, results from such ensemble time-history analyses are not available and they would be prohibitively costly to generate for the bridge structure with more than 4,000 degrees of freedom.

In spite of the above shortcoming, a comparison between the results of time-history analysis with a single realization of the input motions, and the results of response spectrum analysis with spectra generated from the same input time histories is often used as a means of validation of the response spectrum method. According to Der Kiureghian (1981), errors of order up to 30% may be expected from such comparison without invalidating the response spectrum method.

Further complication in the present analysis arises from the specification of the coherency function. The time histories for the 18 support motions of the bridge unfortunately were generated without the specification of a coherency function. On the other hand, for the MSRS method, an analytically defined coherency function that describes both the wave passage and incoherence effects is required. For the present application, the coherency model in Eq. 2.32 was used. Values for the two parameters α / v_s and v_{app} of this model were selected by examining the cross-power spectral density of the longitudinal motions at bases of the S.F. and Marin towers. On this basis, as well as considerable amount of judgment, the values $\alpha / v_s = 0$ and $v_{app} = 3000\, m/s$ were chosen. Unfortunately there is no way to ascertain that these values are consistent with the spatial variability inherent in the generated time histories.

One additional problem in the present application is the unavailability of response spectra for damping values other than 5%. Eqs. 5.1 and 5.4 provide only a crude approximation and significant errors relative to time-history results may arise from this approximation.

It should be clear from the foregoing that the comparison presented below should not be taken as proof of validation or invalidation of the multiple-support response spectrum method. The proof of validation of the MSRS method lies in its analytical derivation from the basic principles of random vibration theory, and the fact that it is an extension of the well-tested CQC method (Der Kiureghian and Neuenhofer, 1992).

Fig. 5.13 and 5.14 compare the results of the MSRS and time-history analyses for the peak displacements and base moments of the S.F. and Marin towers of the bridge. Both methods of analysis indicate that the Marin tower response is about 30% larger than the response of the S.F. tower. However, the results based on the MSRS analysis are smaller than the time-history results by 30-35% for the displacement responses and 20-30% for the base moment responses. To better understand the nature of this discrepancy, the MSRS results for the displacement responses are superimposed on the time-history results of Liu and Imbsen (1990) in Figs. 5.15 and 5.16 for the S.F. and Marin towers, respectively. In each figure, the top set of curves are for the dynamic component of the response alone, and the bottom set of curves are for the total displacement. Note that the curves for the mid-height point B of the towers should be compared with the MSRS results.

It is noted in Figs. 5.15 and 5.16 that the MSRS results are in close agreement with the time-history results, if the large negative peak occurring at approximately 12 seconds is neglected. Unfortunately the cause of this peak could not be determined since the individual modal time histories were not available to the investigators. It is noted, however, that this peak has an uncharacteristically large magnitude relative to the neighboring peaks, particularly in the case of the Marin tower (Fig. 5.16), where the peak magnitude is almost twice that of the neighboring peaks in the dynamic component of the response. This kind of response may not be well predicted by the response spectrum method which works best when the response includes a quasi-stationary strong-motion phase. Beyond this, no conclusions are derived from the comparison of the MSRS and time-history results.

5.4 Concluding Remarks

From the results in this chapter, the following main conclusions can be derived:

(1) The MSRS method provides a practical means for dynamic analysis of the bridge, accounting for the effects of wave passage and incoherence. The method is particularly convenient for parametric studies to investigate the influences of input parameters and the contribution of the pseudo-static and dynamic components of the response.

(2) For the displacement responses of the bridge, the dynamic component is dominant, although the contributions of the pseudo-static component and the cross term are not negligible. The base moment responses of the bridge are primarily contributed by the dynamic component. This is due to the flexible nature of the bridge.

(3) The influence of wave passage and incoherence effects are stronger on the dynamic component of the response, than on the pseudo-static component or the cross term. Compared to the MSRS results, the assumption of uniform support excitation results in increased responses of both the S.F. and Marin towers, whereas the assumption of independent excitations results in decreased responses for the Marin tower and insignificant change in the responses of the S.F. tower.

(4) The MSRS estimates of the two tower responses show trends which are consistent with the trend observed in the time-history results. However, there is a significant discrepancy between the two sets of results. This discrepancy is attributed to several factors, including: (a) the statistical nature of the MSRS results versus the time-history results which represent a single realization, (b) the uncertainty in specifying the coherency function for the generated time histories, (c) the error in the assumed response spectra for modal damping values other than 0.05, and (d) the appearance of an uncharacteristically large peak in the time-history results.

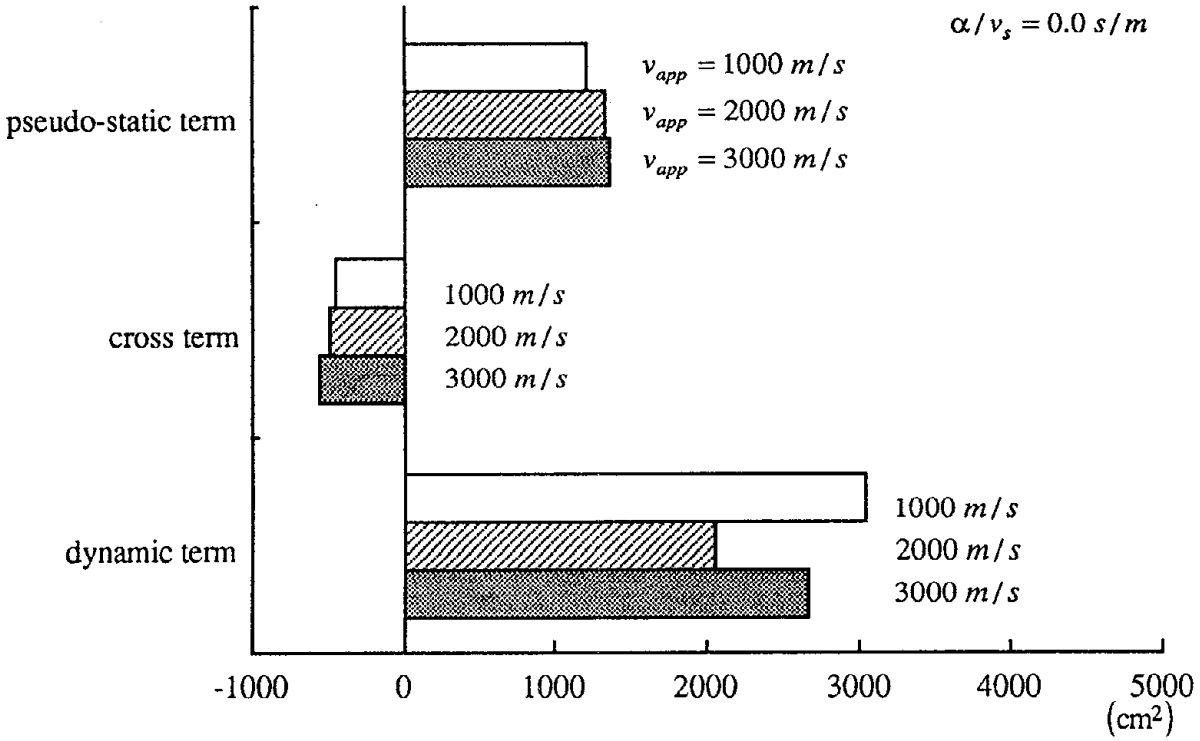

Fig. 5.1 Squared Displacement Responses of Mid-height Point (East Side) of the S.F. Tower

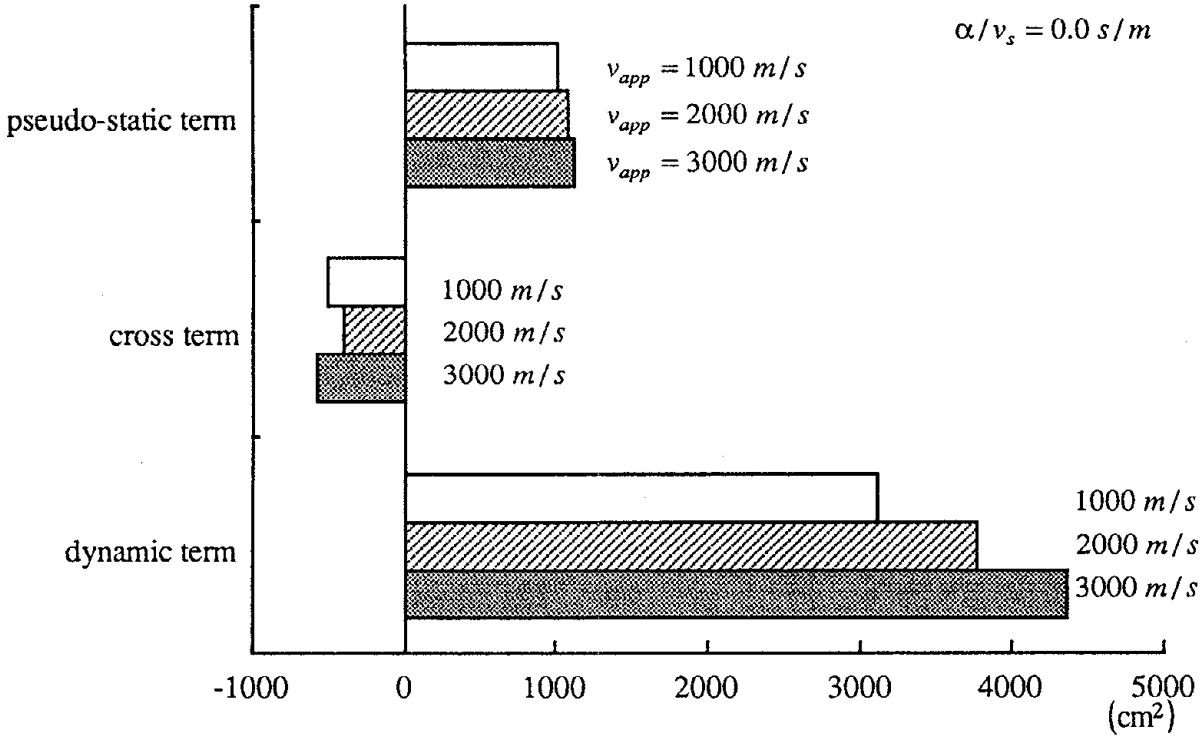

Fig. 5.2 Squared Displacement Responses of Mid-height Point (East Side) of the Marin Tower

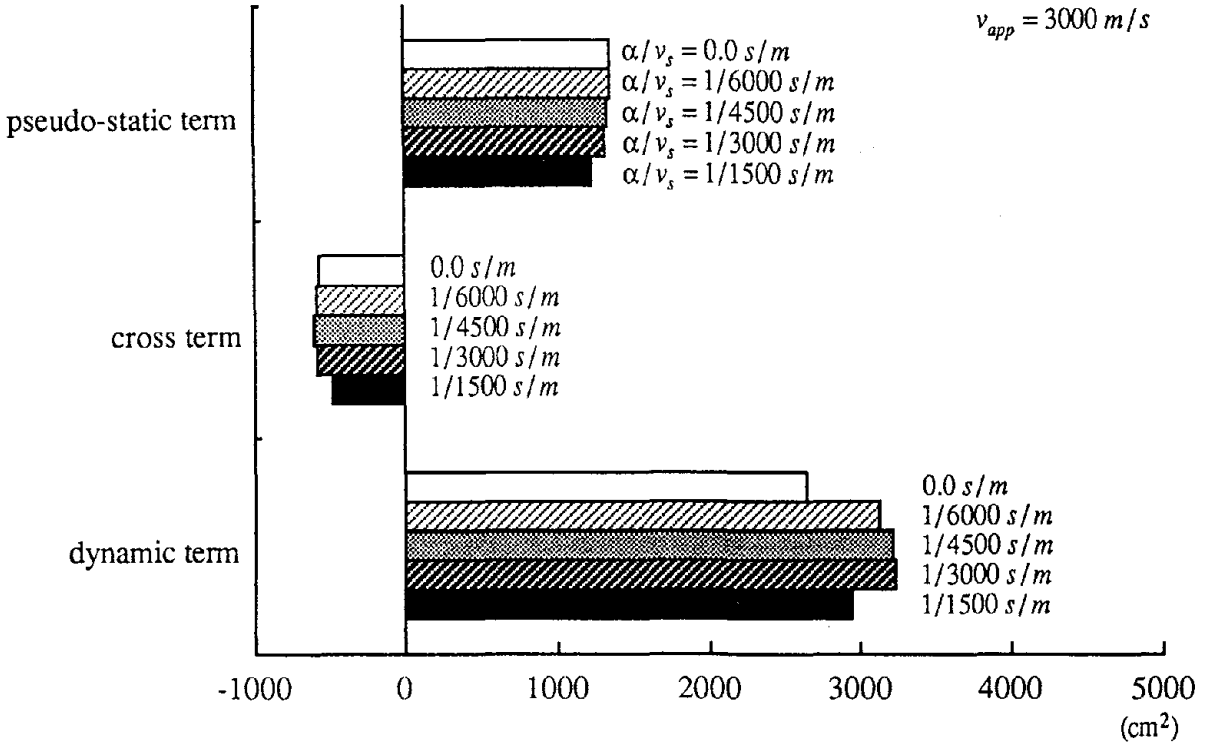

Fig. 5.3 Squared Displacement Responses of Mid-height Point (East Side) of the S.F. Tower

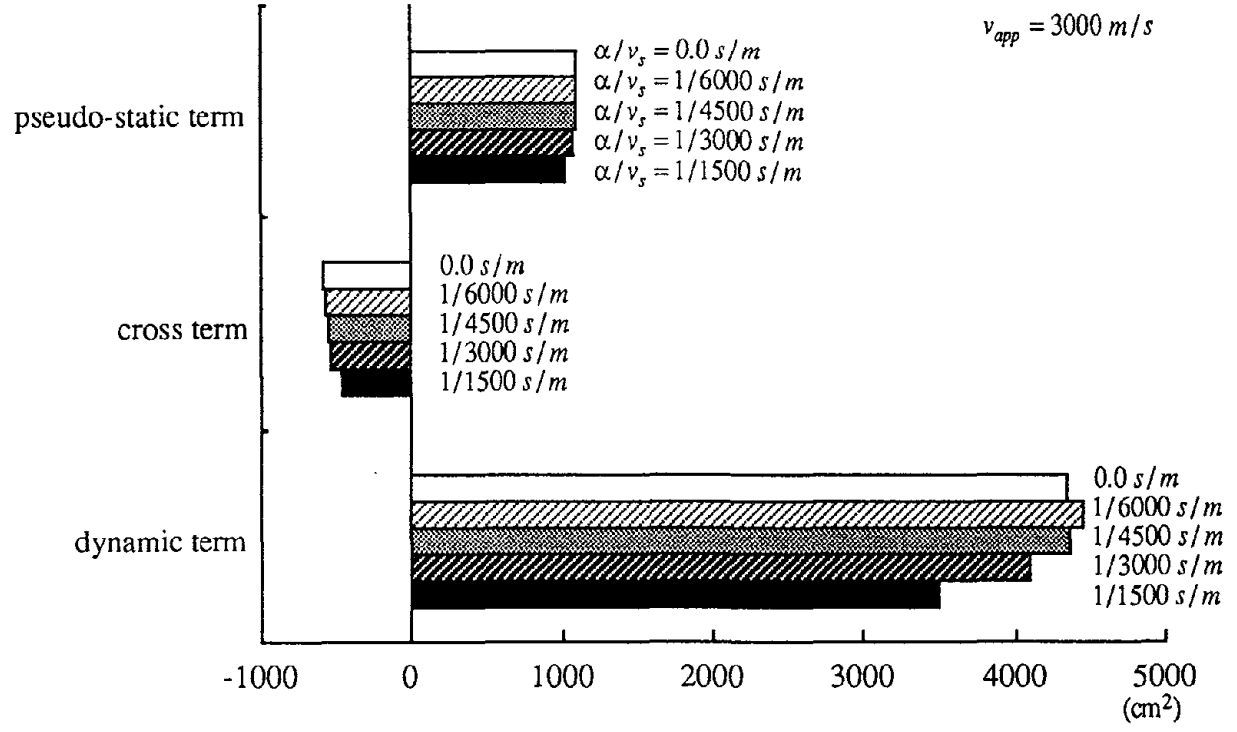

Fig. 5.4 Squared Displacement Responses of Mid-height Point (East Side) of the Marin Tower

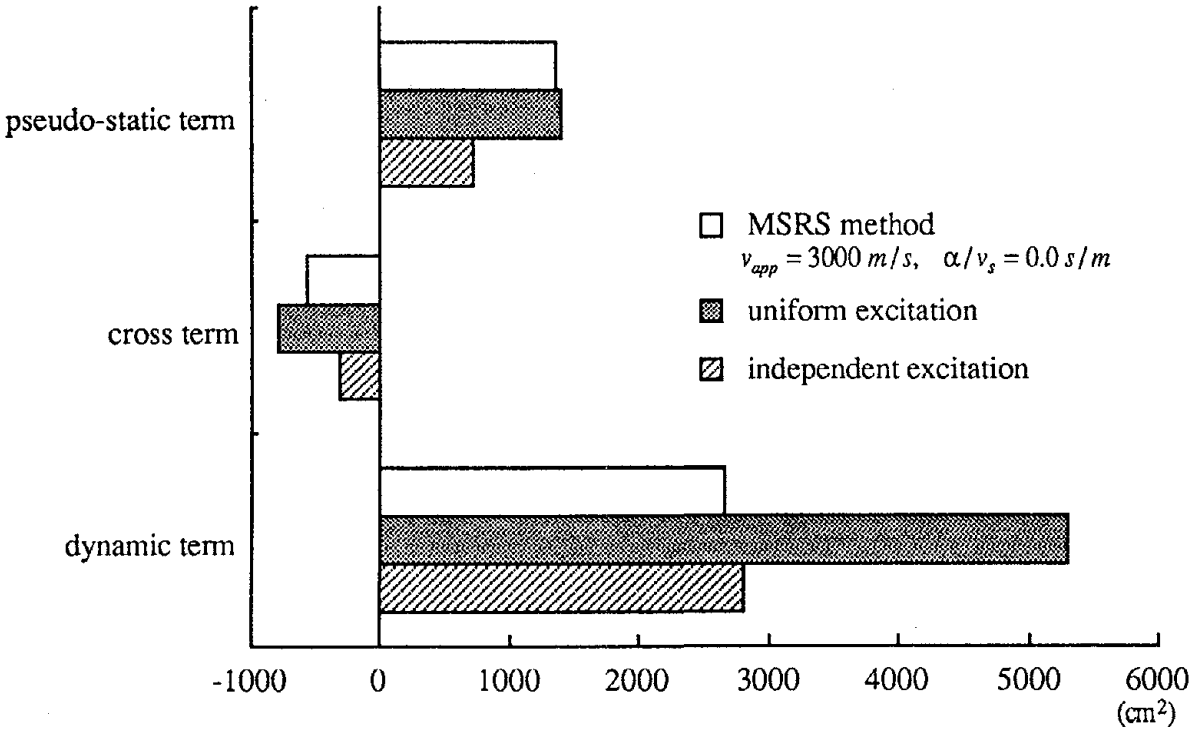

Fig. 5.5 Squared Displacement Responses of Mid-height Point (East Side) of the S.F. Tower

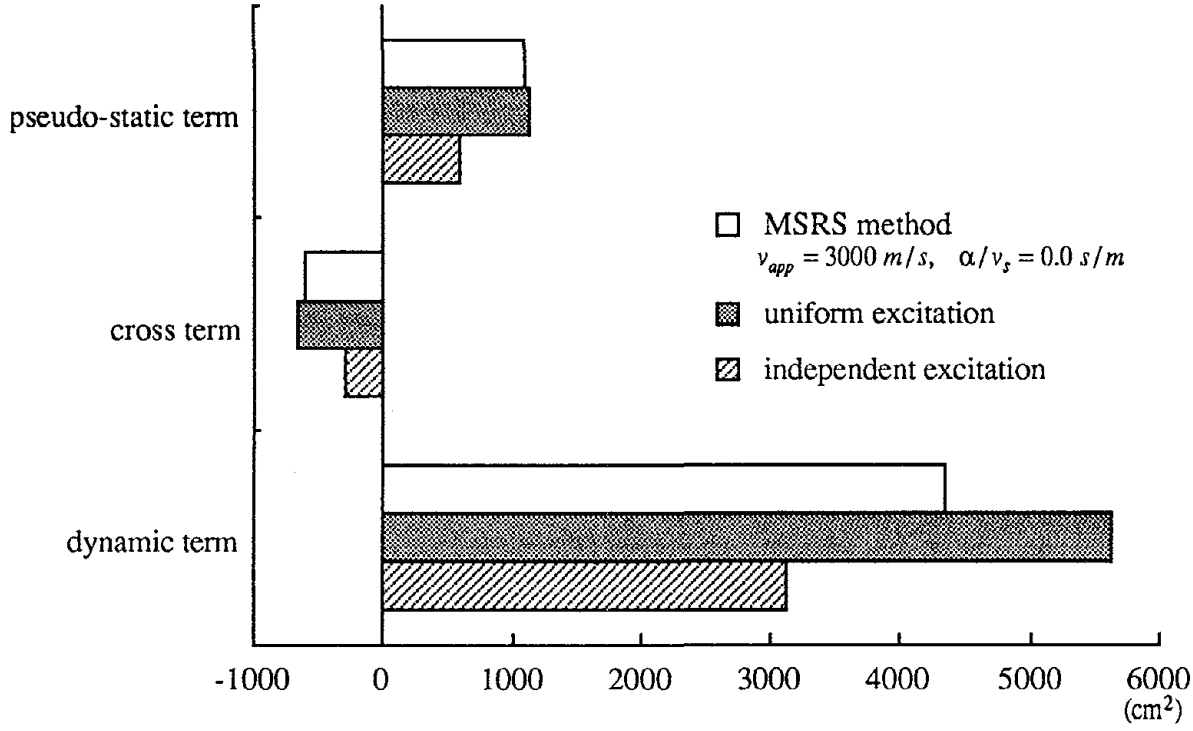

Fig. 5.6 Squared Displacement Responses of Mid-height Point (East Side) of the Marin Tower

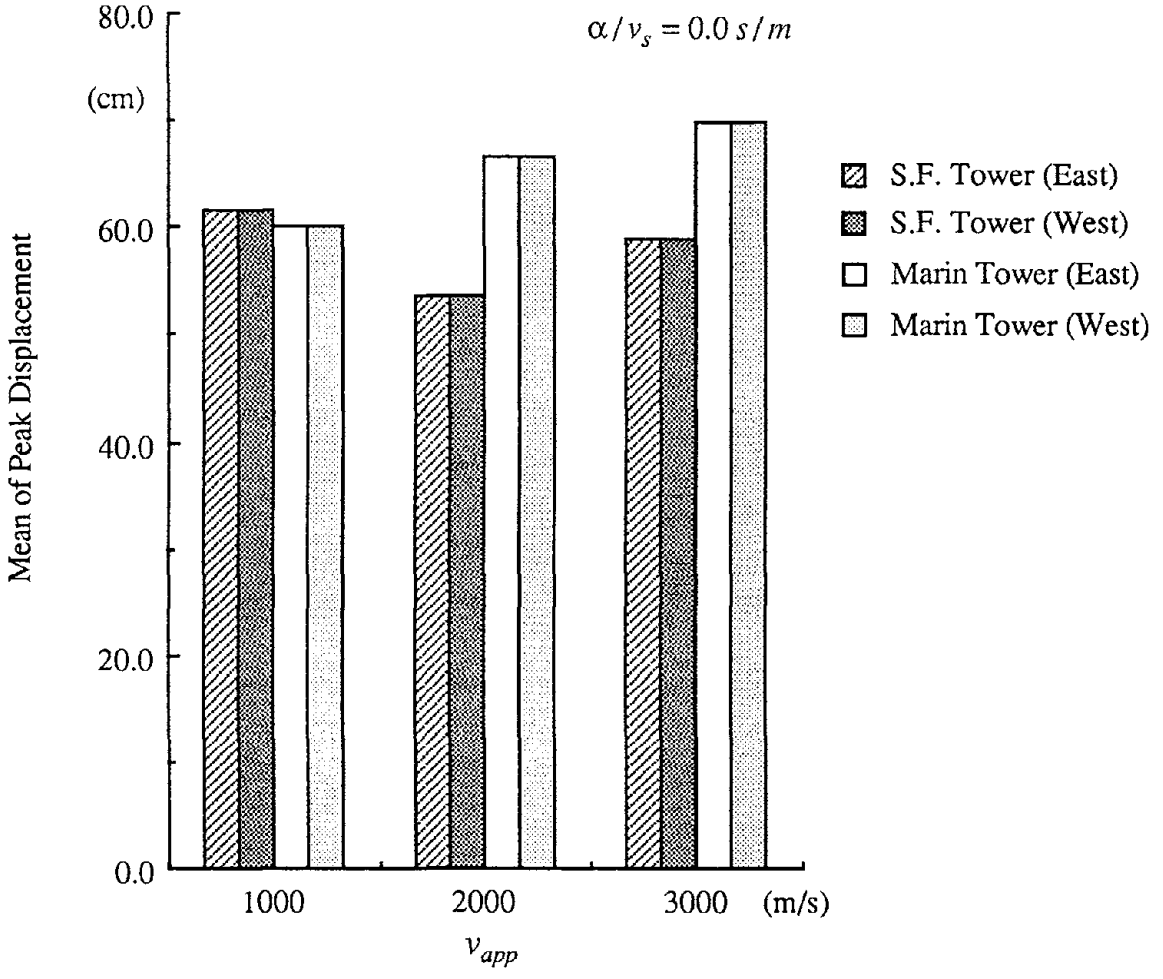

Fig. 5.7 Mean of Peak Longitudinal Displacements of Mid-height Points of the S.F. and Marin Towers

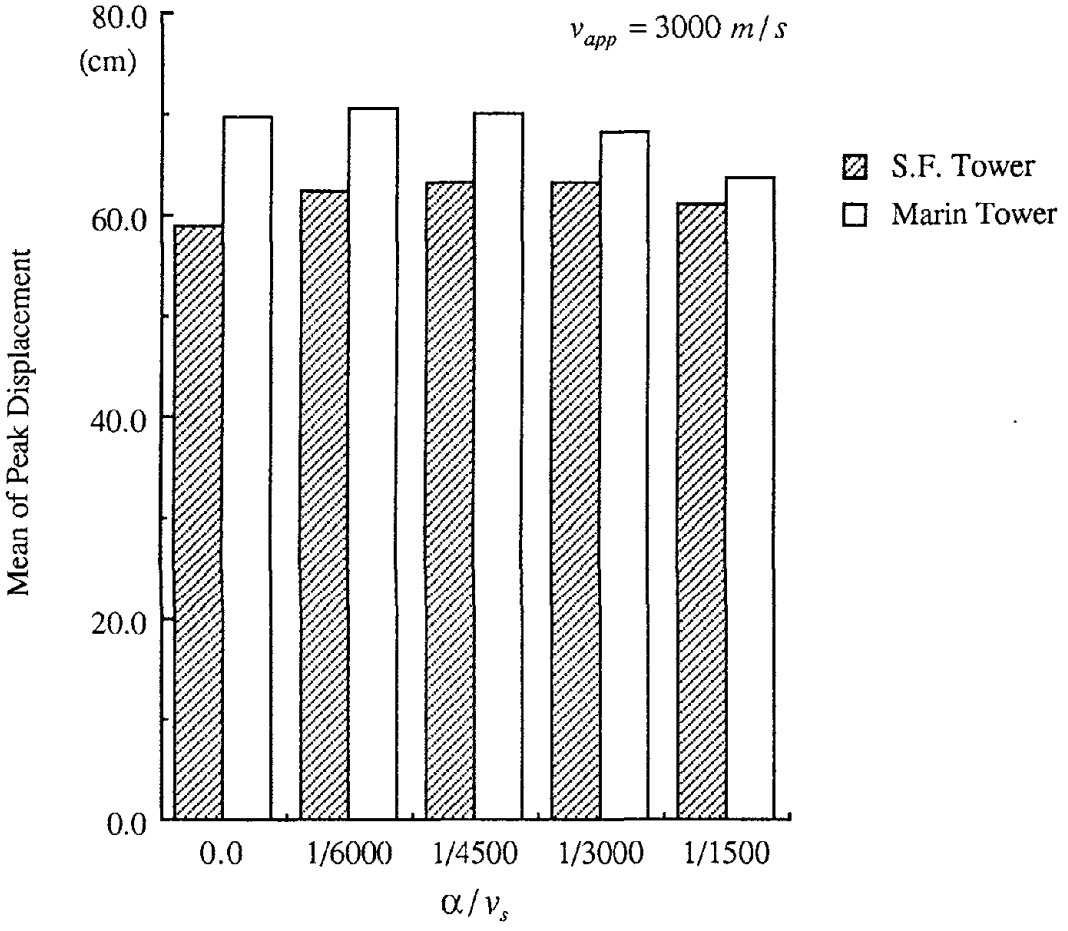

Fig. 5.8 Mean of Peak Longitudinal Displacements of Mid-height Points (East Side) of the S.F. and Marin Towers

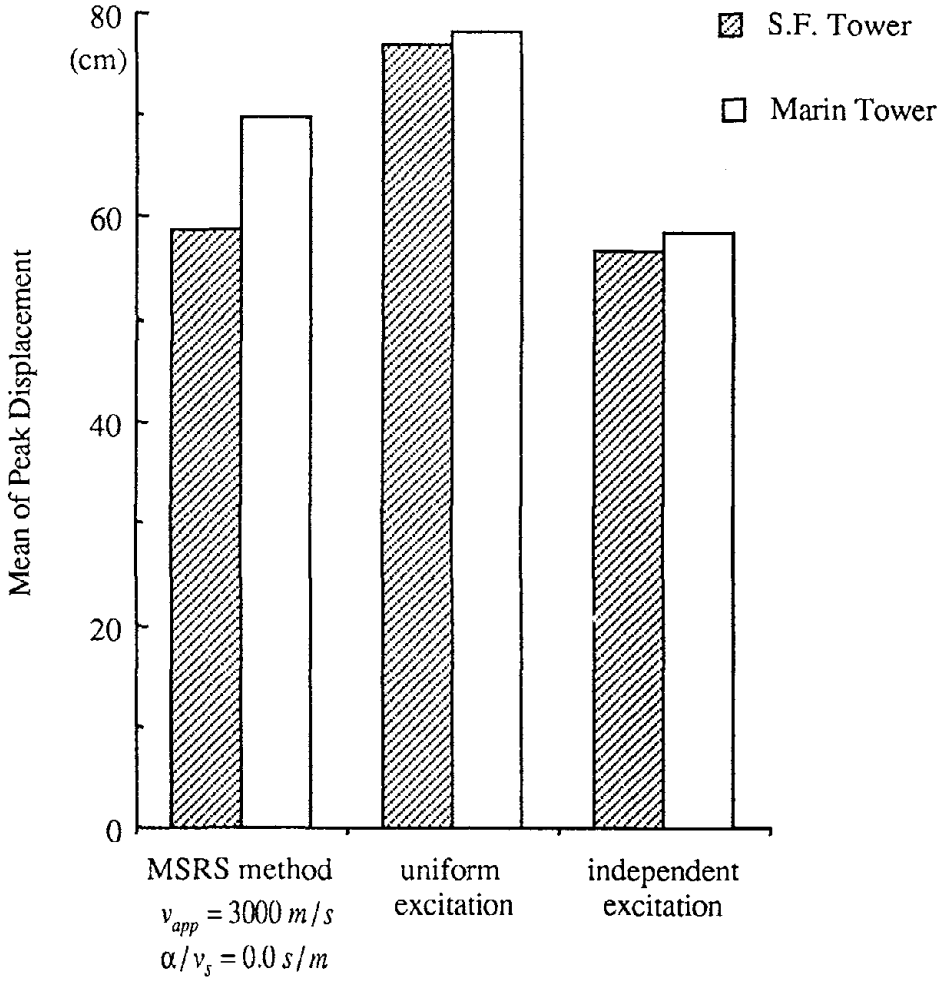

Fig. 5.9 Mean of Peak Longitudinal Displacements of Mid-height Points (East Side) of the S.F. and Marin Towers

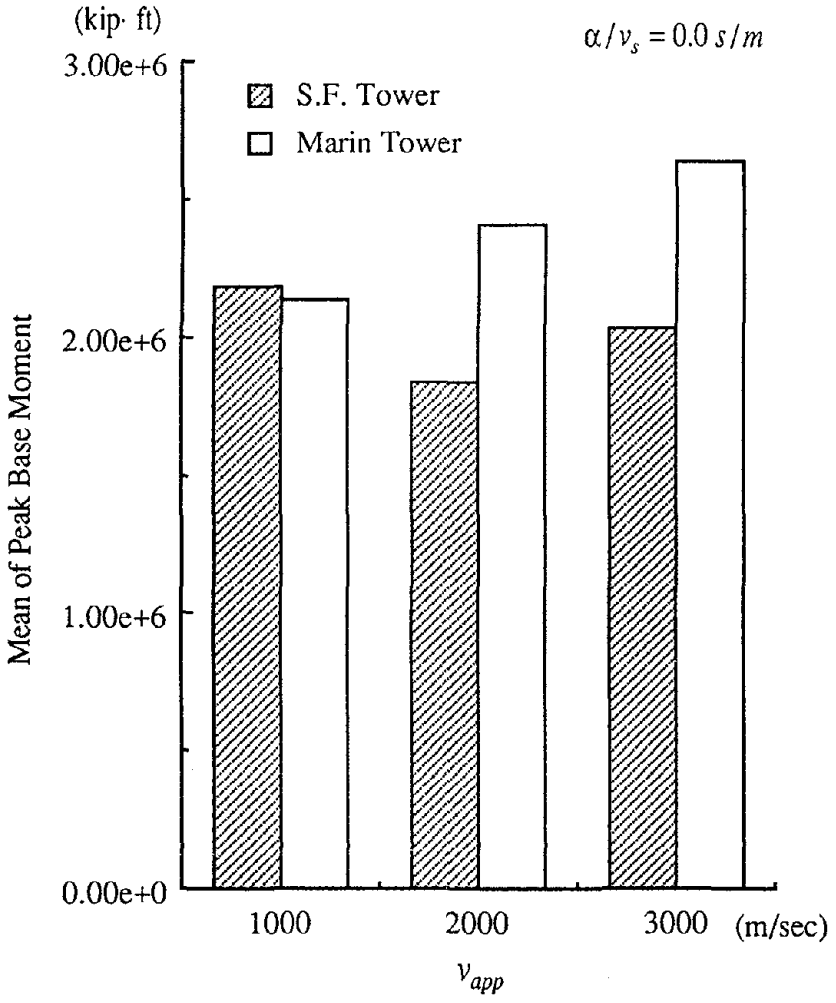

Fig. 5.10 Mean of Peak Base Moments of the S.F. and Marin Towers

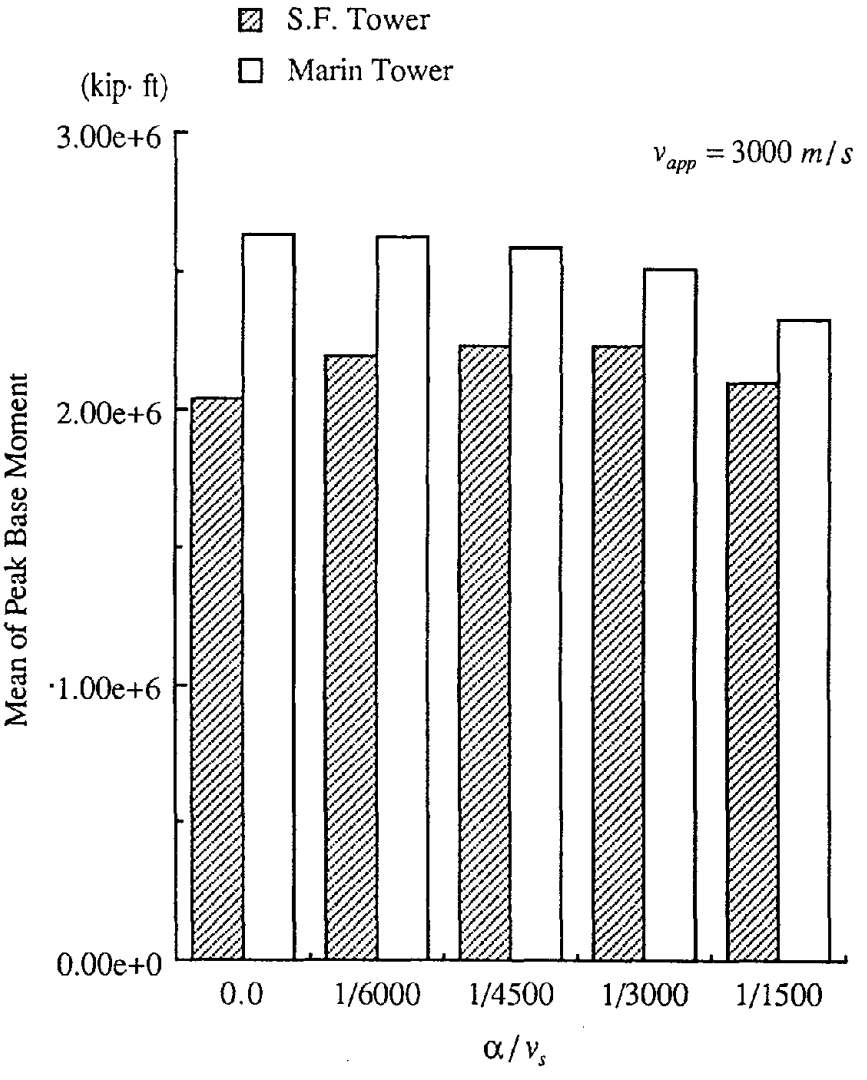

Fig. 5.11 Mean of Peak Base Moments of the S.F. and Marin Towers

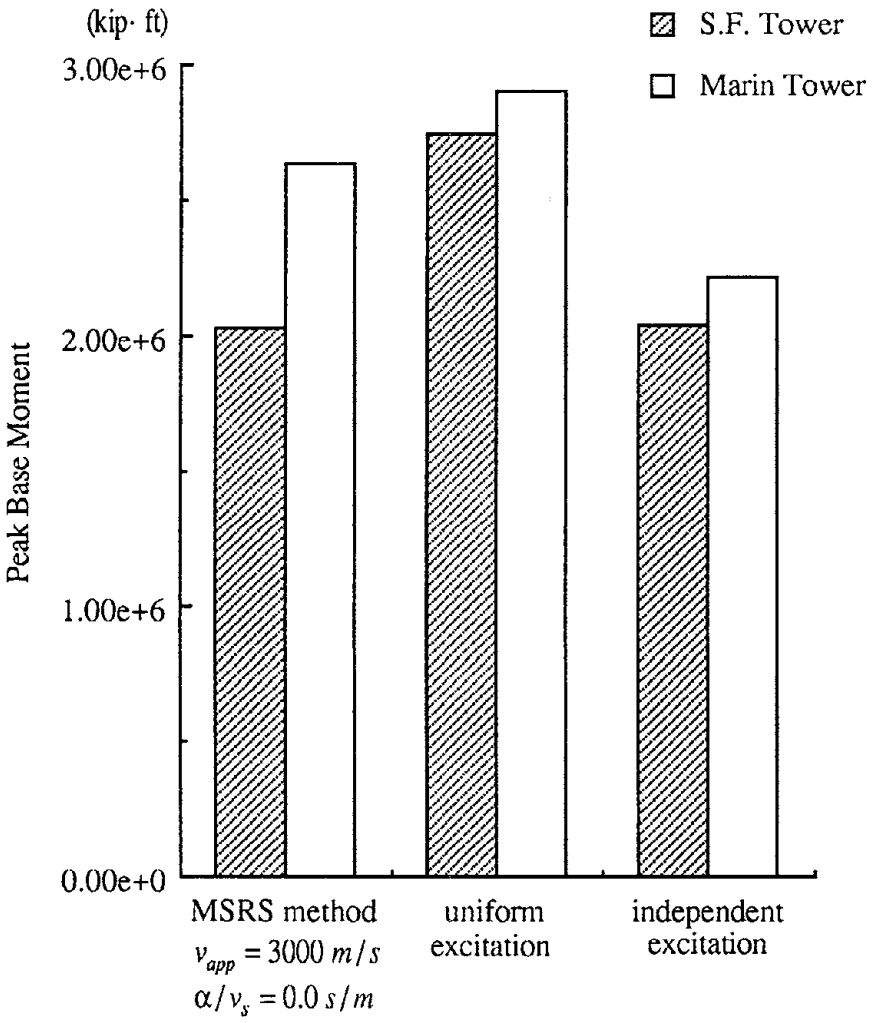

Fig. 5.12 Mean of Peak Base Moments of the S.F. and Marin Towers

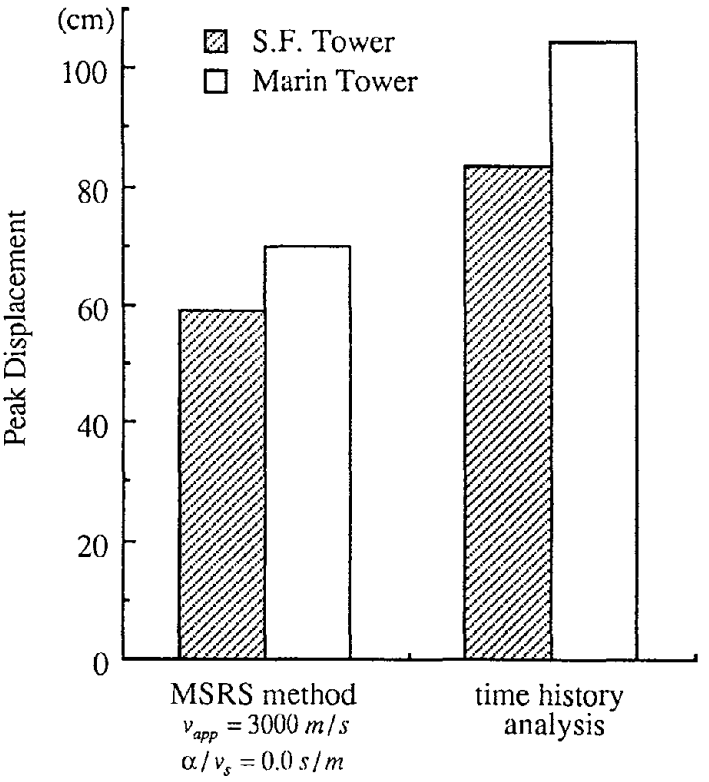

Fig. 5.13 Estimated Peak Longitudinal Displacement of the S.F. and Marin Towers

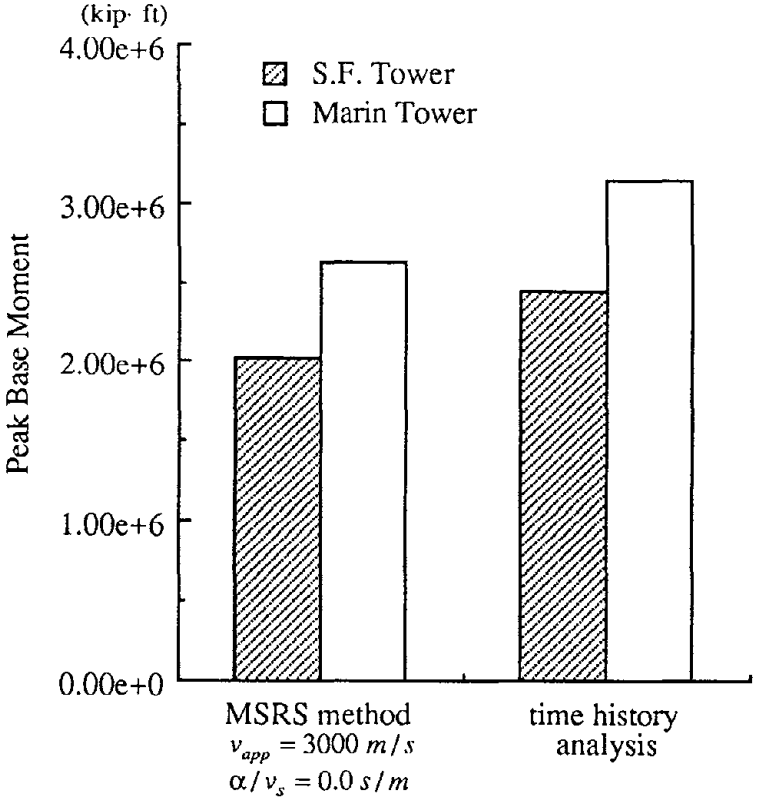

Fig. 5.14 Estimated Peak Base Moments of the S.F. and Marin Towers

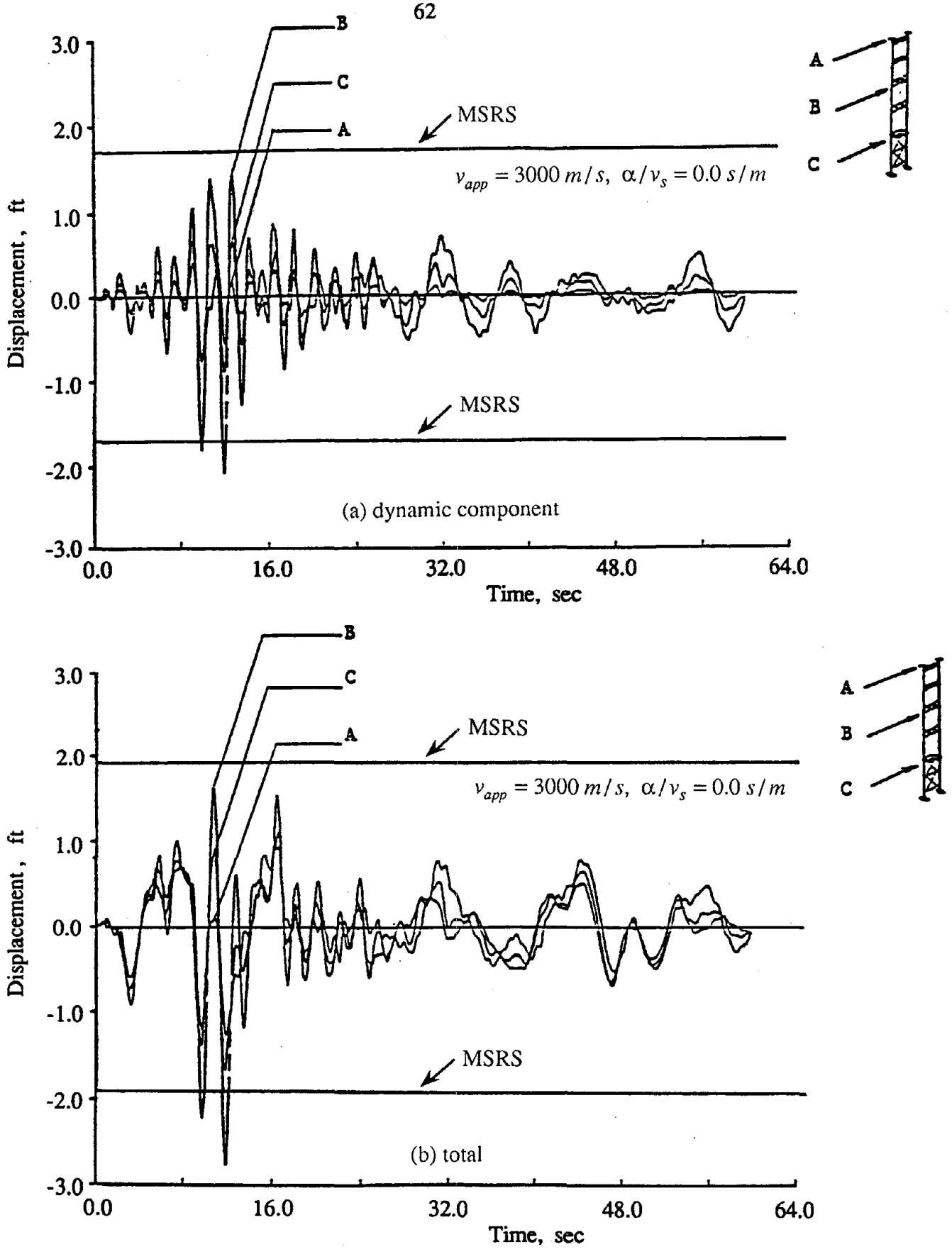

Fig. 5.15 Longitudinal Time Histories of the S.F. Tower: (a) dynamic component, (b) total

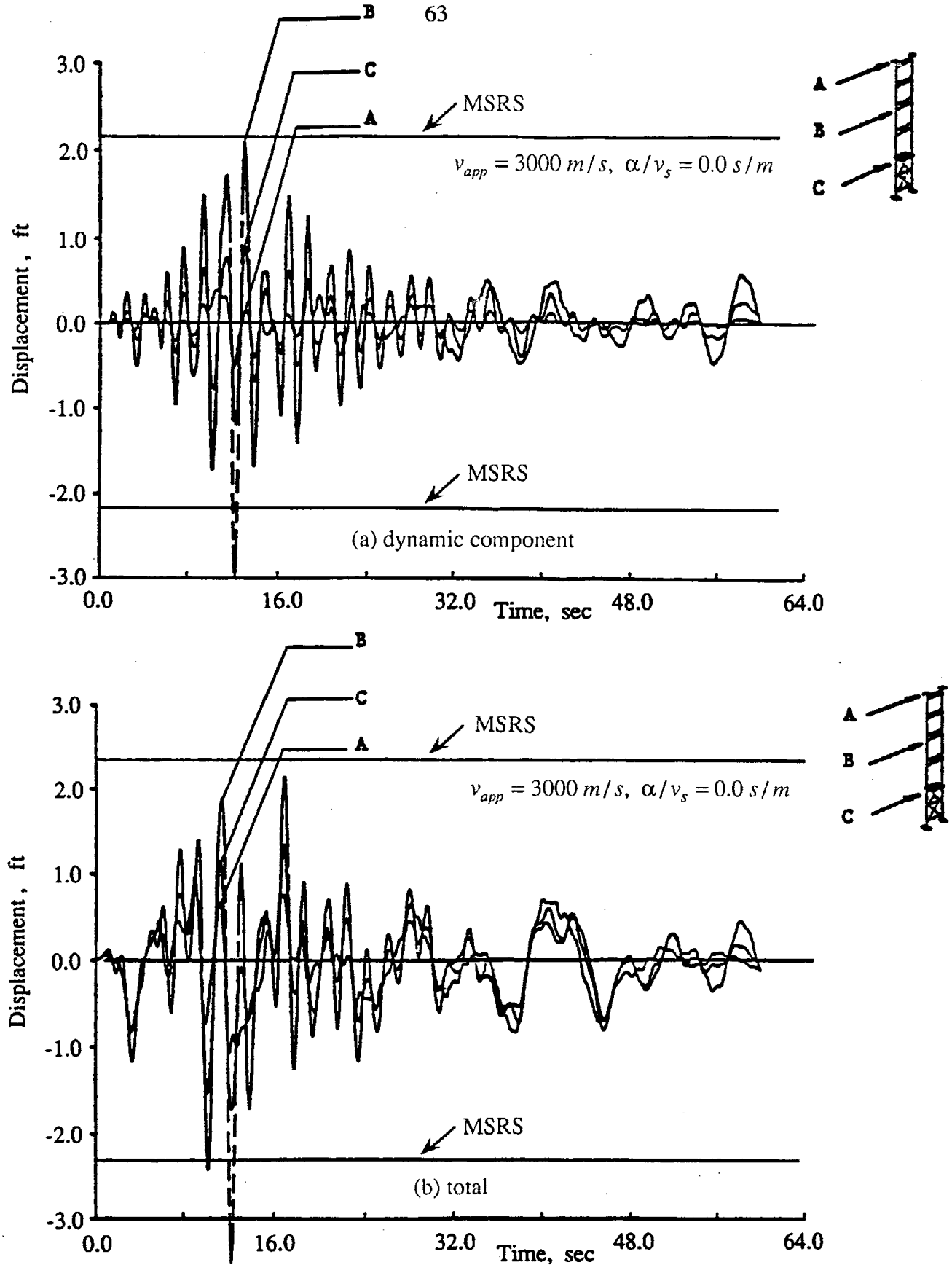

Fig. 5.16 Longitudinal Time Histories of the Marin Tower: (a) dynamic component, (b) total

CHAPTER 6
SUMMARY AND CONCLUSIONS

The newly developed Multiple-Support Response Spectrum (MSRS) method is reviewed. This method properly accounts for the effects of wave passage and incoherence of the support motions, the effect of local site conditions, and the effects of correlation between the support motions and between the dynamic modes of the structure. New properties concerning the influence matrix, effective influence coefficients, and effective modal participation factors that are required in the modal combination rule are developed.

The MSRS method is applied to the Golden Gate Bridge, which is a three-span suspension bridge connecting San Francisco and Marin counties. A 3-dimensional model with a total of 4,074 degrees of freedom and 6 pairs of support points is used for the analysis. Response spectra obtained from generated time histories are used for the three components of the ground motion at each support point.

The significances of the modal and support cross-correlation coefficients of the Golden Gate Bridge are investigated. It is found that the cross-correlation coefficients involved in terms representing the pseudo-static and dynamic components of the response are significant and are influenced by the wave passage effect and the incoherence effect. The cross-correlation coefficients involved in the covariance between the pseudo-static and dynamic contributions of the response are relatively small.

The mean peak longitudinal displacements of the mid-height points of the S.F. and Marin towers and their mean peak base moments are computed by the MSRS method. The method provides a convenient means for parametric study, which is performed to determine the influences of the wave passage and incoherence effects, as well as the influences of assuming uniform or statistically independent support motions. Results indicate that the assumption of uniform support motion increases the response estimates for both towers of the bridge, whereas the assumption of independent motions decreases the Marin tower response but has little effect on the S.F. tower response.

Comparison of MSRS results with results generated by a single time-history analysis show consistent trends, although relatively significant discrepancies between the two sets of results are observed. Possible reasons for the discrepancy are discussed.

REFERENCES

1. Abdel-Ghaffar, A., and Rubin, L.I. (1982). "Suspension bridge response to multiple- support excitations." *J. Eng. Mech*, 108, 419-435.
2. Abrahamson, N.A., and Bolt, B.A. (1985). "The spatial variation of the phasing of seismic strong ground motion." *Bull. Seism. Soc. America*, 75, 1247-1264.
3. Abrahamson, N.A., and Bolt, B.A. (1987). "The SMART-1 accelerograph array (1980-1987): a review." *Earthq. Spectra*, 3(2), 263-287.
4. Abrahamson, N.A., Schneider, J.F., and Stepp, J.C. (1991) "Empirical spatial coherency functions for application to soil-structure interaction analysis." *Earthq. Spectra*, 7, 1-28.
5. Asfura, A., and Der Kiureghian, A. (1986). "Floor response spectrum method for seismic analysis of multiply supported secondary systems." *Earthq. Eng. Struct. Dyn.*, 14, 245-265
6. Berrah, M., and Kausel E. (1989). "Modified response spectrum model for the design of structures subjected to spatially varying seismic excitations." *Report R90-2, Department of Civil Engineering, MIT, Cambridge, Mass.*
7. Bogdanoff, J.L., Goldberg, J.E., and Schiff, A.J. (1965). "The effect of ground transmission time on the response of long structures." *Bull. Seism. Soc. America*, 55, 627-640
8. Bolt, B.A., Loh, C.H., Penzien, J., Tsai, Y.B., and Yeh, Y.T. (1982a). Preliminary report on the SMART 1 strong motion array in Taiwan. *Report UCB/EERC-82/13*, Earthquake Engineering Research Center, University of California at Berkeley, CA.
9. Bolt, B.A., Loh, C.H., Penzien, J., Tsai, Y.B., and Yeh, Y.T. (1982b). Earthquake strong motions recorded by a large near-source array of digital seismographs. *Earthq. Eng. Struct. Dyn.*, 10, 561-573.
10. Christian, J.T. (1989). "Generating seismic design power spectral density functions." *Earthq. Spectra*, 5, 351-368
11. Clough, R.W., and Penzien, J. (1975) *Dynamics of Structures*. McGraw-Hill Book Co., New York, NY.
12. Der Kiureghian, A. (1980). "Structural response to stationary excitation." *J. Eng. Mechanics Division*, ASCE, 106, 1195-1213.

13. Der Kiureghian, A. (1981). "A response spectrum method for random vibration analysis of MDF systems." *Earthq. Eng. Struct. Dyn.*, 9, 419-435.
14. Der Kiureghian, A. (1991). "CQC modal combination rule for high-frequency modes." *Trans. 11th Int. Conf. on Struct. Mech. in Reactor Technology,* Tokyo, Japan.
15. Der Kiureghian, A., and Neuenhofer, A. (1991). A response spectrum method for multiple-support response spectrum method. *Report UCB/EERC-91/08*, Earthquake Engineering Research Center, University of California at Berkeley, Berkeley, CA.
16. Der Kiureghian, A., and Neuenhofer, A. (1992). "Response spectrum method for multi-support seismic excitations." *Earthq. Eng. Struct. Dyn.*, 21, 713-740.
17. Dong, K.K., and Wieland, M. (1988) "Application of response spectrum method to a bridge subjected to multiple support excitation." *Proc. 9th World Conf. Earthq. Eng.*, Tokyo, Japan, VI, 531-536.
18. Hao, H. (1989). Effects of spatial variation of ground motions on large multiply-supported structures. *Report UCB/EERC-89/06*, Earthquake Engineering Research Center, University of California at Berkeley, CA.
19. Hao, H., Olivera, C.S., and Penzien, J. (1989). "Multiple-station ground motion processing and simulation based on SMART-1 array data." *Nuclear Eng. and Design*, 111, 293-310.
20. Harichandran, R.S., and Vanmarcke E. (1986). "Stochastic variation of earthquake ground motion in space and time." *J. Eng. Mechanics*, ASCE, 112, 154-174.
21. Harichandran, R.S., and Wang, W. (1988a). "Response of simple beam to spatially varying earthquake excitation." *J. Eng. Mechanics*, ASCE, 114, 1526-1541.
22. Harichandran, R.S., and Wang, W. (1988a). "Response of indeterminate two-span beams to spatially varying earthquake excitation." *Earthq. Eng. Struct. Dyn.*,19, 173-187.
23. Humar J.L. (1990) *Dynamics of Structures.* Prentice-Hall, Inc., New Jersey.
24. Igusa, T., and Der Kiureghian, A. (1983). "Response spectrum method for systems with nonclassical damping." *Proc. of ASCE-EMD Specialty Conference,* West Lafayette, Indiana, 380-384

25. Igusa, T., and Der Kiureghian, A. (1985). "Generation of floor response spectra including oscillator-structure interaction." *Earthq. Eng. Struct. Dyn.*, 13, 661-676.
26. Johnson, N.E., and Gallety, R.D. (1972). "The comparison of the response of a highway bridge to uniform ground shock and moving ground excitation." *Shock Vibration Bull.*, 42, 75-85.
27. Kaul, M.K. (1978). "Stochastic characterization of earthquake through their response spectrum." *Earthq. Eng. Struct. Dyn.*, 6, 497-509.
28. Kawashima, K., and Aizawa, K. (1986). "Modification of earthquake response spectra with respect to damping ratio." *Proc., Third U.S. Natl. Conf. Earthq. Eng.*, South Carolina, II, 1107-1116.
29. Lin, Y.K. (1967) *Probabilistic theory of structural dynamics.* McGraw-Hill, New York, NY.
30. Liu, W.D., and Imbsen, R.A. (1990). Seismic evaluation of Golden Gate Bridge and tower structure. Imbsen & Associates, Inc. Sacramento, CA.
31. Loh, C.H., Penzien, J., and Tsai, Y.B. (1982). "Engineering analysis of SMART-1 array accelerograms." *Earthq. Eng. Struct. Dyn.*, 10, 575-591.
32. Loh, C.H., and Yeh, Y.T. (1988). "Spatial variation and stochastic modeling of seismic differential ground movement." *Earthq. Eng. Struct. Dyn.*, 16, 583-596.
33. Luco, J.E., and Wong, H.L. (1986). "Response of a rigid foundation to a spatially random ground motion." *Earthq. Eng. Struct. Dyn.*, 14, 891-908.
34. Newmark, N.M., and Hall, W.J. (1969). "Seismic design criteria for nuclear Reactor facilities." *Proc. 4th World Conf. Earthq. Eng.*, Santiago, Chile, II, 37-50
35. Penzien, J., and Watabe, M. (1975). "Characteristic of 3-dimensional earthquake ground motion." *Earthq. Eng. Struct. Dyn.*, 3, 365-374.
36. Rosenblueth, E., and Elorduy, J. (1969). "Responses of linear systems to certain transient disturbances." *Proc. 4th World Conf. Earthq. Eng.*, Santiago, Chile, I, 185-196.
37. Smeby, W., and Der Kiureghian, A. (1985). "Modal combination rule for multi-component earthquake excitation." *Earthq. Eng. Struct. Dyn.*, 13, 1-12.
38. SEAOC (1990). *Recommended lateral force requirements and commentary.* Structural Engineers Association of California, Sacramento, CA.

39. Singh, M.P., and Chu, S.L. (1976). "Stochastic consideration in seismic analysis of structures." *Earthq. Eng. Struct. Dyn.*, 4, 295-307.
40. Unruh, J.F., and Kana, D.D. (1981). "An alternative procedure for the generation of consistent power/response spectrum." *Nuclear Eng. and Design*, 66, 427-435.
41. Werner, S.D., Lee, L.C., Wong, H.L., and Trifunac, M.D. (1979). "Structural response to traveling seismic waves." J. Structural Division, ASCE, 105, 2547-2564.
42. Wilson, E.L., Der Kiureghian, A., and Bayo, E.P. (1981). "A replacement for the SRSS method in seismic analysis." *Earthq. Eng. Struct. Dyn.*, 9, 187-194.
43. Yamamura, N., and Tanaka, H. (1990). "Response analysis of flexible MDF systems for multiple-support seismic excitations." *Earthq. Eng. Struct. Dyn.*, 19, 345-357.
44. Zerva, A. (1990). "Response of multi-span beams to spatially incoherent seismic ground motions." *Earthq. Eng. Struct. Dyn.*, 19, 819-832.
45. Zerva, A. (1991). "Effect of spatial variability and propagation of seismic ground motions on the response of multiply-supported structures." *Probabilistic Eng. Mechanics.*
46. Zerva, A., Ang, A. H-S., and Wen, Y.K. (1988). "Lifeline response to spatially variable ground motions." *Earthq. Eng. Struct. Dyn.*, 16, 361-379.

EARTHQUAKE ENGINEERING RESEARCH CENTER REPORT SERIES

EERC reports are available from the National Information Service for Earthquake Engineering (NISEE) and from the National Technical Information Service (NTIS). Numbers in parentheses are Accession Numbers assigned by the National Technical Information Service; these are followed by a price code. Contact NTIS, 5285 Port Royal Road, Springfield Virginia, 22161 for more information. Reports without Accession Numbers were not available from NTIS at the time of printing. For a current complete list of EERC reports (from EERC 67-1) and availablity information, please contact University of California, EERC, NISEE, 1301 South 46th Street, Richmond, California 94804.

UCB/EERC-82/01 "Dynamic Behavior of Ground for Seismic Analysis of Lifeline Systems," by Sato, T. and Der Kiureghian, A., January 1982, (PB82 218 926)A05.

UCB/EERC-82/02 "Shaking Table Tests of a Tubular Steel Frame Model," by Ghanaat, Y. and Clough, R.W., January 1982, (PB82 220 161)A07.

UCB/EERC-82/03 "Behavior of a Piping System under Seismic Excitation: Experimental Investigations of a Spatial Piping System supported by Mechanical Shock Arrestors," by Schneider, S., Lee, H.-M. and Godden, W. G., May 1982, (PB83 172 544)A09.

UCB/EERC-82/04 "New Approaches for the Dynamic Analysis of Large Structural Systems," by Wilson, E.L., June 1982, (PB83 148 080)A05.

UCB/EERC-82/05 "Model Study of Effects of Damage on the Vibration Properties of Steel Offshore Platforms," by Shahrivar, F. and Bouwkamp, J.G., June 1982, (PB83 148 742)A10.

UCB/EERC-82/06 "States of the Art and Practice in the Optimum Seismic Design and Analytical Response Prediction of R/C Frame Wall Structures," by Aktan, A.E. and Bertero, V.V., July 1982, (PB83 147 736)A05.

UCB/EERC-82/07 "Further Study of the Earthquake Response of a Broad Cylindrical Liquid-Storage Tank Model," by Manos, G.C. and Clough, R.W., July 1982, (PB83 147 744)A11.

UCB/EERC-82/08 "An Evaluation of the Design and Analytical Seismic Response of a Seven Story Reinforced Concrete Frame," by Charney, F.A. and Bertero, V.V., July 1982, (PB83 157 628)A09.

UCB/EERC-82/09 "Fluid-Structure Interactions: Added Mass Computations for Incompressible Fluid," by Kuo, J.S.-H., August 1982, (PB83 156 281)A07.

UCB/EERC-82/10 "Joint-Opening Nonlinear Mechanism: Interface Smeared Crack Model," by Kuo, J.S.-H., August 1982, (PB83 149 195)A05.

UCB/EERC-82/11 "Dynamic Response Analysis of Techi Dam," by Clough, R.W., Stephen, R.M. and Kuo, J.S.-H., August 1982, (PB83 147 496)A06.

UCB/EERC-82/12 "Prediction of the Seismic Response of R/C Frame-Coupled Wall Structures," by Aktan, A.E., Bertero, V.V. and Piazzo, M., August 1982, (PB83 149 203)A09.

UCB/EERC-82/13 "Preliminary Report on the Smart 1 Strong Motion Array in Taiwan," by Bolt, B.A., Loh, C.H., Penzien, J. and Tsai, Y.B., August 1982, (PB83 159 400)A10.

UCB/EERC-82/14 "Seismic Behavior of an Eccentrically X-Braced Steel Structure," by Yang, M.S., September 1982, (PB83 260 778)A12.

UCB/EERC-82/15 "The Performance of Stairways in Earthquakes," by Roha, C., Axley, J.W. and Bertero, V.V., September 1982, (PB83 157 693)A07.

UCB/EERC-82/16 "The Behavior of Submerged Multiple Bodies in Earthquakes," by Liao, W.-G., September 1982, (PB83 158 709)A07.

UCB/EERC-82/17 "Effects of Concrete Types and Loading Conditions on Local Bond-Slip Relationships," by Cowell, A.D., Popov, E.P. and Bertero, V.V., September 1982, (PB83 153 577)A04.

UCB/EERC-82/18 "Mechanical Behavior of Shear Wall Vertical Boundary Members: An Experimental Investigation," by Wagner, M.T. and Bertero, V.V., October 1982, (PB83 159 764)A05.

UCB/EERC-82/19 "Experimental Studies of Multi-support Seismic Loading on Piping Systems," by Kelly, J.M. and Cowell, A.D., November 1982, (PB90 262 684)A07.

UCB/EERC-82/20 "Generalized Plastic Hinge Concepts for 3D Beam-Column Elements," by Chen, P. F.-S. and Powell, G.H., November 1982, (PB83 247 981)A13.

UCB/EERC-82/21 "ANSR-III: General Computer Program for Nonlinear Structural Analysis," by Oughourlian, C.V. and Powell, G.H., November 1982, (PB83 251 330)A12.

UCB/EERC-82/22 "Solution Strategies for Statically Loaded Nonlinear Structures," by Simons, J.W. and Powell, G.H., November 1982, (PB83 197 970)A06.

UCB/EERC-82/23 "Analytical Model of Deformed Bar Anchorages under Generalized Excitations," by Ciampi, V., Eligehausen, R., Bertero, V.V. and Popov, E.P., November 1982, (PB83 169 532)A06.

UCB/EERC-82/24 "A Mathematical Model for the Response of Masonry Walls to Dynamic Excitations," by Sucuoglu, H., Mengi, Y. and McNiven, H.D., November 1982, (PB83 169 011)A07.

UCB/EERC-82/25 "Earthquake Response Considerations of Broad Liquid Storage Tanks," by Cambra, F.J., November 1982, (PB83 251 215)A09.

UCB/EERC-82/26 "Computational Models for Cyclic Plasticity, Rate Dependence and Creep," by Mosaddad, B. and Powell, G.H., November 1982, (PB83 245 829)A08.

UCB/EERC-82/27 "Inelastic Analysis of Piping and Tubular Structures," by Mahasuverachai, M. and Powell, G.H., November 1982, (PB83 249 987)A07.

UCB/EERC-83/01 "The Economic Feasibility of Seismic Rehabilitation of Buildings by Base Isolation," by Kelly, J.M., January 1983, (PB83 197 988)A05.

UCB/EERC-83/02 "Seismic Moment Connections for Moment-Resisting Steel Frames.," by Popov, E.P., January 1983, (PB83 195 412)A04.

UCB/EERC-83/03 "Design of Links and Beam-to-Column Connections for Eccentrically Braced Steel Frames," by Popov, E.P. and Malley, J.O., January 1983, (PB83 194 811)A04.

UCB/EERC-83/04 "Numerical Techniques for the Evaluation of Soil-Structure Interaction Effects in the Time Domain," by Bayo, E. and Wilson, E.L., February 1983, (PB83 245 605)A09.

UCB/EERC-83/05 "A Transducer for Measuring the Internal Forces in the Columns of a Frame-Wall Reinforced Concrete Structure," by Sause, R. and Bertero, V.V., May 1983, (PB84 119 494)A06.

UCB/EERC-83/06 "Dynamic Interactions Between Floating Ice and Offshore Structures," by Croteau, P., May 1983, (PB84 119 486)A16.

UCB/EERC-83/07 "Dynamic Analysis of Multiply Tuned and Arbitrarily Supported Secondary Systems," by Igusa, T. and Der Kiureghian, A., July 1983, (PB84 118 272)A11.

UCB/EERC-83/08 "A Laboratory Study of Submerged Multi-body Systems in Earthquakes," by Ansari, G.R., June 1983, (PB83 261 842)A17.

UCB/EERC-83/09 "Effects of Transient Foundation Uplift on Earthquake Response of Structures," by Yim, C.-S. and Chopra, A.K., June 1983, (PB83 261 396)A07.

UCB/EERC-83/10 "Optimal Design of Friction-Braced Frames under Seismic Loading," by Austin, M.A. and Pister, K.S., June 1983, (PB84 119 288)A06.

UCB/EERC-83/11 "Shaking Table Study of Single-Story Masonry Houses: Dynamic Performance under Three Component Seismic Input and Recommendations," by Manos, G.C., Clough, R.W. and Mayes, R.L., July 1983, (UCB/EERC-83/11)A08.

UCB/EERC-83/12 "Experimental Error Propagation in Pseudodynamic Testing," by Shing, P.B. and Mahin, S.A., June 1983, (PB84 119 270)A09.

UCB/EERC-83/13 "Experimental and Analytical Predictions of the Mechanical Characteristics of a 1/5-scale Model of a 7-story R/C Frame-Wall Building Structure," by Aktan, A.E., Bertero, V.V., Chowdhury, A.A. and Nagashima, T., June 1983, (PB84 119 213)A07.

UCB/EERC-83/14 "Shaking Table Tests of Large-Panel Precast Concrete Building System Assemblages," by Oliva, M.G. and Clough, R.W., June 1983, (PB86 110 210/AS)A11.

UCB/EERC-83/15 "Seismic Behavior of Active Beam Links in Eccentrically Braced Frames," by Hjelmstad, K.D. and Popov, E.P., July 1983, (PB84 119 676)A09.

UCB/EERC-83/16 "System Identification of Structures with Joint Rotation," by Dimsdale, J.S., July 1983, (PB84 192 210)A06.

UCB/EERC-83/17 "Construction of Inelastic Response Spectra for Single-Degree-of-Freedom Systems," by Mahin, S. and Lin, J., June 1983, (PB84 208 834)A05.

UCB/EERC-83/18 "Interactive Computer Analysis Methods for Predicting the Inelastic Cyclic Behaviour of Structural Sections," by Kaba, S. and Mahin, S., July 1983, (PB84 192 012)A06.

UCB/EERC-83/19 "Effects of Bond Deterioration on Hysteretic Behavior of Reinforced Concrete Joints," by Filippou, F.C., Popov, E.P. and Bertero, V.V., August 1983, (PB84 192 020)A10.

UCB/EERC-83/20 "Correlation of Analytical and Experimental Responses of Large-Panel Precast Building Systems," by Oliva, M.G., Clough, R.W., Velkov, M. and Gavrilovic, P., May 1988, (PB90 262 692)A06.

UCB/EERC-83/21 "Mechanical Characteristics of Materials Used in a 1/5 Scale Model of a 7-Story Reinforced Concrete Test Structure," by Bertero, V.V., Aktan, A.E., Harris, H.G. and Chowdhury, A.A., October 1983, (PB84 193 697)A05.

UCB/EERC-83/22 "Hybrid Modelling of Soil-Structure Interaction in Layered Media," by Tzong, T.-J. and Penzien, J., October 1983, (PB84 192 178)A08.

UCB/EERC-83/23 "Local Bond Stress-Slip Relationships of Deformed Bars under Generalized Excitations," by Eligehausen, R., Popov, E.P. and Bertero, V.V., October 1983, (PB84 192 848)A09.

UCB/EERC-83/24 "Design Considerations for Shear Links in Eccentrically Braced Frames," by Malley, J.O. and Popov, E.P., November 1983, (PB84 192 186)A07.

UCB/EERC-84/01 "Pseudodynamic Test Method for Seismic Performance Evaluation: Theory and Implementation," by Shing, P.-S.B. and Mahin, S.A., January 1984, (PB84 190 644)A08.

UCB/EERC-84/02 "Dynamic Response Behavior of Kiang Hong Dian Dam," by Clough, R.W., Chang, K.-T., Chen, H.-Q. and Stephen, R.M., April 1984, (PB84 209 402)A08.

UCB/EERC-84/03 "Refined Modelling of Reinforced Concrete Columns for Seismic Analysis," by Kaba, S.A. and Mahin, S.A., April 1984, (PB84 234 384)A06.

UCB/EERC-84/04 "A New Floor Response Spectrum Method for Seismic Analysis of Multiply Supported Secondary Systems," by Asfura, A. and Der Kiureghian, A., June 1984, (PB84 239 417)A06.

UCB/EERC-84/05 "Earthquake Simulation Tests and Associated Studies of a 1/5th-scale Model of a 7-Story R/C Frame-Wall Test Structure," by Bertero, V.V., Aktan, A.E., Charney, F.A. and Sause, R., June 1984, (PB84 239 409)A09.

UCB/EERC-84/06 "Unassigned," by Unassigned, 1984.

UCB/EERC-84/07 "Behavior of Interior and Exterior Flat-Plate Connections Subjected to Inelastic Load Reversals," by Zee, H.L. and Moehle, J.P., August 1984, (PB86 117 629/AS)A07.

UCB/EERC-84/08 "Experimental Study of the Seismic Behavior of a Two-Story Flat-Plate Structure," by Moehle, J.P. and Diebold, J.W., August 1984, (PB86 122 553/AS)A12.

UCB/EERC-84/09 "Phenomenological Modeling of Steel Braces under Cyclic Loading," by Ikeda, K., Mahin, S.A. and Dermitzakis, S.N., May 1984, (PB86 132 198/AS)A08.

UCB/EERC-84/10 "Earthquake Analysis and Response of Concrete Gravity Dams," by Fenves, G.L. and Chopra, A.K., August 1984, (PB85 193 902/AS)A11.

UCB/EERC-84/11 "EAGD-84: A Computer Program for Earthquake Analysis of Concrete Gravity Dams," by Fenves, G.L. and Chopra, A.K., August 1984, (PB85 193 613/AS)A05.

UCB/EERC-84/12 "A Refined Physical Theory Model for Predicting the Seismic Behavior of Braced Steel Frames," by Ikeda, K. and Mahin, S.A., July 1984, (PB85 191 450/AS)A09.

UCB/EERC-84/13 "Earthquake Engineering Research at Berkeley - 1984," by EERC, August 1984, (PB85 197 341/AS)A10.

UCB/EERC-84/14 "Moduli and Damping Factors for Dynamic Analyses of Cohesionless Soils," by Seed, H.B., Wong, R.T., Idriss, I.M. and Tokimatsu, K., September 1984, (PB85 191 468/AS)A04.

UCB/EERC-84/15 "The Influence of SPT Procedures in Soil Liquefaction Resistance Evaluations," by Seed, H.B., Tokimatsu, K., Harder, L.F. and Chung, R.M., October 1984, (PB85 191 732/AS)A04.

UCB/EERC-84/16 "Simplified Procedures for the Evaluation of Settlements in Sands Due to Earthquake Shaking," by Tokimatsu, K. and Seed, H.B., October 1984, (PB85 197 887/AS)A03.

UCB/EERC-84/17 "Evaluation of Energy Absorption Characteristics of Highway Bridges Under Seismic Conditions - Volume I (PB90 262 627)A16 and Volume II (Appendices) (PB90 262 635)A13," by Imbsen, R.A. and Penzien, J., September 1986.

UCB/EERC-84/18 "Structure-Foundation Interactions under Dynamic Loads," by Liu, W.D. and Penzien, J., November 1984, (PB87 124 889/AS)A11.

UCB/EERC-84/19 "Seismic Modelling of Deep Foundations," by Chen, C.-H. and Penzien, J., November 1984, (PB87 124 798/AS)A07.

UCB/EERC-84/20 "Dynamic Response Behavior of Quan Shui Dam," by Clough, R.W., Chang, K.-T., Chen, H.-Q., Stephen, R.M., Ghanaat, Y. and Qi, J.-H., November 1984, (PB86 115177/AS)A07.

UCB/EERC-85/01 "Simplified Methods of Analysis for Earthquake Resistant Design of Buildings," by Cruz, E.F. and Chopra, A.K., February 1985, (PB86 112299/AS)A12.

UCB/EERC-85/02 "Estimation of Seismic Wave Coherency and Rupture Velocity using the SMART 1 Strong-Motion Array Recordings," by Abrahamson, N.A., March 1985, (PB86 214 343)A07.

UCB/EERC-85/03 "Dynamic Properties of a Thirty Story Condominium Tower Building," by Stephen, R.M., Wilson, E.L. and Stander, N., April 1985, (PB86 118965/AS)A06.

UCB/EERC-85/04 "Development of Substructuring Techniques for On-Line Computer Controlled Seismic Performance Testing," by Dermitzakis, S. and Mahin, S., February 1985, (PB86 132941/AS)A08.

UCB/EERC-85/05 "A Simple Model for Reinforcing Bar Anchorages under Cyclic Excitations," by Filippou, F.C., March 1985, (PB86 112 919/AS)A05.

UCB/EERC-85/06 "Racking Behavior of Wood-framed Gypsum Panels under Dynamic Load," by Oliva, M.G., June 1985, (PB90 262 643)A04.

UCB/EERC-85/07 "Earthquake Analysis and Response of Concrete Arch Dams," by Fok, K.-L. and Chopra, A.K., June 1985, (PB86 139672/AS)A10.

UCB/EERC-85/08 "Effect of Inelastic Behavior on the Analysis and Design of Earthquake Resistant Structures," by Lin, J.P. and Mahin, S.A., June 1985, (PB86 135340/AS)A08.

UCB/EERC-85/09 "Earthquake Simulator Testing of a Base-Isolated Bridge Deck," by Kelly, J.M., Buckle, I.G. and Tsai, H.-C., January 1986, (PB87 124 152/AS)A06.

UCB/EERC-85/10 "Simplified Analysis for Earthquake Resistant Design of Concrete Gravity Dams," by Fenves, G.L. and Chopra, A.K., June 1986, (PB87 124 160/AS)A08.

UCB/EERC-85/11 "Dynamic Interaction Effects in Arch Dams," by Clough, R.W., Chang. K.-T., Chen, H.-Q. and Ghanaat, Y., October 1985, (PB86 135027/AS)A05.

UCB/EERC-85/12 "Dynamic Response of Long Valley Dam in the Mammoth Lake Earthquake Series of May 25-27, 1980," by Lai, S. and Seed, H.B., November 1985, (PB86 142304/AS)A05.

UCB/EERC-85/13 "A Methodology for Computer-Aided Design of Earthquake-Resistant Steel Structures," by Austin, M.A., Pister, K.S. and Mahin, S.A., December 1985, (PB86 159480/AS)A10 .

UCB/EERC-85/14 "Response of Tension-Leg Platforms to Vertical Seismic Excitations," by Liou, G.-S., Penzien, J. and Yeung, R.W., December 1985, (PB87 124 871/AS)A08.

UCB/EERC-85/15 "Cyclic Loading Tests of Masonry Single Piers: Volume 4 - Additional Tests with Height to Width Ratio of 1," by Sveinsson, B., McNiven, H.D. and Sucuoglu, H., December 1985, (PB87 165031/AS)A08.

UCB/EERC-85/16 "An Experimental Program for Studying the Dynamic Response of a Steel Frame with a Variety of Infill Partitions," by Yanev, B. and McNiven, H.D., December 1985, (PB90 262 676)A05.

UCB/EERC-86/01 "A Study of Seismically Resistant Eccentrically Braced Steel Frame Systems," by Kasai, K. and Popov, E.P., January 1986, (PB87 124 178/AS)A14.

UCB/EERC-86/02 "Design Problems in Soil Liquefaction," by Seed, H.B., February 1986, (PB87 124 186/AS)A03.

UCB/EERC-86/03 "Implications of Recent Earthquakes and Research on Earthquake-Resistant Design and Construction of Buildings," by Bertero, V.V., March 1986, (PB87 124 194/AS)A05.

UCB/EERC-86/04 "The Use of Load Dependent Vectors for Dynamic and Earthquake Analyses," by Leger, P., Wilson, E.L. and Clough, R.W., March 1986, (PB87 124 202/AS)A12.

UCB/EERC-86/05 "Two Beam-To-Column Web Connections," by Tsai, K.-C. and Popov, E.P., April 1986, (PB87 124 301/AS)A04.

UCB/EERC-86/06 "Determination of Penetration Resistance for Coarse-Grained Soils using the Becker Hammer Drill," by Harder, L.F. and Seed, H.B., May 1986, (PB87 124 210/AS)A07.

UCB/EERC-86/07 "A Mathematical Model for Predicting the Nonlinear Response of Unreinforced Masonry Walls to In-Plane Earthquake Excitations," by Mengi, Y. and McNiven, H.D., May 1986, (PB87 124 780/AS)A06.

UCB/EERC-86/08 "The 19 September 1985 Mexico Earthquake: Building Behavior," by Bertero, V.V., July 1986.

UCB/EERC-86/09 "EACD-3D: A Computer Program for Three-Dimensional Earthquake Analysis of Concrete Dams," by Fok, K.-L., Hall, J.F. and Chopra, A.K., July 1986, (PB87 124 228/AS)A08.

UCB/EERC-86/10 "Earthquake Simulation Tests and Associated Studies of a 0.3-Scale Model of a Six-Story Concentrically Braced Steel Structure," by Uang, C.-M. and Bertero, V.V., December 1986, (PB87 163 564/AS)A17.

UCB/EERC-86/11 "Mechanical Characteristics of Base Isolation Bearings for a Bridge Deck Model Test," by Kelly, J.M., Buckle, I.G. and Koh, C.-G., November 1987, (PB90 262 668)A04.

UCB/EERC-86/12 "Effects of Axial Load on Elastomeric Isolation Bearings," by Koh, C.-G. and Kelly, J.M., November 1987.

UCB/EERC-87/01 "The FPS Earthquake Resisting System: Experimental Report," by Zayas, V.A., Low, S.S. and Mahin, S.A., June 1987, (PB88 170 287)A06.

UCB/EERC-87/02 "Earthquake Simulator Tests and Associated Studies of a 0.3-Scale Model of a Six-Story Eccentrically Braced Steel Structure," by Whittaker, A., Uang, C.-M. and Bertero, V.V., July 1987, (PB88 166 707/AS)A18.

UCB/EERC-87/03 "A Displacement Control and Uplift Restraint Device for Base-Isolated Structures," by Kelly, J.M., Griffith, M.C. and Aiken, I.D., April 1987, (PB88 169 933)A04.

UCB/EERC-87/04 "Earthquake Simulator Testing of a Combined Sliding Bearing and Rubber Bearing Isolation System," by Kelly, J.M. and Chalhoub, M.S., December 1990.

UCB/EERC-87/05 "Three-Dimensional Inelastic Analysis of Reinforced Concrete Frame-Wall Structures," by Moazzami, S. and Bertero, V.V., May 1987, (PB88 169 586/AS)A08.

UCB/EERC-87/06 "Experiments on Eccentrically Braced Frames with Composite Floors," by Ricles, J. and Popov, E., June 1987, (PB88 173 067/AS)A14.

UCB/EERC-87/07 "Dynamic Analysis of Seismically Resistant Eccentrically Braced Frames," by Ricles, J. and Popov, E., June 1987, (PB88 173 075/AS)A16.

UCB/EERC-87/08 "Undrained Cyclic Triaxial Testing of Gravels-The Effect of Membrane Compliance," by Evans, M.D. and Seed, H.B., July 1987, (PB88 173 257)A19.

UCB/EERC-87/09 "Hybrid Solution Techniques for Generalized Pseudo-Dynamic Testing," by Thewalt, C. and Mahin, S.A., July 1987, (PB 88 179 007)A07.

UCB/EERC-87/10 "Ultimate Behavior of Butt Welded Splices in Heavy Rolled Steel Sections," by Bruneau, M., Mahin, S.A. and Popov, E.P., September 1987, (PB90 254 285)A07.

UCB/EERC-87/11 "Residual Strength of Sand from Dam Failures in the Chilean Earthquake of March 3, 1985," by De Alba, P., Seed, H.B., Retamal, E. and Seed, R.B., September 1987, (PB88 174 321/AS)A03.

UCB/EERC-87/12 "Inelastic Seismic Response of Structures with Mass or Stiffness Eccentricities in Plan," by Bruneau, M. and Mahin, S.A., September 1987, (PB90 262 650/AS)A14.

UCB/EERC-87/13 "CSTRUCT: An Interactive Computer Environment for the Design and Analysis of Earthquake Resistant Steel Structures," by Austin, M.A., Mahin, S.A. and Pister, K.S., September 1987, (PB88 173 339/AS)A06.

UCB/EERC-87/14 "Experimental Study of Reinforced Concrete Columns Subjected to Multi-Axial Loading," by Low, S.S. and Moehle, J.P., September 1987, (PB88 174 347/AS)A07.

UCB/EERC-87/15 "Relationships between Soil Conditions and Earthquake Ground Motions in Mexico City in the Earthquake of Sept. 19, 1985," by Seed, H.B., Romo, M.P., Sun, J., Jaime, A. and Lysmer, J., October 1987, (PB88 178 991)A06.

UCB/EERC-87/16 "Experimental Study of Seismic Response of R. C. Setback Buildings," by Shahrooz, B.M. and Moehle, J.P., October 1987, (PB88 176 359)A16.

UCB/EERC-87/17 "The Effect of Slabs on the Flexural Behavior of Beams," by Pantazopoulou, S.J. and Moehle, J.P., October 1987, (PB90 262 700)A07.

UCB/EERC-87/18 "Design Procedure for R-FBI Bearings," by Mostaghel, N. and Kelly, J.M., November 1987, (PB90 262 718)A04.

UCB/EERC-87/19 "Analytical Models for Predicting the Lateral Response of R C Shear Walls: Evaluation of their Reliability," by Vulcano, A. and Bertero, V.V., November 1987, (PB88 178 983)A05.

UCB/EERC-87/20 "Earthquake Response of Torsionally-Coupled Buildings," by Hejal, R. and Chopra, A.K., December 1987.

UCB/EERC-87/21 "Dynamic Reservoir Interaction with Monticello Dam," by Clough, R.W., Ghanaat, Y. and Qiu, X-F., December 1987, (PB88 179 023)A07.

UCB/EERC-87/22 "Strength Evaluation of Coarse-Grained Soils," by Siddiqi, F.H., Seed, R.B., Chan, C.K., Seed, H.B. and Pyke, R.M., December 1987, (PB88 179 031)A04.

UCB/EERC-88/01 "Seismic Behavior of Concentrically Braced Steel Frames," by Khatib, I., Mahin, S.A. and Pister, K.S., January 1988, (PB91 210 898/AS)A11.

UCB/EERC-88/02 "Experimental Evaluation of Seismic Isolation of Medium-Rise Structures Subject to Uplift," by Griffith, M.C., Kelly, J.M., Coveney, V.A. and Koh, C.G., January 1988, (PB91 217 950/AS)A09.

UCB/EERC-88/03 "Cyclic Behavior of Steel Double Angle Connections," by Astaneh-Asl, A. and Nader, M.N., January 1988, (PB91 210 872)A05.

UCB/EERC-88/04 "Re-evaluation of the Slide in the Lower San Fernando Dam in the Earthquake of Feb. 9, 1971," by Seed, H.B., Seed, R.B., Harder, L.F. and Jong, H.-L., April 1988, (PB91 212 456/AS)A07.

UCB/EERC-88/05 "Experimental Evaluation of Seismic Isolation of a Nine-Story Braced Steel Frame Subject to Uplift," by Griffith, M.C., Kelly, J.M. and Aiken, I.D., May 1988, (PB91 217 968/AS)A07.

UCB/EERC-88/06 "DRAIN-2DX User Guide.," by Allahabadi, R. and Powell, G.H., March 1988, (PB91 212 530)A12.

UCB/EERC-88/07 "Theoretical and Experimental Studies of Cylindrical Water Tanks in Base-Isolated Structures," by Chalhoub, M.S. and Kelly, J.M., April 1988, (PB91 217 976/AS)A05.

UCB/EERC-88/08 "Analysis of Near-Source Waves: Separation of Wave Types Using Strong Motion Array Recording," by Darragh, R.B., June 1988, (PB91 212 621)A08.

UCB/EERC-88/09 "Alternatives to Standard Mode Superposition for Analysis of Non-Classically Damped Systems," by Kusainov, A.A. and Clough, R.W., June 1988, (PB91 217 992/AS)A04.

UCB/EERC-88/10 "The Landslide at the Port of Nice on October 16, 1979," by Seed, H.B., Seed, R.B., Schlosser, F., Blondeau, F. and Juran, I., June 1988, (PB91 210 914)A05.

UCB/EERC-88/11 "Liquefaction Potential of Sand Deposits Under Low Levels of Excitation," by Carter, D.P. and Seed, H.B., August 1988, (PB91 210 880)A15.

UCB/EERC-88/12 "Nonlinear Analysis of Reinforced Concrete Frames Under Cyclic Load Reversals," by Filippou, F.C. and Issa, A., September 1988, (PB91 212 589)A07.

UCB/EERC-88/13 "Implications of Recorded Earthquake Ground Motions on Seismic Design of Building Structures," by Uang, C.-M. and Bertero, V.V., November 1988, (PB91 212 548)A06.

UCB/EERC-88/14 "An Experimental Study of the Behavior of Dual Steel Systems," by Whittaker, A.S. , Uang, C.-M. and Bertero, V.V., September 1988, (PB91 212 712)A16.

UCB/EERC-88/15 "Dynamic Moduli and Damping Ratios for Cohesive Soils," by Sun, J.I., Golesorkhi, R. and Seed, H.B., August 1988, (PB91 210 922)A04.

UCB/EERC-88/16 "Reinforced Concrete Flat Plates Under Lateral Load: An Experimental Study Including Biaxial Effects," by Pan, A. and Moehle, J.P., October 1988, (PB91 210 856)A13.

UCB/EERC-88/17 "Earthquake Engineering Research at Berkeley - 1988," by EERC, November 1988, (PB91 210 864)A10.

UCB/EERC-88/18 "Use of Energy as a Design Criterion in Earthquake-Resistant Design," by Uang, C.-M. and Bertero, V.V., November 1988, (PB91 210 906/AS)A04.

UCB/EERC-88/19 "Steel Beam-Column Joints in Seismic Moment Resisting Frames," by Tsai, K.-C. and Popov, E.P., November 1988, (PB91 217 984/AS)A20.

UCB/EERC-88/20 "Base Isolation in Japan, 1988," by Kelly, J.M., December 1988, (PB91 212 449)A05.

UCB/EERC-89/01 "Behavior of Long Links in Eccentrically Braced Frames," by Engelhardt, M.D. and Popov, E.P., January 1989, (PB92 143 056)A18.

UCB/EERC-89/02 "Earthquake Simulator Testing of Steel Plate Added Damping and Stiffness Elements," by Whittaker, A., Bertero, V.V., Alonso, J. and Thompson, C., January 1989, (PB91 229 252/AS)A10.

UCB/EERC-89/03 "Implications of Site Effects in the Mexico City Earthquake of Sept. 19, 1985 for Earthquake-Resistant Design Criteria in the San Francisco Bay Area of California," by Seed, H.B. and Sun, J.I., March 1989, (PB91 229 369/AS)A07.

UCB/EERC-89/04 "Earthquake Analysis and Response of Intake-Outlet Towers," by Goyal, A. and Chopra, A.K., July 1989, (PB91 229 286/AS)A19.

UCB/EERC-89/05 "The 1985 Chile Earthquake: An Evaluation of Structural Requirements for Bearing Wall Buildings," by Wallace, J.W. and Moehle, J.P., July 1989, (PB91 218 008/AS)A13.

UCB/EERC-89/06 "Effects of Spatial Variation of Ground Motions on Large Multiply-Supported Structures," by Hao, H., July 1989, (PB91 229 161/AS)A08.

UCB/EERC-89/07 "EADAP - Enhanced Arch Dam Analysis Program: Users's Manual," by Ghanaat, Y. and Clough, R.W., August 1989, (PB91 212 522)A06.

UCB/EERC-89/08 "Seismic Performance of Steel Moment Frames Plastically Designed by Least Squares Stress Fields," by Ohi, K. and Mahin, S.A., August 1989, (PB91 212 597)A05.

UCB/EERC-89/09 "Feasibility and Performance Studies on Improving the Earthquake Resistance of New and Existing Buildings Using the Friction Pendulum System," by Zayas, V., Low, S., Mahin, S.A. and Bozzo, L., July 1989, (PB92 143 064)A14.

UCB/EERC-89/10 "Measurement and Elimination of Membrane Compliance Effects in Undrained Triaxial Testing," by Nicholson, P.G., Seed, R.B. and Anwar, H., September 1989, (PB92 139 641/AS)A13.

UCB/EERC-89/11 "Static Tilt Behavior of Unanchored Cylindrical Tanks," by Lau, D.T. and Clough, R.W., September 1989, (PB92 143 049)A10.

UCB/EERC-89/12 "ADAP-88: A Computer Program for Nonlinear Earthquake Analysis of Concrete Arch Dams," by Fenves, G.L., Mojtahedi, S. and Reimer, R.B., September 1989, (PB92 139 674/AS)A07.

UCB/EERC-89/13 "Mechanics of Low Shape Factor Elastomeric Seismic Isolation Bearings," by Aiken, I.D., Kelly, J.M. and Tajirian, F.F., November 1989, (PB92 139 732/AS)A09.

UCB/EERC-89/14 "Preliminary Report on the Seismological and Engineering Aspects of the October 17, 1989 Santa Cruz (Loma Prieta) Earthquake," by EERC, October 1989, (PB92 139 682/AS)A04.

UCB/EERC-89/15 "Experimental Studies of a Single Story Steel Structure Tested with Fixed, Semi-Rigid and Flexible Connections," by Nader, M.N. and Astaneh-Asl, A., August 1989, (PB91 229 211/AS)A10.

UCB/EERC-89/16 "Collapse of the Cypress Street Viaduct as a Result of the Loma Prieta Earthquake," by Nims, D.K., Miranda, E., Aiken, I.D., Whittaker, A.S. and Bertero, V.V., November 1989, (PB91 217 935/AS)A05.

UCB/EERC-90/01 "Mechanics of High-Shape Factor Elastomeric Seismic Isolation Bearings," by Kelly, J.M., Aiken, I.D. and Tajirian, F.F., March 1990.

UCB/EERC-90/02 "Javid's Paradox: The Influence of Preform on the Modes of Vibrating Beams," by Kelly, J.M., Sackman, J.L. and Javid, A., May 1990, (PB91 217 943/AS)A03.

UCB/EERC-90/03 "Earthquake Simulator Testing and Analytical Studies of Two Energy-Absorbing Systems for Multistory Structures," by Aiken, I.D. and Kelly, J.M., October 1990, (PB92 192 988)A13.

UCB/EERC-90/04 "Damage to the San Francisco-Oakland Bay Bridge During the October 17, 1989 Earthquake," by Astaneh-Asl, A., June 1990.

UCB/EERC-90/05 "Preliminary Report on the Principal Geotechnical Aspects of the October 17, 1989 Loma Prieta Earthquake," by Seed, R.B., Dickenson, S.E., Riemer, M.F., Bray, J.D., Sitar, N., Mitchell, J.K., Idriss, I.M., Kayen, R.E., Kropp, A., Harder, L.F., Jr. and Power, M.S., April 1990, (PB 192 970)A08.

UCB/EERC-90/06 "Models of Critical Regions in Reinforced Concrete Frames Under Seismic Excitations," by Zulfiqar, N. and Filippou, F.C., May 1990.

UCB/EERC-90/07 "A Unified Earthquake-Resistant Design Method for Steel Frames Using ARMA Models," by Takewaki, I., Conte, J.P., Mahin, S.A. and Pister, K.S., June 1990.

UCB/EERC-90/08 "Soil Conditions and Earthquake Hazard Mitigation in the Marina District of San Francisco," by Mitchell, J.K., Masood, T., Kayen, R.E. and Seed, R.B., May 1990, (PB 193 267/AS)A04.

UCB/EERC-90/09 "Influence of the Earthquake Ground Motion Process and Structural Properties on Response Characteristics of Simple Structures," by Conte, J.P., Pister, K.S. and Mahin, S.A., July 1990, (PB92 143 064)A15.

UCB/EERC-90/10 "Experimental Testing of the Resilient-Friction Base Isolation System," by Clark, P.W. and Kelly, J.M., July 1990, (PB92 143 072)A08.

UCB/EERC-90/11 "Seismic Hazard Analysis: Improved Models, Uncertainties and Sensitivities," by Araya, R. and Der Kiureghian, A., March 1988.

UCB/EERC-90/12 "Effects of Torsion on the Linear and Nonlinear Seismic Response of Structures," by Sedarat, H. and Bertero, V.V., September 1989, (PB92 193 002/AS)A15.

UCB/EERC-90/13 "The Effects of Tectonic Movements on Stresses and Deformations in Earth Embankments," by Bray, J. D., Seed, R. B. and Seed, H. B., September 1989.

UCB/EERC-90/14 "Inelastic Seismic Response of One-Story, Asymmetric-Plan Systems," by Goel, R.K. and Chopra, A.K., October 1990.

UCB/EERC-90/15 "Dynamic Crack Propagation: A Model for Near-Field Ground Motion.," by Seyyedian, H. and Kelly, J.M., 1990.

UCB/EERC-90/16 "Sensitivity of Long-Period Response Spectra to System Initial Conditions," by Blasquez, R., Ventura, C. and Kelly, J.M., 1990.

UCB/EERC-90/17 "Behavior of Peak Values and Spectral Ordinates of Near-Source Strong Ground-Motion over a Dense Array," by Niazi, M., June 1990.

UCB/EERC-90/18 "Material Characterization of Elastomers used in Earthquake Base Isolation," by Papoulia, K.D. and Kelly, J.M., 1990.

UCB/EERC-90/19 "Cyclic Behavior of Steel Top-and-Bottom Plate Moment Connections," by Harriott, J.D. and Astaneh-Asl, A., August 1990, (PB91 229 260/AS)A05.

UCB/EERC-90/20 "Seismic Response Evaluation of an Instrumented Six Story Steel Building," by Shen, J.-H. and Astaneh-Asl, A., December 1990, (PB91 229 294/AS)A04.

UCB/EERC-90/21 "Observations and Implications of Tests on the Cypress Street Viaduct Test Structure," by Bollo, M., Mahin, S.A., Moehle, J.P., Stephen, R.M. and Qi, X., December 1990.

UCB/EERC-91/01 "Experimental Evaluation of Nitinol for Energy Dissipation in Structures," by Nims, D.K., Sasaki, K.K. and Kelly, J.M., 1991.

UCB/EERC-91/02 "Displacement Design Approach for Reinforced Concrete Structures Subjected to Earthquakes," by Qi, X. and Moehle, J.P., January 1991.

UCB/EERC-91/03 "A Long-Period Isolation System Using Low-Modulus High-Damping Isolators for Nuclear Facilities at Soft-Soil Sites," by Kelly, J.M., March 1991.

UCB/EERC-91/04 "Dynamic and Failure Characteristics of Bridgestone Isolation Bearings," by Kelly, J.M., April 1991.

UCB/EERC-91/05 "Base Sliding Response of Concrete Gravity Dams to Earthquakes," by Chopra, A.K. and Zhang, L., May 1991.

UCB/EERC-91/06 "Computation of Spatially Varying Ground Motion and Foundation-Rock Impedance Matrices for Seismic Analysis of Arch Dams," by Zhang, L. and Chopra, A.K., May 1991.

UCB/EERC-91/07 "Estimation of Seismic Source Processes Using Strong Motion Array Data," by Chiou, S.-J., July 1991.

UCB/EERC-91/08 "A Response Spectrum Method for Multiple-Support Seismic Excitations," by Der Kiureghian, A. and Neuenhofer, A., August 1991.

UCB/EERC-91/09 "A Preliminary Study on Energy Dissipating Cladding-to-Frame Connection," by Cohen, J.M. and Powell, G.H., September 1991.

UCB/EERC-91/10 "Evaluation of Seismic Performance of a Ten-Story RC Building During the Whittier Narrows Earthquake," by Miranda, E. and Bertero, V.V., October 1991.

UCB/EERC-91/11 "Seismic Performance of an Instrumented Six Story Steel Building," by Anderson, J.C. and Bertero, V.V., November 1991.

UCB/EERC-91/12 "Performance of Improved Ground During the Loma Prieta Earthquake," by Mitchell, J.K. and Wentz, Jr., F.J., October 1991.

UCB/EERC-91/13 "Shaking Table - Structure Interaction," by Rinawi, A.M. and Clough, R.W., October 1991.

UCB/EERC-91/14 "Cyclic Response of RC Beam-Column Knee Joints: Test and Retrofit," by Mazzoni, S., Moehle, J.P. and Thewalt, C.R., October 1991.

UCB/EERC-91/15 "Design Guidelines for Ductility and Drift Limits: Review of State-of-the-Practice and State-of-the-Art in Ductility and Drift-Based Earthquake-Resistant Design of Buildings," by Bertero, V.V., Anderson, J.C., Krawinkler, H., Miranda, E. and The CUREe and The Kajima Research Teams,, July 1991.

UCB/EERC-91/16 "Evaluation of the Seismic Performance of a Thirty-Story RC Building," by Anderson, J.C., Miranda, E., Bertero, V.V. and The Kajima Project Research Team,, July 1991.

UCB/EERC-91/17 "A Fiber Beam-Column Element for Seismic Response Analysis of Reinforced Concrete Structures," by Taucer, F., Spacone, E. and Filippou, F.C., December 1991.

UCB/EERC-91/18 "Investigation of the Seismic Response of a Lightly-Damped Torsionally-Coupled Building," by Boroschek, R. and Mahin, S.A., December 1991.

UCB/EERC-92/01 "Studies of a 49-Story Instrumented Steel Structure Shaken During the Loma Prieta Earthquake," by Chen, C.-C., Bonowitz, D. and Astaneh-Asl, A., February 1992.

UCB/EERC-92/02 "Response of the Dumbarton Bridge in the Loma Prieta Earthquake," by Fenves, G.L., Filippou, F.C. and Sze, D.T., January 1992.

UCB/EERC-92/03 "Models for Nonlinear Earthquake Analysis of Brick Masonry Buildings," by Mengi, Y., McNiven, H.D. and Tanrikulu, A.K., March 1992.

UCB/EERC-92/04 "Shear Strength and Deformability of RC Bridge Columns Subjected to Inelastic Cyclic Displacements," by Aschheim, M. and Moehle, J.P., March 1992.

UCB/EERC-92/05 "Parameter Study of Joint Opening Effects on Earthquake Response of Arch Dams," by Fenves, G.L., Mojtahedi, S. and Reimer, R.B., April 1992.

UCB/EERC-92/06 "Seismic Behavior and Design of Semi-Rigid Steel Frames," by Nader, M.N. and Astaneh-Asl, A., May 1992.

UCB/EERC-92/07 "A Beam Element for Seismic Damage Analysis," by Spacone, E., Ciampi, V. and Filippou, F.C., August 1992.

UCB/EERC-92/08 "Nonlinear Static and Dynamic Analysis of Reinforced Concrete Subassemblages," by Filippou, F.C., D'Ambrisi, A. and Issa, A., August 1992.

UCB/EERC-92/09 "Evaluation of Code Accidental-Torsion Provisions Using Earthquake Records from Three Nominally Symmetric-Plan Buildings," by De la Llera, J.C. and Chopra, A.K., September 1992.

UCB/EERC-92/10 "Slotted Bolted Connection Energy Dissipators," by Grigorian, C.E., Yang, T.-S. and Popov, E.P., July 1992.

UCB/EERC-92/11 "Mechanical Characteristics of Neoprene Isolation Bearings," by Kelly, J.M. and Quiroz, E., August 1992.

UCB/EERC-92/12 "Application of a Mass Damping System to Bridge Structures," by Hasegawa, K. and Kelly, J.M., August 1992.

UCB/EERC-92/13 "Earthquake Engineering Research at Berkeley - 1992," by EERC, October 1992.

UCB/EERC-92/14 "Earthquake Risk and Insurance," by Brillinger, D.R., October 1992.

UCB/EERC-92/15 "A Friction Mass Damper for Vibration Control," by Inaudi, J.A. and Kelly, J.M., October 1992.

UCB/EERC-92/16 "Tall Reinforced Concrete Buildings: Conceptual Earthquake-Resistant Design Methology," by Bertero, R.D. and Bertero, V.V., December 1992.

UCB/EERC-92/17 "Performance of Tall Buildings During the 1985 Mexico Earthquakes," by Terán-Gilmore, A. and Bertero, V.V., December 1992.

UCB/EERC-92/18 "Dynamic Analysis of Nonlinear Structures using State-Space Formulation and Partitioned Integration Schemes," by Inaudi, J.A. and De la Llera, J.C., December 1992.

UCB/EERC-93/01 "Seismic Performance of an Instrumented Six-Story Reinforced-Concrete Building," by Anderson, J.C. and Bertero, V.V., 1993.

UCB/EERC-93/02 "Evaluation of an Active Variable-Damping-Structure," by Polak, E., Meeker, G., Yamada, K. and Kurata, N., 1993.

UCB/EERC-93/03 "Innovative Semi-Rigid Steel Frames for Control of the Seismic Response of Buildings," by McMullin, K.M., Astaneh-Asl, A. and Fenves, G.L., 1993.

UCB/EERC-93/04 "Seismic Performance of a 30-Story Building located on Soft Soil and designed according to UBC 1991," by Terán-Gilmore, A. and Bertero, V.V., 1993.

UCB/EERC-93/05 "Multiple-Support Response Spectrum Analysis of the Golden Gate Bridge," by Nakamura, Y., Der Kiureghian, A. and Liu, D., May 1993.